2005-06

Performance analysis of the IEEE 802.11G waveform transmitted over a fading channel with pulse-noise interference

Taxeidis, Konstantinos

Monterey California. Naval Postgraduate School

NAVAL POSTGRADUATE SCHOOL

MONTEREY, CALIFORNIA

THESIS

PERFORMANCE ANALYSIS OF THE *IEEE* 802.11G WAVEFORM TRANSMITTED OVER A FADING CHANNEL WITH PULSE-NOISE INTERFERENCE

by

Konstantinos Taxeidis

June 2006

Thesis Advisor:	Clark Robertson
Thesis Co-Advisor:	David Jenn

Approved for public release; distribution is unlimited.

THIS PAGE INTENTIONALLY LEFT BLANK

REPORT DOCUMENTATION PAGE			Form Approved OMB No. 0704-0188
Public reporting burden for this collection of information is estimated to average 1 hour per response, including the time for reviewing instruction, searching existing data sources, gathering and maintaining the data needed, and completing and reviewing the collection of information. Send comments regarding this burden estimate or any other aspect of this collection of information, including suggestions for reducing this burden, to Washington headquarters Services, Directorate for Information Operations and Reports, 1215 Jefferson Davis Highway, Suite 1204, Arlington, VA 22202-4302, and to the Office of Management and Budget, Paperwork Reduction Project (0704-0188) Washington DC 20503.			
1. AGENCY USE ONLY ***(Leave blank)***	**2. REPORT DATE** June 2006	**3. REPORT TYPE AND DATES COVERED** Master's Thesis	
4. TITLE AND SUBTITLE: Performance Analysis of *IEEE 802.11g* Waveform Transmitted Over A Fading Channel with Pulse-Noise Interference			**5. FUNDING NUMBERS**
6. AUTHOR(S) Konstantinos Taxeidis			
7. PERFORMING ORGANIZATION NAME(S) AND ADDRESS(ES) Naval Postgraduate School Monterey, CA 93943-5000			**8. PERFORMING ORGANIZATION REPORT NUMBER**
9. SPONSORING /MONITORING AGENCY NAME(S) AND ADDRESS(ES) N/A			**10. SPONSORING/MONITORING AGENCY REPORT NUMBER**
11. SUPPLEMENTARY NOTES The views expressed in this thesis are those of the author and do not reflect the official policy or position of the Department of Defense or the U.S. Government.			
12a. DISTRIBUTION / AVAILABILITY STATEMENT Approved for public release; distribution is unlimited.			**12b. DISTRIBUTION CODE**

13. ABSTRACT (maximum 200 words)

The performance of the most promising wireless local area network (WLAN) standards today, *IEEE* 802.11*g*, which specifies orthogonal frequency-division multiplexing in order to avoid multi-path effects and at the same time achieve high data rates, was examined in this thesis. We investigated four different receivers and analyzed their performance with Viterbi soft decision decoding when the signal was transmitted over a slow, flat fading Nakagami channel for AWGN only, as well as for AWGN plus pulse-noise interference. The implementation of forward error correction coding with soft decision decoding improves the performance compared to uncoded signal if pulse-noise interference is not present. The scenarios when no side information is available (linear-combining receiver), when perfect side information is available (noise-normalizing receiver), and two alternatives to the noise-normalized receiver with much coarser side information (modified noise-normalized receiver and noise-normalized receiver with normalization error) are examined. All the scenarios are examined for various fading and interference conditions. The performance of the noise-normalized receiver is, as expected, much improved compared to the linear-combining receiver when PNI is present. Finally, the noise-normalized receiver with normalization error achieves the same or better performance than the noise-normalized receiver without the exact interference noise power.

14. SUBJECT TERMS *IEEE* 802.11g WLAN Standard, Nakagami Fading Channel, OFDM, Soft Decision Decoding, Pulse-Noise Interference, Noise-Normalization			**15. NUMBER OF PAGES** 123
			16. PRICE CODE
17. SECURITY CLASSIFICATION OF REPORT Unclassified	**18. SECURITY CLASSIFICATION OF THIS PAGE** Unclassified	**19. SECURITY CLASSIFICATION OF ABSTRACT** Unclassified	**20. LIMITATION OF ABSTRACT** UL

NSN 7540-01-280-5500 Standard Form 298 (Rev. 2-89)
Prescribed by ANSI Std. 239-18

THIS PAGE INTENTIONALLY LEFT BLANK

Approved for public release; distribution is unlimited.

PERFORMANCE ANALYSIS OF *IEEE* 802.11G WAVEFORM TRANSMITTED OVER A FADING CHANNEL WITH PULSE-NOISE INTERFERENCE

Konstantinos Taxeidis
Lieutenant Junior Grade, Hellenic Navy
Bachelor of Science, Hellenic Naval Academy, 1998

Submitted in partial fulfillment of the
requirements for the degree of

MASTER OF SCIENCE IN ELECTRICAL ENGINEERING
and
MASTER OF SCIENCE IN SYSTEMS ENGINEERING

from the

NAVAL POSTGRADUATE SCHOOL
June 2006

Author: Konstantinos Taxeidis

Approved by: Clark Robertson
Thesis Advisor

David Jenn
Co-Advisor

Jeffrey B. Knorr
Chairman, Department of Electrical and Computer Engineering

Dan C. Boger
Chairman, Department of Information Science

THIS PAGE INTENTIONALLY LEFT BLANK

ABSTRACT

The performance of the most promising wireless local area network (WLAN) standards today, *IEEE* 802.11*g*, which specifies orthogonal frequency-division multiplexing (OFDM) in order to avoid multi-path effects and at the same time achieve high data rates, was examined in this thesis. We investigated four different receivers and analyzed their performance with Viterbi soft decision decoding when the signal was transmitted over a slow, flat fading Nakagami channel for additive white Gaussian noise (AWGN) only, as well as for AWGN plus pulse-noise interference (PNI). The implementation of forward error correction (FEC) coding with soft decision decoding (SDD) improves the performance compared to uncoded signal if pulse-noise interference is not present. The scenarios when no side information is available (linear-combining receiver), when perfect side information is available (noise-normalizing receiver), and two alternatives to the noise-normalized receiver with much coarser side information (modified noise-normalized receiver and noise-normalized receiver with normalization error) are examined. All the scenarios are examined for various fading and interference conditions. The performance of the noise-normalized receiver is, as expected, much improved compared to the linear-combining receiver when PNI is present. Finally, the noise-normalized receiver with normalization error achieves the same or better performance than the noise-normalized receiver without the exact interference noise power.

THIS PAGE INTENTIONALLY LEFT BLANK

TABLE OF CONTENTS

THIS PAGE INTENTIONALLY LEFT BLANK

LIST OF FIGURES

THIS PAGE INTENTIONALLY LEFT BLANK

LIST OF TABLES

THIS PAGE INTENTIONALLY LEFT BLANK

ACKNOWLEDGMENTS

This thesis is dedicated to my Father who passed away three years ago. He was a teacher, and he always used to say that the major goal of studying is not the knowledge, but to learn thinking. When you know how to think, you can find the knowledge anywhere.

I also wish to dedicate this thesis to my thoughtful Mother, who taught me the values of education, diligence and conscientiousness, and all my relatives in the U.S., but especially my cousin Maria, who helped me have a good time the last two years.

I would like to express my sincere appreciation to my advisors Professor Clark Robertson and Professor David Jenn. Without their support, coupled with clear explanations and supervision, this thesis would not have been possible.

Lastly, I must thank the Hellenic Navy for providing an opportunity for me to pursue my postgraduate study here at the Naval Postgraduate School.

THIS PAGE INTENTIONALLY LEFT BLANK

EXECUTIVE SUMMARY

The performance of *IEEE* 802.11*g* wireless local area network (WLAN) standard compliant receivers for signals transmitted over slow, flat fading channels with pulse-noise interference (PNI) was examined in this thesis. This standard specifies orthogonal frequency-division multiplexing (OFDM) in order to overcome fading caused by multipath propagation due to reflections, diffractions, and scattering processes and, at the same time, achieve high data rates. The Nakagami-*m* distribution was used to model different fading conditions. The performance of four different receivers that implement forward error correction (FEC) coding with soft decision decoding (SDD) in order to improve the performance compared to uncoded signal were investigated.

We first examined the performance of the linear-combining receiver, which is designed to operate without the need for side information. In other words, the amplitude fluctuations of the received signal and the noise power that corrupts every received bit are not known. The linear-combining receiver with additive white Gaussian noise in a fading channel was investigated. We also examined the case of PNI for both non fading channels as well as for fading channel.

We then analyzed the performance of a receiver which required side information. In this case, the exact noise power for every received bit was assumed known. This receiver, named noise-normalized receiver, normalizes the received bits with the noise power. It is found that noise-normalization significantly improves the performance of the receiver in a fading channel for small E_b/N_i (signal-to-interference ratio), something that does not happen for large E_b/N_i.

The next topic considered was the modified noise-normalized receiver. A major problem that the designer of the noise-normalized combining receiver has to face is the difficulty in measuring the power of the jammer in real time in order to use it as side information for the receiver. The modified noise-normalized receiver was proposed in order to overcome this difficulty. Instead of the exact interference power, a multiple of

the AWGN is used. When interference is detected, generally, for small values of E_b/N_i, this receiver has better performance than the linear-combining receiver.

The last topic examined was the noise-normalized receiver with normalization error. When the interference power is overestimated, the performance of the receiver is better than the performance of the noise-normalized receiver with perfect interference power estimation. Summarizing, our analysis indicates that the noise-normalized receiver results in the best performance in PNI.

I. INTRODUCTION

A. BACKGROUND

The rapidly growing demand for reliable wireless communications has led to a great deal of research on wireless local networks (WLAN). The most promising wireless communication standard today is *IEEE* 802.11, which was adopted by the Standard of the Institute of Electrical and Electronics Engineers in 1997. This standard provides for three physical layer (PHY) specifications including infrared 1-2 Mbps frequency-hopping spread spectrum (FHSS) and 1-2 Mbps direct sequence spread spectrum (DSSS) in the 2.4 GHz ISM band. Since its introduction, three more offshoots of this standard have been adopted.

The first one was in 1999 and was designated as *IEEE* 802.11*b*. The *IEEE* 802.11b specification increased data rates well beyond 10 Mbps, maintained compatibility with the original 802.11 DSSS standard, and incorporated a modulation scheme known as complimentary code keying (CCK) to attain a top-end data rate of 11 Mbps. A second scheme, called packet binary convolutional code (PBCC), was included as an option for performance at rate of either 5.5 or 11 Mpbs.

The second offshoot of 802.11 was designated as 802.11*a*. It utilized a different frequency band, the 5.2 GHz U-NII band, and was specified to achieve data rates up to 54 Mbps. Unlike 802.11b, which is a single carrier system, 802.11*a* utilized a multi-carrier modulation technique known as orthogonal frequency-division multiplexing (OFDM) [1]. By utilizing the 5.2 GHz radio spectrum, 802.11*a* is not interoperable with either 802.11*b* or the initial 802.11 WLAN standard. In March 2000, the *IEEE* 802.11 Working Group formed a study group to explore the feasibility of establishing an extension to the 802.11*b* standard for data rates greater than 20 Mbps. In July 2000, this study group became a full task group, Task Group G (TG *g*), with a mission to define the next standard for higher data rates in the 2.4 GHz band.

In November 2001, the 802.11*g* standard was submitted. The 802.11*g* draft standard utilizes existing elements from the original CCK-OFDM and PBCC-22 proposals. The 802.11*g* draft standard makes OFDM a mandatory technology, offering

802.11*a* data rates in the 2.4 GHz band, requires mandatory implementation of 802.11*b* modes, and offers optional modes of CCK-OFDM and PBCC-22. The *IEEE* 802.11g standard achieves the 54 Mbps data rates of 802.11*a* in the 2.4 GHz band, thereby maintaining compatibility with installed 802.11*b* equipment [2].

B. OBJECTIVE

A continuing issue for modern digital communication systems is how to immunize the receiver against the negative effects of narrowband interference and other types of noise that may be present in addition to additive white Gaussian noise (AWGN). Numerous papers have been written on the subject of reducing the effects of narrowband noise that affects some of the received bits (or chips, as the case may be) but not others, such as occurs for a fast frequency-hopped system with diversity when partial-band noise interference is present or for a direct sequence spread spectrum system or a conventional, non-spread spectrum system with forward error correction coding when pulse-noise interference is present. One technique that works quite well in conjunction with soft decision demodulation is noise-normalization combining, which effectively eliminates the negative effects of pulse-noise interference or partial-band noise interference in either direct sequence spread spectrum systems and conventional, non-spread spectrum systems with forward error correction coding or fast frequency-hopped systems with diversity, respectively [3, 4, 5, 6]. The problem with noise-normalization combining is that it requires a real-time estimate of the received noise power for each bit, which may be impractical to implement. A technique that has been suggested to side-step this problem is self-normalization combining, which works quite well to eliminate the negative effects of partial-band noise interference in fast frequency-hopped systems with diversity and does not require a real-time estimate of the received noise power for each bit [7, 8, 9]. Instead, the received signal itself is used to provide the required normalization. The chief drawback to self-normalization is that, while it works quite well for *M*-ary frequency-shift keyed (*M*FSK) waveforms, it cannot be implemented for binary phase-shift keyed (BPSK) waveforms.

In this thesis, the performance of a system utilizing a BPSK waveform transmitted over a frequency-selective, slowly fading Nakagami channel with pulse-noise interference in addition to AWGN is examined. The underlying information bits are assumed to be convolutionally encoded prior to transmission over the channel, and the receiver is assumed to use soft decision Viterbi decoding with modified noise-normalization of the soft receiver output. This waveform corresponds to that specified for the 6 Mbps data rate by both the IEEE 802.11*a* and *g* OFDM standards. Two modifications of noise-normalized combining are considered. In the first, when interference power is determined to be present, the normalization factor is taken to be four or more times the noise power of AWGN alone, thus providing a deemphasis of bits that are affected by the pulse-noise interference that relies only on a measurement of the relative noise power instead of an exact measurement of the noise power for a particular bit. The idea is to examine a modification of noise-normalized combining that does not require an accurate, real-time estimate of the noise power received for each bit, making implementation much more practical. In the second, the interference power present during a bit is multiplied by some factor prior to normalization, providing the means to determine the effect of either underestimating or overestimating the interference noise power on receiver performance. If receiver performance does not suffer significant degradation when the noise power estimate for each bit is poor, then implementation of the noise-normalized receiver is much more practical than if an accurate noise power estimate is required to effectively eliminate degradation due to pulse-noise interference. In either case, it is assumed that an accurate measure of the AWGN power is available.

THIS PAGE INTENTIONALLY LEFT BLANK

II. REVIEW OF THEORY

A. INTRODUCTION

Both *IEEE* 802.11*a* and *IEEE* 802.11*g* specify OFDM in order to achieve high data rates over the frequency-selective channel. Forward error correction coding (FEC) and Viterbi soft decision decoding (SDD) are implemented in order to achieve reliable communications. The fading channel is modeled as a Nakagami fading channel.

B. ORTHOGONAL FREQUENCY-DIVISION MULTIPLEXING (OFDM)

OFDM is a special case of multicarrier transmission, where a single data stream is transmitted over a number of subcarriers. OFDM can be seen as either a modulation technique or a multiplexing technique. One of the main reasons to use OFDM is to minimize the effect of the frequency-selective channel. In a single carrier system, a high data rate signal might cause the channel to be frequency selective, but in a multicarrier system, the data rate on each subcarrier is much lower than the overall data rate and the channel for each subcarrier is flat, or frequency non-selective.

In a classical parallel data stream, the total single frequency band is divided into N non-overlapping frequency subchannels. Each subchannel is modulated with a different data stream, and the N subchannels are frequency-multiplexed. It is best to avoid spectral overlap of channels to eliminate interchannel interference; however, this leads to inefficient use of the available spectrum. To minimize this inefficiency, the idea is to use parallel data and FDM with overlapping subchannels in which each subcarrier has a signaling rate R and is spaced R Hz apart in frequency to fully utilize the available bandwidth.

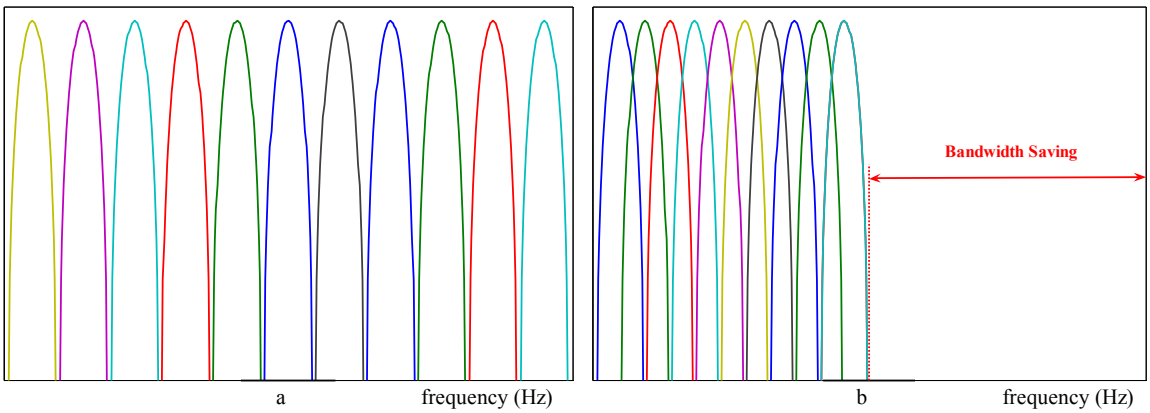

Figure 1. Concept of OFDM signals: (a) Conventional multicarrier technique; (b) Orthogonal multicarrier modulation technique.

Figure 1 illustrates the difference between a conventional, non-overlapping multicarrier technique and the overlapping multicarrier technique. As shown in Figure 1, by using the overlapping multicarrier modulation technique, we save almost 50% of the bandwidth. To realize the overlapping technique, however, we need to reduce crosstalk between subcarriers, which means we require orthogonality between the different modulated carriers.

The word orthogonal indicates that there is a precise mathematical relationship between the frequencies of the carriers in the system. In a normal frequency-division system, many carriers are spaced apart in such a way that the signals can be received using conventional filters and demodulators. In such receivers, guard bands are introduced between the different carriers and in the frequency domain which results in a lowering of spectral efficiency.

It is possible, however, to arrange the carriers in an OFDM signal so that the sidebands of the individual carriers overlap and the signals are still received without adjacent carrier interference. To do this the carriers must be mathematically orthogonal. The receiver acts as bank of demodulators, translating each carrier down to baseband, with the results integrated over a symbol period to recover data. If the other carriers all down convert to a frequency that, in the time domain, has an integer number of cycles in

the symbol period T_s, then the integration process results in a zero contribution from all the other carriers. Thus, the carriers are linearly independent if the carrier spacing is a multiple of $1/T_s$ Hz.

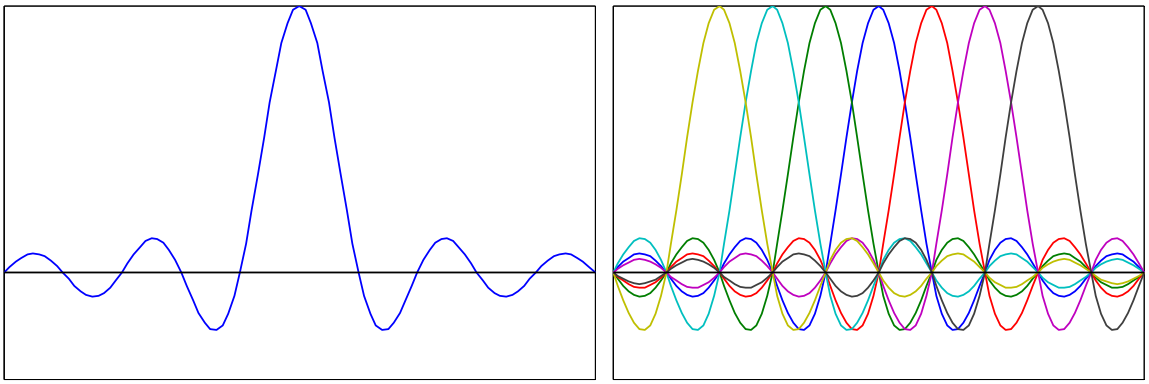

Figure 2. Spectrum of (a) an OFDM subchannel and (b) an OFDM signal.

OFDM utilizes the discrete Fourrier transform (DFT) as part of the modulation and demodulation process. In Figure 2a we see the spectrum of an individual subchannel. The OFDM signal, with the individual spectra multiplexed with a frequency spacing R Hz, equal to the transmission speed of each subcarrier, is shown in Figure 2b. Figure 2b shows that at the center frequency of each subcarrier there is no interference from other channels. Therefore, if we use a DFT at the receiver and calculate correlation values with the center of the frequency of each subcarrier, we recover the transmitted data with no crosstalk.

The OFDM transmission scheme has the following key advantages [10]:

- OFDM is an efficient way to deal with multipath for a given delay spread; the implementation complexity is significantly lower than that of a single carrier system with an equalizer.
- OFDM is robust against narrowband interference because such interference affects only a small percentage of the subcarriers.

- OFDM makes single-frequency networks possible, which is especially attractive for broadcast applications.

On the other hand, OFDM also has some drawbacks compared with single carrier modulation:

- OFDM is more sensitive to frequency offset and phase noise.
- OFDM has relatively large peak-to-average power ratio, which tends to reduce the power efficiency of the RF amplifier.

C. MULTIPATH CHANNELS

IEEE 802.11 is a WLAN standard designed to operate in a variety of environmental link conditions, from line-of-sight (LOS) to obstructed line-of-sight (OLOS) and non-line-of-sight (NLOS). This results from the inherent capability of OFDM technology to overcome multipath phenomena, which is typical for NLOS links. *Multipath propagation phenomena* is the propagation phenomena that a signal will arrive at the receiver multiple times with different amplitudes, phases and arrival times due to reflection of the original signal off of buildings, terrain features, the ionosphere or troposphere and so on.

In the frequency domain, this results in different spectral components of the signal being affected differently by the channel, thus the frequency response of the channel is not flat over the bandwidth of the channel which results in distortion to the received signal. The number of multiple paths and their characteristics such as attenuation and propagation delay will differ from one multipath channel to the other.

Another characteristic of a multipath channel is that it is time-varying. Thus, if an identical pulse is transmitted at a later time, a different number of pulses with different amplitudes, phases and arrival times will be received as compared to that received the first time.

In order to classify the time characteristics of the channel, the coherence time or the Doppler spread are important parameters. The coherence time is the time duration over which the channel characteristics do not change significantly. The time variation of

the channel is evidenced as a Doppler spread in the frequency domain, which is determined as the width of the spectrum when a single sinusoid (constant envelope) is transmitted. The time correlation function $\varphi_c(\Delta t)$ and the Doppler power spectrum $S_c(f)$ are related to each other by the Fourier transform [11].

The range of values of the frequency f over which $S_c(f)$ is essentially nonzero is called the Doppler spread B_d of the channel. Because $S_c(f)$ is related to $\varphi_c(\Delta t)$ by the Fourier transform, the reciprocal of B_d is a measure of the coherence time $(\Delta t)_c$ of the channel [11], that is:

$$(\Delta t)_c = \frac{1}{B_d} \tag{2.1}$$

The coherence time is a measure of the width of the time correlation function. A slowly-changing channel has a large coherence time, or equivalently a small Doppler spread. The rapidity of the fading can be determined either from the correlation function $\varphi_c(\Delta t)$ or from the Doppler power spectrum $S_c(f)$. If the symbol duration T_s is large compared to the coherence time, then the channel is subject to fast fading and the channel is said to be a fast fading channel. On the contrary, if the symbol duration T_s is small compared to the coherence time, then the channel is not subject to fast fading and the channel is said to be a slowly fading channel.

Another categorization of the communication channel is whether it is a frequency-selective or a flat fading channel. The range of τ over which the correlation function $\varphi_c(\tau)$ is nonzero is called *multipath spread* of the channel, T_m, and the range of Δf over which the Doppler power spectrum $S_c(\Delta f)$ is greater than some defined value is the *coherence bandwidth* of the channel $(\Delta f)_c$ where [11]:

$$(\Delta f)_c \approx \frac{1}{T_m} \tag{2.2}$$

The channel is characterized by comparing the noise equivalent bandwidth of the signal to the coherence bandwidth. If the noise equivalent bandwidth is greater than the

coherence bandwidth, then the signal faces significant distortion and the channel is said to be *frequency-selective*:

$$W > (\Delta f)_c \tag{2.3}$$

If the noise equivalent bandwidth is less than the coherence bandwidth, all the frequency components of the signal are affected equally by the channel and the channel is said to be *frequency-nonselective* or *flat fading*:

$$W < (\Delta f)_c \tag{2.4}$$

According to the *IEEE* 802.11*g* standard, the data are divided into 48 low-data rate subcarriers and transmitted in parallel. As a result, the symbol duration of each data subcarrier is significantly smaller than the symbol duration and therefore, the subcarrier's symbol duration is sufficiently small compared to the channel coherence time to be considered slowly fading. In the same way, the bandwidth of each data subcarrier is significantly smaller than the system bandwidth and, therefore, the subcarrier's bandwidth is sufficiently small compared to the coherence bandwidth to be assumed flat fading [2].

D. NAKAGAMI FADING MODEL

The probability of bit error for all digital modulation techniques can be expressed as a function of the average signal energy per symbol:

$$E_s = A_c^2 T_s \tag{2.5}$$

where $\sqrt{2}A_c$ is the amplitude of the received signal.

For a non-fading channel, E_s is simply a parameter, but for the case of a fading channel, the signal energy fluctuates, and the signal energy cannot be modeled as a parameter but must be modeled as a random variable.

The distribution we used to model the fading channel is the Nakagami distribution, where the amplitude of the received signal α_c is modeled as a Nakagami-*m* random variable.

The *probability density function* (PDF) for the Nakagami random variable is

$$f_{A_c}(\alpha_c) = \frac{2}{\Gamma(m)}\left(\frac{m}{\Omega}\right) a_c^{2m-1} e^{-\frac{ma_c}{\Omega}} \tag{2.6}$$

where Γ(m) is the Gamma function defined as

$$\Gamma(m) = \int_0^\infty t^{m-1} e^{-t}\, dt \tag{2.7}$$

and Ω is defined as

$$\Omega = E[A_c^2] \tag{2.8}$$

The parameter *m*, the fading figure, is defined as

$$m = \frac{\Omega^2}{E[(A_c^2 - \Omega)^2]}, \qquad m \geq \frac{1}{2} \tag{2.9}$$

The Nakagami–*m* PDF is determined by two parameters: the parameter *m* and the second moment Ω. As a consequence, this PDF provides more flexibility and accuracy in modeling the observed signal statistics than other distributions. The Nakagami-*m* distribution can be used to model fading channel conditions that are either more or less severe than the Rayleigh distribution and includes the Rayleigh distribution as a special case (*m*=1). For small values of *m* (i.e., $0.5 \leq m \leq 1$), the fading conditions are severe, while for larger values of *m* the fading conditions are less severe. As $m \to \infty$, no fading is present. The Nakagami-*m* distribution is the best fit for a signal received over an urban radio multipath channel [11].

In Figure 3, we see the Nakagami-*m* distribution for different values of *m*.

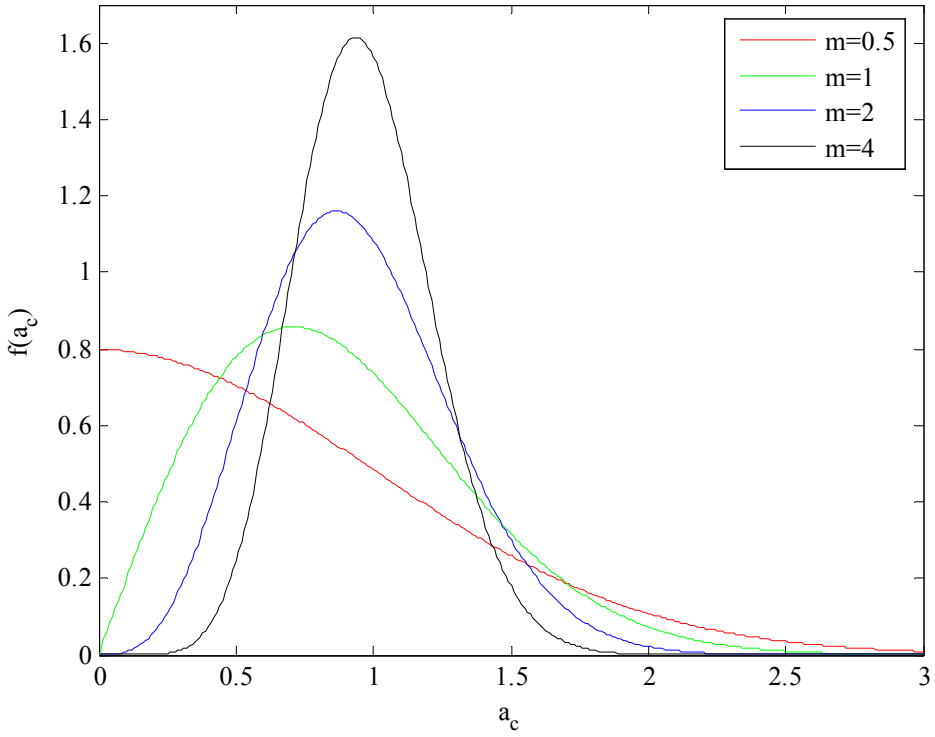

Figure 3. The Nakagami-*m* PDF.

E. WAVEFORM CHARACTERISTICS

1. Subcarrier Modulation Types

For subcarrier modulation, the *IEEE* 802.11*g* standard specifies BPSK, QPSK, 16QAM and 64QAM. These modulation types belong to the category of bandwidth efficient modulation schemes. One of the major problems all communication standards have to overcome is the lack of sufficient bandwidth.

2. Data Error Correction Management

As with most of the modern digital communication systems, error correction coding is utilized. The reason for this is to reduce errors that occur as a consequence of transmission over a noisy, fading channel and, thus, increase the integrity of the channel. The use of varying data rates is accommodated by the use of various code rates in combination with different modulation techniques as shown in Table 1. This allows the *IEEE* 802.11*g* transmitter to select the modulation scheme, which, when combined with

correct code rate, allows the highest reliable data rate for the signal-to-noise ratio (SNR) at the time of the communication.

Table 1. Code rates and modulation techniques for various data rates [From Ref. 6].

Data rate (Mbits/s)	Modulation	Coding rate (R)	Coded bits per subcarrier (N_{BPSC})	Coded bits per OFDM symbol (N_{CBPS})	Data bits per OFDM symbol (N_{DBPS})
6	BPSK	1/2	1	48	24
9	BPSK	3/4	1	48	36
12	QPSK	1/2	2	96	48
18	QPSK	3/4	2	96	72
24	16-QAM	1/2	4	192	96
36	16-QAM	3/4	4	192	144
48	64-QAM	2/3	6	288	192
54	64-QAM	3/4	6	288	216

3. Forward Error Correction (FEC)

The *IEEE* 802.11*a* standard uses a convolutional encoder with the industry-standard generator polynomials $g_0 = 133_8$ and $g_1 = 171_8$. A k/n convolutional code produces *n* coded bits for each *k* data bits, where each set of *n* coded bits is determined by the *k* data bits and between $(\nu - 1)$ and $k(\nu - 1)$ of the preceding data bits. The parameter ν is the constraint length of the convolutional code, and the code rate is $r = k/n$. A general convolutional encoder can be implemented with *k* shift-registers and *n* modulo-2 adders. Higher rates can be derived from lower rate codes by employing "puncturing." Puncturing is a procedure for omitting some of the encoded bits in the transmitter (thus reducing the number of transmitted bits and increasing the code rate) and inserting a dummy "zero" metric into the convolutional decoder on the receive side in place of the omitted bits [6]. The *IEEE* 802.11*a* and *g* standards specify the convolutional encoder shown in Figure 4.

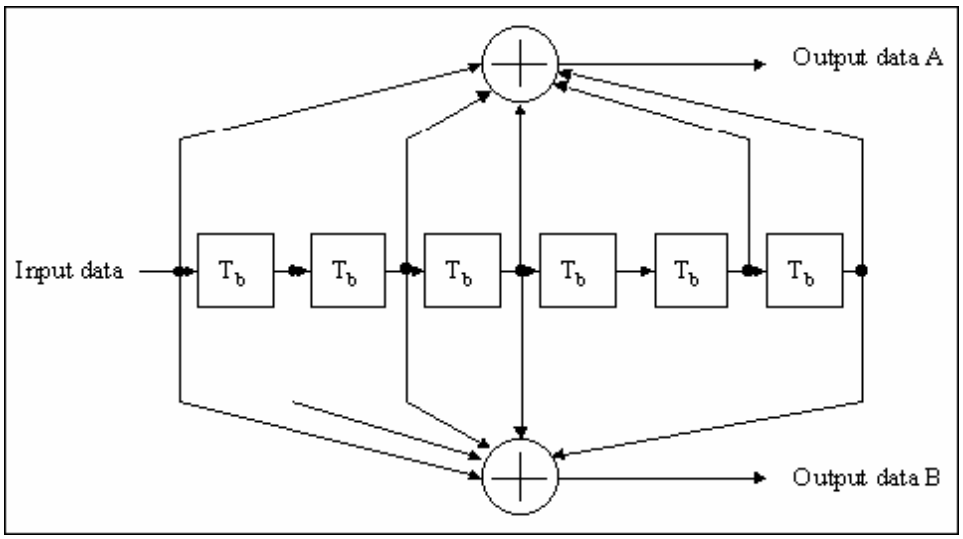

Figure 4. The convolutional encoder with industry standard generator polynomials $g_o = 133_8$ and $g_1 = 171_8$ with constraint length ν=7 [From Ref. 6].

4. Viterbi Decoding

The data decoding at the receiver is performed via the Viterbi decoding algorithm. The Viterbi algorithm is used to determine the maximum-likelihood code sequence associated with a given received sequence. The Viterbi algorithm chooses the path through the convolutional code trellis which differs from the received sequence in the fewest places in order to decode the encoded data. The Viterbi algorithm computes path metrics for all possible paths through the trellis and selects the path with the best metric.

The *IEEE* 802.11*g* standard specifies 3-bit soft decision decoding (SDD) at the receiver. As a result, eight decision regions are specified for the received signal for both the inphase and the quadrature components of the signal. For example, for a binary signal, instead of simply assigning a "one" or a "zero," there are four decision regions for the "one" and four for the "zero."

An exact expression for the probability of bit error (P_b) cannot be derived, but a widely accepted upper bound is [11]

$$P_b < \frac{1}{k} \sum_{d=d_{free}}^{\infty} B_d P_d \tag{2.10}$$

where k is the number of information bits encoded per clock cycle, d is the weight of the path, d_{free} is the minimum Hamming distance between all pairs of non-zero convolutional code sequences, B_d is the sum of all possible bit errors that can occur when a path a distance d from the correct path is selected, and P_d represents the probability that the decoder will select a path a distance d from the correct path.

The values of B_d generally are determined by computer search. The values of B_d are shown for the codes specified by the *IEEE* 802.11*g* standard in Table 2.

Table 2. Weight structure for the best $r = 1/2$ and punctured $r = 2/3$ and $r = 3/4$ convolutional FEC [After Ref. 6].

Rates	d_{free}	$B_{d_{free}}$	$B_{d_{free}+1}$	$B_{d_{free}+2}$	$B_{d_{free}+3}$	$B_{d_{free}+4}$
r=1/2	10	36	0	211	0	1404
r=2/3	6	3	81	402	1487	6793
r=3/4	5	42	252	1903	11995	72115

F. SUMMARY

In this chapter, we discussed OFDM and the reasons this type of multiplexing was specified by IEEE 802.11*g*. Then we discussed the effects of multipath channels on a communication system. We also addressed the Nakagami fading model and explained the reasons it was selected to model the fading channel. Finally, we introduced the waveform characteristics, such as the subcarrier modulation types, and the data error correction management, FEC and Viterbi decoding.

In the next chapter we present the linear-combining receiver and its performance over frequency-selective, slowly fading Nakagami channels in an AWGN plus pulse-noise interference environment with Viterbi soft decision decoding.

THIS PAGE INTENTIONALLY LEFT BLANK

III. PERFORMANCE ANALYSIS OF OFDM SIGNALS TRANSMITTED OVER FREQUENCY-SELECTIVE, SLOWLY FADING NAKAGAMI CHANNELS IN AN AWGN PLUS PULSE-INTERFERENCE ENVIRONMENT WITH LINEAR COMBINING AND VITERBI SOFT DECISION DECODING (SDD)

In this chapter the performance of OFDM signals transmitted over frequency-selective, slowly fading Nakagami channels in an AWGN plus pulse-interference environment with a linear-combining receiver is examined. This receiver was examined by Christos Kalogrias in [12] is examined here in order to compare the performance of the linear-combining receiver with the performance of the receivers considered in later chapters.

A. THE LINEAR-COMBINING RECEIVER

The linear-combining receiver (LC) examined in this chapter is designed to operate without the need for side information. In other words, the amplitude of the received signal and the noise power that corrupts every received bit are not known.

The linear-combining receiver for BPSK modulation with soft decision Viterbi decoding is equivalent to Figure 5 for the purpose of finding P_d.

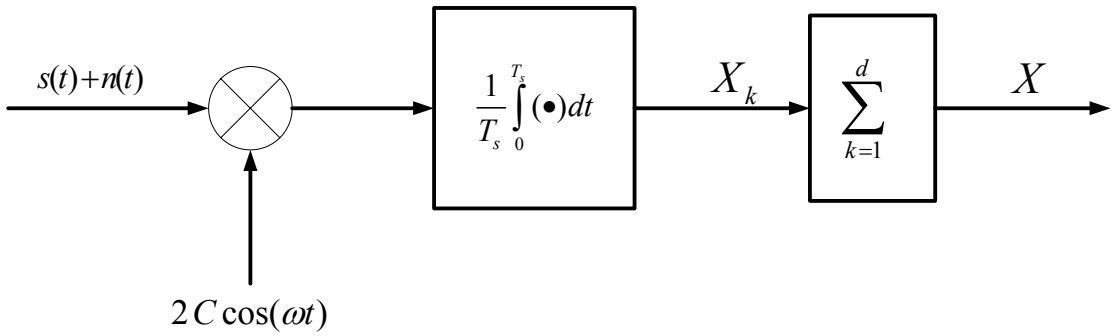

Figure 5. The linear-combining receiver.

At the input of the receiver is the desired signal $\sqrt{2}a_c d(t)\cos(\omega_c t)$ and the AWGN, where a_c represents the amplitude of the received signal, $d(t)$ the baseband

information waveform, T_s the time duration of a symbol, and ω_c is the frequency of the sub-carrier signal. At the input of the receiver, the signal is corrupted by the noise $n(t)$.

The integrator's output X_k represents those sequence bits that have been affected in a random way by the channel can be modelled as Gaussian random variables (GRV). The PDFs of these random variables are

$$f_{X_k}(x_k/1) = \frac{1}{\sqrt{2\pi}\sigma_k} e^{\left[-\frac{(x_k-\sqrt{2}a_c)^2}{2\sigma_k^2}\right]} \tag{3.1}$$

for a bit "1" and

$$f_{X_k}(x_k/0) = \frac{1}{\sqrt{2\pi}\sigma_k} e^{\left[-\frac{(x_k+\sqrt{2}a_c)^2}{2\sigma_k^2}\right]} \tag{3.2}$$

for bit "0." The mean and the variance of these GRVs at the output of the integrator are, respectively,

$$\overline{X_k} = \sqrt{2}Ca_c \tag{3.3}$$

and

$$\sigma_{x_k}^2 = C^2\sigma_k^2 \tag{3.4}$$

The probability P_d, if the decision statistic is modelled as GRV, is [11]

$$P_d = Q\left(\frac{\overline{X}}{\sigma_x}\right) = Q\left(\sqrt{\frac{\left(\overline{X}\right)^2}{\sigma_x^2}}\right) \tag{3.5}$$

where $\overline{X}$ and σ_x are the mean and the variance, respectively, of the decision statistic X shown in Figure 5.

B. PERFORMANCE ANALYSIS IN A FADING CHANNEL WITH AWGN

The performance of the linear-combining receiver for a signal transmitted over a fading channel with AWGN and with soft decision Viterbi decoding is now examined. Since the signal $s(t)$ is assumed to be transmitted over a flat, slowly-fading Nakagami channel, the amplitude of the signal $s(t)$ is modeled as a Nakagami-*m* random variable with PDF given by Equation (2.6). At the input of the receiver, the signal $s(t)$ is corrupted by the AWGN channel with power spectral density (PSD) $N_o/2$. Hence, the received signal is equal to $s(t)+n(t)$ and is multiplied by $2C\cos(\omega_c t)$ by the local oscillator.

Because of the multipath channel, each bit of the received signal may be affected differently, and the received amplitude of the received signal a_c may differ from bit to bit.

We now assume that the constant *C* is equal to one. Since the signal X_k can be modeled as a GRV, the mean and the variance are:

$$\overline{X_k} = \sqrt{2}a_c \tag{3.6}$$

and

$$\sigma_{x_k}^2 = \sigma_k^2 \tag{3.7}$$

Since the receiver is subject only to AWGN, we assume that each bit is corrupted by the same amount of noise power, $\sigma_o^2 = N_o/T_s$. Therefore, Equation (3.7) can be rewritten as

$$\sigma_{x_k}^2 = \sigma_o^2 \tag{3.8}$$

The decision variable for the sequence of *d* bits is the summation of *d* independent, random variables

$$X = \sum_{k=1}^{d} X_k \tag{3.9}$$

Hence, the random variable X is also a GRV with mean and variance

$$\overline{X} = \sqrt{2}\sum_{k=1}^{d} a_c \tag{3.10}$$

and

$$\sigma_x^2 = \sum_{k=1}^{d} \sigma_o^2 = d\sigma_o^2 \tag{3.11}$$

The upper bound on the probability of bit error is given by Equation (2.10) and, using the weight structure as specified at Table 2, the upper bound can be rewritten as

$$P_b < \frac{1}{k} \sum_{d=d_{free}}^{d_{free}+4} B_d P_d \tag{3.12}$$

where the probability P_d is given in Equation (3.5). Substituting (3.10) and (3.11) into (3.5), we get

$$P_d\left(\sum_{k=1}^{d} a_c\right) = Q\left(\sqrt{\frac{2}{d}} \frac{\sum_{k=1}^{d} a_c}{\sigma_o}\right) = Q\left(\sqrt{\frac{2}{d}} \sum_{k=1}^{d} \frac{a_c}{\sigma_o}\right) \tag{3.13}$$

We can express the conditional probability P_d with linear-combining as

$$P_d\left(\gamma_b\right) = Q\left(\sqrt{\frac{2}{d}}\gamma_b\right) \tag{3.14}$$

where

$$\gamma_b = \sum_{k=1}^{d} \gamma_{b_k} = \sum_{k=1}^{d} \frac{a_c}{\sigma_o} \tag{3.15}$$

In order to obtain the unconditional probability of a weight-*d* output sequence, we have to calculate the integral

$$P_d = \int_0^{\infty} P_d(\gamma_b) f_{\Gamma_b}(\gamma_b) d\gamma_b \tag{3.16}$$

where $f_{\Gamma_b}(\gamma_b)$ is the PDF of the random variable γ_b given by Equation (3.15).

In order to evaluate $f_{\Gamma_b}(\gamma_b)$, we need first to evaluate $f_{\Gamma_{b_k}}(\gamma_{b_k})$. This can be done by a change of variables

$$f_{\Gamma_{b_k}}(\gamma_{b_k}) = \left|\frac{da_c}{d\gamma_{b_k}}\right| f_{A_c}(a_c)\Big|_{a_c=\gamma_{b_k}\sigma_o} \tag{3.17}$$

where $f_{A_c}(a_c)$ is the Nakagami-*m* PDF as defined in Equation (2.6) and Ω is given by Equation (2.8).

Substituting Equation (2.6) into (3.17), we have

$$\begin{aligned} f_{\Gamma_{b_k}}(\gamma_{b_k}) &= \sigma_o \frac{2}{\Gamma(m)}\left(\frac{m}{\overline{a_c^2}}\right)^m \left(\gamma_{b_k}\sigma_o\right)^{2m-1} \exp\left(-\frac{m\left(\gamma_{b_k}\sigma_o\right)^2}{\overline{a_c^2}}\right) \\ &= \frac{2}{\Gamma(m)}\left(\frac{m\sigma_o^2}{\overline{a_c^2}}\right)^m \left(\gamma_{b_k}\right)^{2m-1} \exp\left(-\frac{m\gamma_{b_k}^2\sigma_o^2}{\overline{a_c^2}}\right) \end{aligned} \tag{3.18}$$

If we substitute $\overline{\gamma_b} = \frac{\sigma_o^2}{\overline{a_c^2}}$ into Equation (3.18) we get

$$f_{\Gamma_{b_k}}(\gamma_{b_k}) = \frac{2}{\Gamma(m)}\left(m\overline{\gamma_b}\right)^m \left(\gamma_{b_k}\right)^{2m-1} e^{\left(-m\gamma_{b_k}^2\overline{\gamma_b}\right)} \tag{3.19}$$

where

$$\overline{\gamma_b} = \frac{\sigma_o^2}{\overline{a_c^2}} = \frac{N_o}{T_s\overline{a_c^2}} = \frac{N_o}{rT_b\overline{a_c^2}} = \frac{1}{r}\frac{N_o}{E_b} = \frac{1}{r}\left(\frac{E_b}{N_o}\right)^{-1} \tag{3.20}$$

Now that we have $f_{\Gamma_{b_k}}(\gamma_{b_k})$, we must find $f_{\Gamma_b}(\gamma_b)$. Since $\gamma_b = \sum_{k=1}^{d}\gamma_{b_k}$, then the PDF of the sum of *d* independent random variables is given by the *d*-fold convolution of the PDFs of the d random variables [12]. This evaluation cannot be done analytically in this case, so a numerical evaluation is required. In order to evaluate $f_{\Gamma_b}(\gamma_b)$ numerically, we take the advantage of the properties of the Laplace transform. As is well known, the

Laplace transform $L\{\square\}$ of the convolution of d functions is equal to the product of the Laplace transforms of the PDFs of each variable. Hence,

$$L\{X_1 \otimes X_2 \otimes ... \otimes X_d\} = L\{X_1\} \times L\{X_2\} \times ... \times L\{X_d\} \tag{3.21}$$

Thus, if we evaluate the Laplace transform for each $f_{\Gamma_{b_k}}(\gamma_{b_k})$, multiply the result d times, and inverse Laplace transform the overall result, we obtain the desired $f_{\Gamma_b}(\gamma_b)$. The Laplace transform of $f_{\Gamma_{b_k}}(\gamma_{b_k})$ is:

$$F_{\Gamma_{b_k}}(\gamma_{b_k}) = L\left\{f_{\Gamma_{b_k}}(\gamma_{b_k})\right\} = \int_0^\infty f_{\Gamma_{b_k}}(\gamma_{b_k}) e^{-s\gamma_{b_k}} d\gamma_{b_k} \tag{3.22}$$

and the resulting Laplace transform of $f_{\Gamma_b}(\gamma_b)$ is

$$F_{\Gamma_b}(\gamma_b) = \left[L\left\{f_{\Gamma_{b_k}}(\gamma_{b_k})\right\}\right]^d = \left[F_{\Gamma_{b_k}}(\gamma_{b_k})\right]^d = \left[\int_0^\infty f_{\Gamma_{b_k}}(\gamma_{b_k}) e^{-s\gamma_{b_k}} d\gamma_{b_k}\right]^d \tag{3.23}$$

If we substitute (3.19) into (3.22), we get

$$F_{\Gamma_{b_k}}(\gamma_{b_k}) = \frac{2}{\Gamma(m)}\left(m\overline{\gamma_b}\right)^m \int_0^\infty \left(\gamma_{b_k}\right)^{2m-1} e^{-\left(s\gamma_{b_k} + m\overline{\gamma_b}\gamma_{b_k}^2\right)} d\gamma_{b_k} \tag{3.24}$$

Substituting Equations (3.24) into Equation (3.23), we finally have

$$F_{\Gamma_b}(\gamma_b) = \left(\frac{2}{\Gamma(m)}\left(m\overline{\gamma_b}\right)^m \int_0^\infty \left(\gamma_{b_k}\right)^{2m-1} e^{-\left(s\gamma_{b_k} + m\overline{\gamma_b}\gamma_{b_k}^2\right)} d\gamma_{b_k}\right)^d \tag{3.25}$$

A convenient way to calculate inverse Laplace transform of $F_{\Gamma_b}(\gamma_b)$ is described in Appendix A of [Ref 12], where

$$f_{\Gamma_b}(\gamma_b) = \frac{ce^{c\gamma_b}}{\pi} \int_0^{\frac{\pi}{2}} \left[\begin{array}{l} \mathrm{Re}\left\{F_{\Gamma_b}\left(c + jc\tan(\phi)\right)\right\}\cos\left(c\gamma_b \tan(\phi)\right) \\ \quad -\mathrm{Im}\left\{F_{\Gamma_b}\left(c + jc\tan(\phi)\right)\right\}\sin\left(c\gamma_b \tan(\phi)\right) \end{array}\right] \sec^2(\phi) d\phi \tag{3.26}$$

and c must be in the strip of convergence of $F_{\Gamma_b}(\gamma_b)$.

With the use of Equations (3.14), (3.16), (3.25), (3.12), and (3.26), we can now calculate the probability of bit error of the linear-combining receiver with AWGN over a flat, slowly-fading Nakagami channel. For the *IEEE* 802.11*g* standard, data rates of 6 and 12 Mbps are specified as BPSK and QPSK, respectively, where the code rate is $r = 1/2$ and B_d and d_{free} are specified in Table 2. The upper bound on P_b is plotted in Figure 6 as a function of the SNR at the receiver for different values of the parameter *m*. From Figure 6 we see that as the parameter *m* increases the receiver's performance decreases. In other words, as the fading conditions get less severe, the performance improves. As we see for $P_b = 10^{-4}$, the difference in required E_b/N_o between *m*=0.5 and *m*=1 is 4.2 dB, while the difference between *m*=1 and *m*=2 is 2.1 dB, and the difference between *m*=2 and *m*=4 is 0.8 dB.

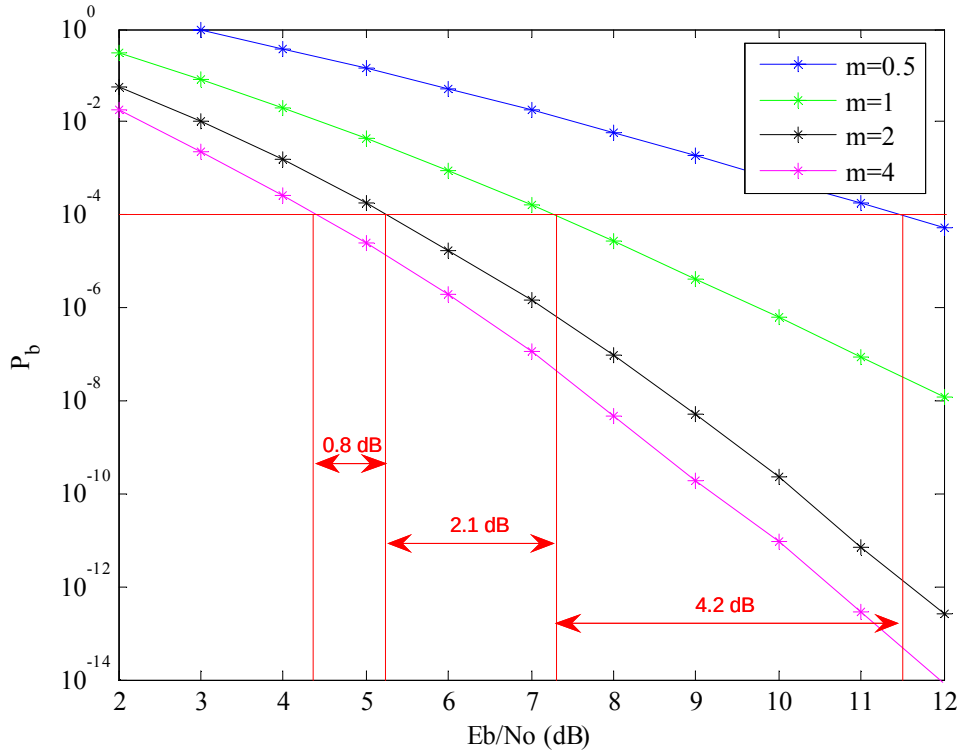

Figure 6. Linear-combining receiver for a Nakagami fading channel with AWGN for bit data rate of 6 and 12 Mbps

C. PERFORMANCE ANALYSIS WITH HOSTILE PULSE-NOISE INTERFERENCE IN A NON FADING CHANNEL

After studying the performance of the linear-combining receiver for fading channels with AWGN, we now examine the performance of the receiver for non fading channel with pulse-noise interference (PNI). Pulse noise-interference is examined since it can result in severe performance degradation. In such a hostile environment, the noise that arrives at the receiver can differ from bit to bit since each bit may be affected by different amounts of noise power σ_{x_k}. A number of bits are affected only by AWGN, while the rest are affected by both AWGN and the interference. Hence, the noise power at the output of the receiver integrator for each received bit can be expressed as

$$\sigma_{x_k}^2 = \begin{cases} \sigma_{x_j}^2 = \sigma_o^2 + \sigma_j^2, & \text{when PNI is operational} \\ \sigma_{x_o}^2 = \sigma_o^2, & \text{otherwise} \end{cases} \tag{3.27}$$

where $\sigma_{x_j}^2$ is the noise power of a jammed bit, σ_o^2 is the AWGN noise power, σ_j^2 is the interference noise power, and $\sigma_{x_o}^2$ is the noise power of a non-interfered bit. The AWGN power is

$$\sigma_o^2 = \frac{N_o}{T_s} \tag{3.28}$$

and the interference power is

$$\sigma_j^2 = \frac{N_i'}{T_s} = \frac{N_i / \rho}{T_s} \tag{3.29}$$

where N_o and N_i are the power spectral densities (PSDs) of the AWGN and the interference signal, respectively. The parameter ρ is the fraction of time that the jammer operates, where $0 < \rho \leq 1$. If we substitute Equations (3.28) and (3.29) into (3.27) we have

$$\sigma_{x_k}^2 = \begin{cases} \sigma_{x_j}^2 = \dfrac{N_o}{T_s} + \dfrac{N_i}{\rho T_s}, & \text{when PNI is operational} \\ \sigma_{x_o}^2 = \dfrac{N_o}{T_s}, & \text{otherwise} \end{cases} \tag{3.30}$$

The probability P_d can be obtained in the same way as for the case of AWGN with the difference that the noise is no longer uniform but i bits of the d bits are jammed and the remaining $d-i$ bits of the d bits are not jammed. Hence,

$$P_d\left(\sum_{k=1}^{d} i\right) = Q\left(\frac{\sqrt{2}\sum_{k=1}^{d} A_c}{\sqrt{\sum_{k=1}^{i}\sigma_{x_j}^2 + \sum_{k=1}^{d-i}\sigma_{x_o}^2}}\right) = Q\left(\frac{\sqrt{2}dA_c}{\sqrt{i\sigma_{x_j}^2 + (d-i)\sigma_{x_o}^2}}\right)$$

$$= Q\left(\sqrt{\frac{2d^2A_c^{\,2}}{d\sigma_{x_o}^2 + i\sigma_j^2}}\right) = Q\left(\sqrt{\frac{2dr}{\frac{N_o}{T_s} + \frac{i}{d}\frac{N_i}{\rho T_s}}}\right) \tag{3.31}$$

$$= Q\left(\sqrt{\frac{2dr}{\left(\frac{E_b}{N_o}\right)^{-1} + \frac{i}{d}\frac{1}{\rho}\left(\frac{E_b}{N_i}\right)^{-1}}}\right)$$

The probability that i bits of the d bits are jammed is given by

$$P_r(i \text{ bits jammed}) = \rho^i(1-\rho)^{d-i} \tag{3.32}$$

and there are $\binom{d}{i}$ different ways that i bits of the d bits can be jammed. The probability, P_d, of selecting a path that has a Hamming distance d from the correct path when i of the d bits are jammed can be expressed as

$$P_d = \sum_{i=0}^{d}\binom{d}{i}\rho^i(1-\rho)^{d-i}P_d(i) \tag{3.33}$$

Finally, the upper bound on the probability P_b is given by Equation (3.12).

For the bit rates of 6 and 12 Mbps, BPSK/QPSK modulation with a code rate of $r = 1/2$ is specified. The weight structure B_d and the free distance d_{free} is given in Table 2. The results are shown in Figure 7, where the probability P_b for different values of the

coefficient ρ are plotted. All the curves are for $E_b / N_o = 5\,\text{dB}$, which yields P_b somewhat less than 10^{-6} for $\frac{E_b}{N_o} \gg 1$.

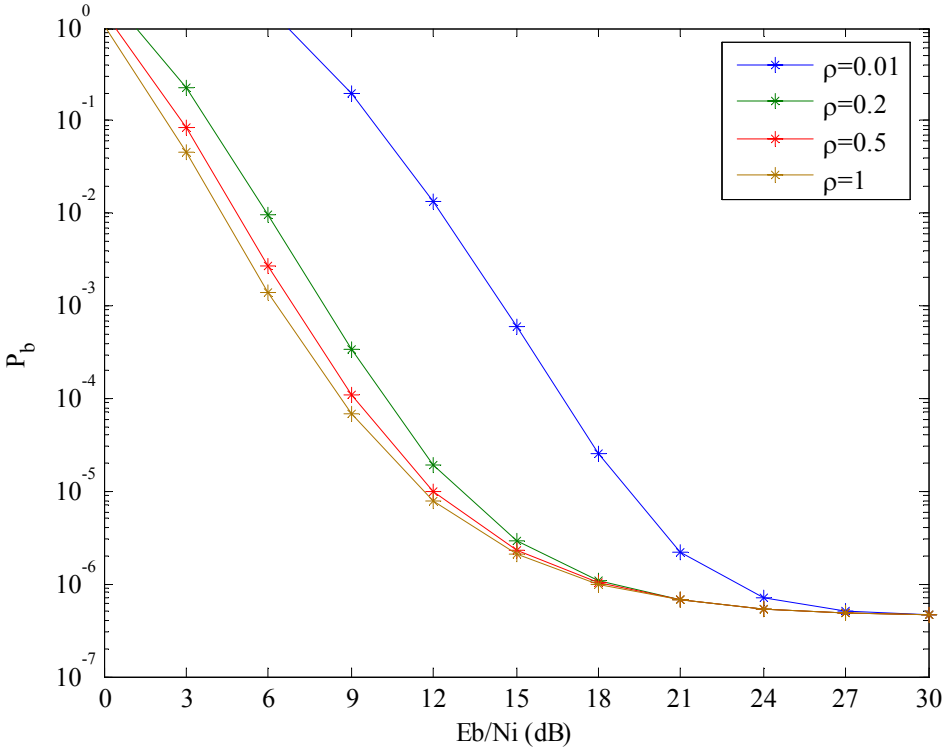

Figure 7. Linear-combining receiver with PNI in a non fading channel.

From Figure 7 we see that as the coefficient ρ increases, resulting in an increase in jammer power, the performance of the receiver decreases. Therefore, in order to obtain the same P_b, more signal power is required as ρ decreases.

D. PERFORMANCE ANALYSIS WITH HOSTILE PULSE NOISE INTERFERENCE IN A FADING CHANNEL

At this point, we will examine the performance of the receiver for a fading channel with PNI.

The noise power at the output of the integrator for each received bit is expressed by Equation (3.30). The conditional probability $P_d(\gamma_b)$ can be obtained in the same way

as for the case of PNI for non fading channel, with the difference that the amplitude of the signal $s(t)$ is not constant due to the fading channel, but differs from bit to bit. The conditional probability $P_d(\gamma_b)$ when i bits are jammed is

$$P_d\left(\sum_{k=1}^{d} a_c, i\right) = Q\left(\frac{\sqrt{2}\sum_{k=1}^{d} a_c}{\sqrt{\sum_{k=1}^{i}\sigma_{x_j}^2 + \sum_{k=1}^{d-i}\sigma_{x_o}^2}}\right) = Q\left(\frac{\sqrt{2}\sum_{k=1}^{d} a_c}{\sqrt{i\sigma_{x_j}^2 + (d-i)\sigma_{x_o}^2}}\right)$$
$$= Q\left(\frac{\sqrt{2}\sum_{k=1}^{d} a_c}{\sigma_{x_j}\sqrt{i + (d-i)\frac{\sigma_{x_o}^2}{\sigma_{x_j}^2}}}\right) = Q\left(\sqrt{\frac{2}{i + (d-i)\frac{\sigma_{x_o}^2}{\sigma_{x_j}^2}}}\sum_{k=1}^{d}\frac{a_c}{\sigma_{x_j}}\right) \tag{3.34}$$

Finally

$$P_d\left(\gamma_{b,} i\right) = Q\left(\sqrt{\frac{2}{i + (d-i)\frac{\sigma_{x_o}^2}{\sigma_{x_j}^2}}}\gamma_b\right) \tag{3.35}$$

where

$$\gamma_b = \sum_{k=1}^{d}\gamma_{b_k} = \sum_{k=1}^{d}\frac{a_c}{\sigma_{x_j}} = \sum_{k=1}^{d}\frac{a_c}{\sqrt{\sigma_j^2 + \sigma_o^2}} \tag{3.36}$$

The PDF $f_{\Gamma_{b_k}}$ of the random variable of the k^{th} bit γ_{b_k} can be evaluated by α change of variables

$$f_{\Gamma_{b_k}}(\gamma_{b_k}) = \left|\frac{da_c}{d\gamma_{b_k}}\right| f_{A_c}(a_c)\Big|_{a_c=\gamma_{b_k}\sigma_{x_j}} \tag{3.37}$$

where $f_{A_c}(a_c)$ is the Nakagami-*m* PDF as defined in Equation (2.6) and, from Equation (3.36), we have

$$\left|\frac{da_c}{d\gamma_{b_k}}\right| = \sigma_{x_j} \tag{3.38}$$

so

$$\begin{aligned} f_{\Gamma_{b_k}}(\gamma_{b_k}) &= \sigma_{x_j}\frac{2}{\Gamma(m)}\left(\frac{m}{\overline{a_c^2}}\right)^m \left(\gamma_{b_k}\sigma_{x_j}\right)^{2m-1} e^{\left(-\frac{m\left(\gamma_{b_k}\sigma_{x_j}\right)^2}{\overline{a_c^2}}\right)} \\ &= \frac{2}{\Gamma(m)}\left(\frac{m\sigma_{x_j}^2}{\overline{a_c^2}}\right)^m \left(\gamma_{b_k}\right)^{2m-1} e^{\left(-\frac{m\gamma_{b_k}^2\sigma_{x_j}^2}{\overline{a_c^2}}\right)} \end{aligned} \tag{3.39}$$

If we substitute $\overline{\gamma_b} = \frac{\sigma_{x_j}^2}{\overline{a_c^2}}$, we have

$$f_{\Gamma_{b_k}}(\gamma_{b_k}) = \frac{2}{\Gamma(m)}\left(m\overline{\gamma_b}\right)^m \left(\gamma_{b_k}\right)^{2m-1} e^{\left(-m\gamma_{b_k}^2\overline{\gamma_b}\right)} \tag{3.40}$$

where

$$\overline{\gamma_b} = \frac{\sigma_{x_j}^2}{\overline{a_c^2}} = \frac{N_o + N_i/\rho}{T_s\overline{a_c^2}} == \frac{1}{r}\left\{\left(\frac{E_b}{N_o}\right)^{-1} + \frac{1}{\rho}\left(\frac{E_b}{N_i}\right)^{-1}\right\} \tag{3.41}$$

The PDF $f_{\Gamma_b}(\gamma_b)$ of the random variable γ_b is the PDF of the sum of d independent random variables $\gamma_b = \sum_{k=1}^{d}\gamma_{b_k}$ and can be calculated numerically with the use of Equations (3.21), (3.22), (3.23), and (3.26).

Now we are ready to calculate P_b from Equation (3.12). The unconditional probability $P_d(i)$ can be calculated numerically by substituting the numerical result for $f_{\Gamma_b}(\gamma_b)$ and Equation (3.35) into Equation (3.16). The probability P_d is obtained by using this result in Equation (3.33).

For the bit rates of 6 and 12 Mbps with BPSK/QPSK modulation and $r = 1/2$ and with weight structure B_d and the free distance d_{free} as given in Table 2, we get Figure 8,

where the probability P_b for different fading conditions and different values of the coefficient ρ are plotted. All the curves are for $E_b / N_o = 15\,\text{dB}$.

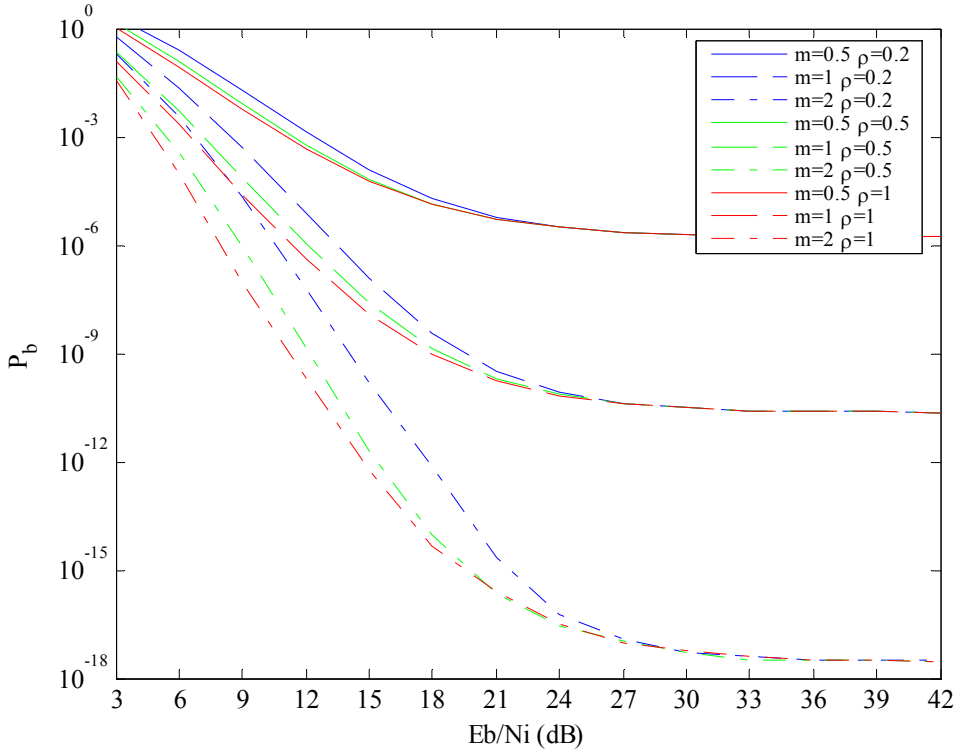

Figure 8. Linear-combining receiver with PNI for various fading conditions and values of the coefficient ρ.

From Figure 8, we see that as the parameter m increases, the receiver's performance decreases. In other words, as the fading conditions get less severe, the performance improves. We also notice that as E_b/N_i increases, the probability P_b for the same values of the parameter m converges. This is because as the ratio E_b/N_i increases, the interference noise becomes AWGN. As we see in Figure 9 for a probability $P_b = 10^{-5}$, the difference in required E_b/N_i between m=0.5 and m=1 and between m=1 and m=2 generally increases as the coefficient ρ increases, which means that the difference in required E_b/N_i increases as the noise power per jammed bit decreases. In other words, the jammer transmits a larger fraction of time.

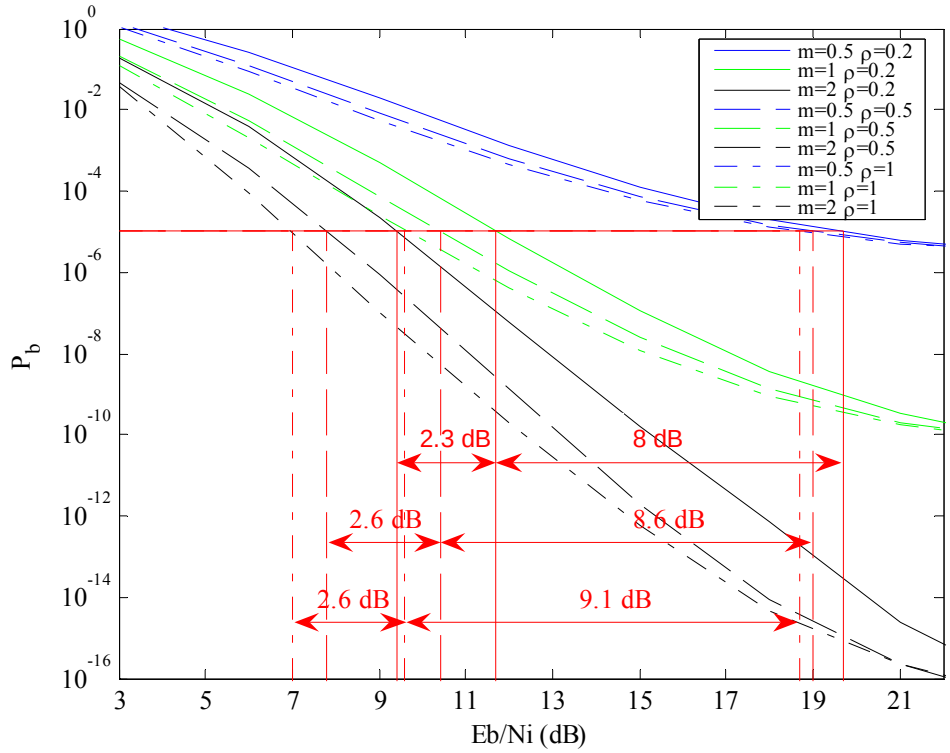

Figure 9. Linear-combining receiver with PNI for various fading conditions and values of the coefficient ρ [$Eb / Ni \in [3, 22]$].

E. SUMMARY

In this chapter, we introduced the performance of OFDM signals transmitted over frequency-selective, slowly fading Nakagami channels in an AWGN plus pulse-interference environment with a linear-combining receiver, which is designed to operate without side information.

In the next chapter, we present the noise-normalized combining receiver, for which we assume the existence of side information in the form of knowledge of the noise power for each received bit.

IV. PERFORMANCE ANALYSIS OF OFDM SIGNALS TRANSMITTED OVER FREQUENCY-SELECTIVE, SLOWLY FADING NAKAGAMI CHANNELS IN AN AWGN PLUS PULSE-INTERFERENCE ENVIRONMENT WITH NOISE-NORMALIZED COMBINING AND VITERBI SOFT DECISION DECODING (SDD)

In this chapter, the performance of OFDM signals transmitted over frequency-selective, slowly fading Nakagami channels in an AWGN plus pulse-interference environment with a noise-normalized combining receiver and Viterbi soft decision decoding is examined.

A. THE NOISE-NORMALIZED COMBINING RECEIVER

For this type of receiver, we assume the existence of side information in the form of knowledge of the noise power for every received bit.

The equivalent model of the noise-normalized combining receiver (NN) when BPSK modulation is used is presented in Figure 10.

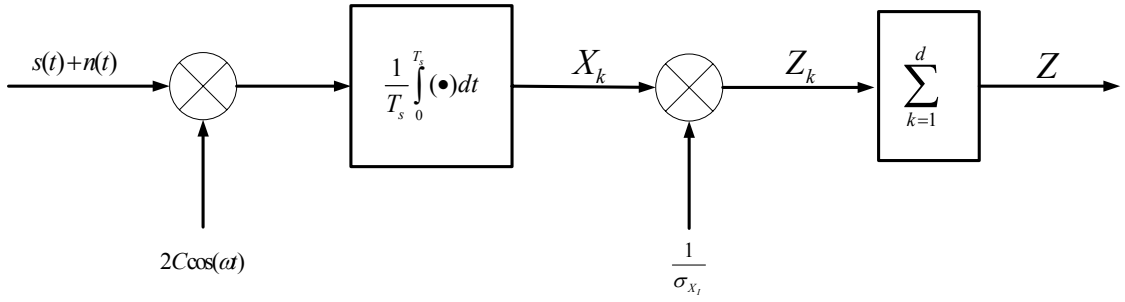

Figure 10. The noise-normalized combining receiver.

At the input of the receiver, as for the linear-combining receiver, there is the desired signal $\sqrt{2}a_c d(t)\cos(\omega_c t)$ and AWGN, where a_c represents the amplitude of the received signal, $d(t)$ the baseband information waveform, T_s the time duration of a symbol, and ω_c the frequency of the sub-carrier signal. At the input of the receiver the signal is corrupted by the noise $n(t)$. The integrator's output X_k is again modelled as a GRV with the mean and the variance given by Equations (3.3) and (3.4), respectively.

After the integrator, the signal X_k is divided by the noise power to yield

$$Z_k = \frac{X_k}{\sigma_k} \tag{4.1}$$

or

$$X_k = Z_k \sigma_k \tag{4.2}$$

The Z_k is also GRV since X_k is. The PDFs of the random variables X_k are given by Equations (3.1) and (3.2). Now changing variables, we obtain

$$f_{Z_k}(z_k) = \left| \frac{dX_k}{dZ_k} \right| f_{X_k}(x_k) \Big|_{X_k = \sigma_{x_k} Z_k} \tag{4.3}$$

From Equation (4.2) we have

$$\left| \frac{dX_k}{dZ_k} \right| = \sigma_k \tag{4.4}$$

Therefore, from Equations (3.1), (4.3), and (4.4), we have

$$f_{Z_k}(z_k) = \frac{\sigma_k}{\sqrt{2\pi} C \sigma_{x_k}} \exp\left[-\frac{(\sigma_k Z_k - \overline{X_k})^2}{2C^2 \sigma_{x_k}^2} \right] = \frac{1}{\sqrt{2\pi} C} \exp\left[-\frac{(Z_k - \overline{X_k}/\sigma_k)^2}{2C^2} \right] \tag{4.5}$$

From Equation (4.5) we see that the mean and the variance of Z_k are

$$\overline{Z_k} = \overline{X_k}/\sigma_k \tag{4.6}$$

and

$$\sigma_{z_k}^2 = C^2 \tag{4.7}$$

B. PERFORMANCE ANALYSIS IN A FADING CHANNEL WITH AWGN

At this point the performance of the noise-normalized combining receiver in a fading channel with AWGN is examined. Since the transmitted signal $s(t)$ is assumed to be transmitted over a flat, slowly-fading Nakagami channel, the amplitude of the signal $s(t)$ is modeled as a Nakagami-*m* random variable with a PDF given by Equation (2.6). At the input to receiver, the signal $s(t)$ is corrupted by the AWGN channel with power

spectral density $N_o/2$. Hence, the received signal is equal to $s(t)+n(t)$, which the local oscillator multiplies by $2C\cos(\omega_c t)$. Due to the fading channel, the amplitude of the received signal a_c differs from bit to bit.

We have assumed that the receiver is subject only to AWGN; therefore, we can assume that each bit is corrupted by the same amount of noise power, $\sigma_o^2 = N_o/T_s$. Hence

$$\sigma_k = \sigma_o \tag{4.8}$$

and Equation (4.6) can be rewritten as

$$\overline{Z_k} = \overline{X_k}/\sigma_o \tag{4.9}$$

We now assume that the constant C is equal to one. The overall decision variable for the sequence of d bits is the summation of independent, random variables:

$$Z = \sum_{k=1}^{d} Z_k \tag{4.10}$$

The random variable Z is also a GRV with mean

$$\overline{Z} = \sqrt{2}\sum_{k=1}^{d} a_c/\sigma_o \tag{4.11}$$

and variance

$$\sigma_z^2 = \sum_{k=1}^{d} C^2 = d \tag{4.12}$$

The probability P_d is given by Equation (3.5). Substituting (4.11) and (4.12) into (3.5), we get

$$P_d\left(\sum_{k=1}^{d} a_c\right) = Q\left(\frac{\sqrt{2}\sum_{k=1}^{d}\frac{a_c}{\sigma_o}}{\sqrt{d}}\right) = Q\left(\sqrt{\frac{2}{d}}\sum_{k=1}^{d}\frac{a_c}{\sigma_o}\right) \tag{4.13}$$

If we substitute $\sum_{k=1}^{d} \frac{a_c}{\sigma_0}$ with γ_b, we can express the probability P_d for the noise-normalized combining receiver

$$P_d(\gamma_b) = Q\left(\sqrt{\frac{2}{d}\gamma_b}\right) \tag{4.14}$$

where

$$\gamma_b = \sum_{k=1}^{d} \gamma_{b_k} = \sum_{k=1}^{d} \frac{a_c}{\sigma_o} \tag{4.15}$$

As we see, Equation (4.14) is identical to Equation (3.14), and Equation (4.15) is identical to Equation (3.17). Therefore, the probability of bit error of the noise-normalized combining receiver is the same as for the linear-combining receiver. This is expected since the receiver is subject to AWGN only and there is no interference. The probability P_b of the noise-normalized combining receiver is the same as that plotted in Figure 6 as a function of E_b/N_o at the receiver for different values of *m*.

C. PERFORMANCE ANALYSIS WITH HOSTILE PULSE-NOISE INTERFERENCE IN A NON FADING CHANNEL

After studying the performance of the noise-normalized combining receiver for a fading channel with AWGN, we now examine the performance of this receiver for a non fading channel with PNI.

As in the case of the linear-combining receiver, the noise that arrives at the receiver differs from bit to bit since each bit may be affected by different amount of noise power σ_{x_k}. A number of bits are affected by both AWGN and the interference signal (i bits), while the rest are affected by AWGN only ($d-i$ bits). Hence, the noise power at the output of the integrator for each received bit can be expressed as

$$\sigma_{x_k}^2 = \begin{cases} \sigma_{x_j}^2 = \sigma_o^2 + \sigma_j^2 = \dfrac{N_o}{T_s} + \dfrac{N_i/\rho}{T_s}, & \text{when PNI is operational} \\ \sigma_{x_o}^2 = \sigma_o^2 = \dfrac{N_o}{T_s}, & \text{otherwise} \end{cases} \tag{4.16}$$

where $\sigma_{x_j}^2$ is the power of a jammed bit, σ_o^2 is the AWGN noise power, σ_j^2 is the jammer noise power, $\sigma_{x_o}^2$ is the power of a non-jammed bit, N_o and N_i are the power spectral densities of the AWGN and the interference signal, respectively, and ρ expresses the fraction of the time that the jammer operates, where $0 < \rho \leq 1$.

If we combine Equations (4.6), (4.10), and (4.16) we have the mean of Z

$$\overline{Z} = \sum_{k=1}^{i} \frac{\sqrt{2}A_c}{\sqrt{\sigma_o^2 + \sigma_j^2}} + \sum_{k=1}^{d-i} \frac{\sqrt{2}A_c}{\sigma_o} \tag{4.17}$$

and its variance:

$$\sigma_z^2 = \sum_{k=1}^{d} C^2 = d \tag{4.18}$$

The conditional probability P_d is

$$\begin{aligned} P_d\left(\sum_{k=1}^{d} A_c, i\right) &= Q\left(\sqrt{\frac{2\left(\sum_{k=1}^{i} \frac{A_c}{\sqrt{\sigma_o^2 + \sigma_j^2}} + \sum_{k=1}^{d-i} \frac{A_c}{\sigma_o}\right)}{d}}\right) \\ &= Q\left(\sqrt{\frac{2}{d}\frac{A_c^2}{\sigma_o^2}\left(\frac{i}{\sqrt{1+\frac{\sigma_j^2}{\sigma_o^2}}} + d - i\right)^2}\right) \end{aligned} \tag{4.19}$$

Finally,

$$P_d(\sum_{k=1}^{d} A_c, i) = Q\left(\sqrt{\frac{2r}{d}\left(\frac{E_b}{N_o}\right)\left(\frac{i}{\sqrt{1+\frac{1}{\rho}\left[\left(\frac{E_b}{N_i}\right)^{-1} \Big/ \left(\frac{E_b}{N_o}\right)^{-1}\right]}} + d - i\right)^2}\right) \tag{4.20}$$

Combining Equations (3.12), (3.33), and (4.20), we obtain the performance of the noise-normalized combining receiver.

1. Performance Analysis of the Noise-Normalized Receiver

For BPSK/QPSK modulation with $r = 1/2$ and the weight structure B_d and the free distance d_{free} given in Table 2, we get Figure 11 for the probability P_b. Figures 11 and 12 are for $E_b / N_o = 5\,\text{dB}$.

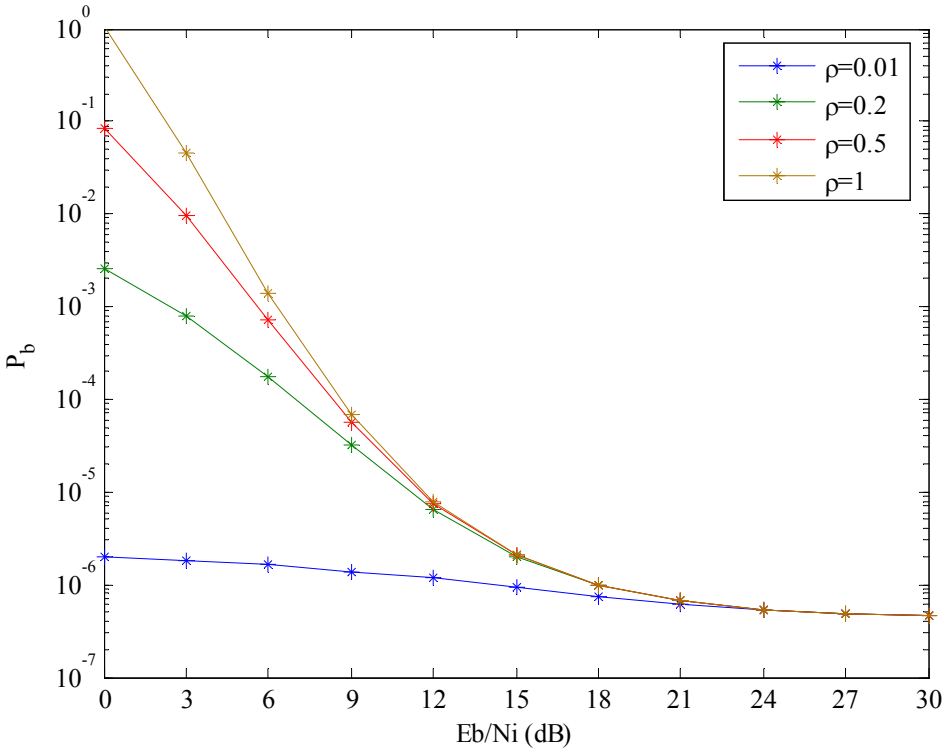

Figure 11. Noise-normalized receiver with PNI for non fading channel.

As we can see, as the coefficient ρ increases, the receiver's performance decreases. Also, as E_b/N_i increases, the probabilities P_b for different values of the parameter ρ converge since, as E_b/N_i increases, the interfering signal becomes AWGN. This is something that also happens with the linear-combining receiver. Note that the behaviour of P_b with decreasing ρ is the opposite of that obtained for the linear-combining receiver.

2. Comparison of the Noise–Normalized Combining Receiver with the Linear-Combining Receiver

From Figure 12 it is obvious that the probability P_b of the noise-normalized combining receiver is always better than the performance of the linear-combining receiver when $\rho < 1$. For the case of ρ=1, the two receivers have the same performance as expected. The two receivers converge to the same probability P_b as E_b/N_i increases regardless of ρ.

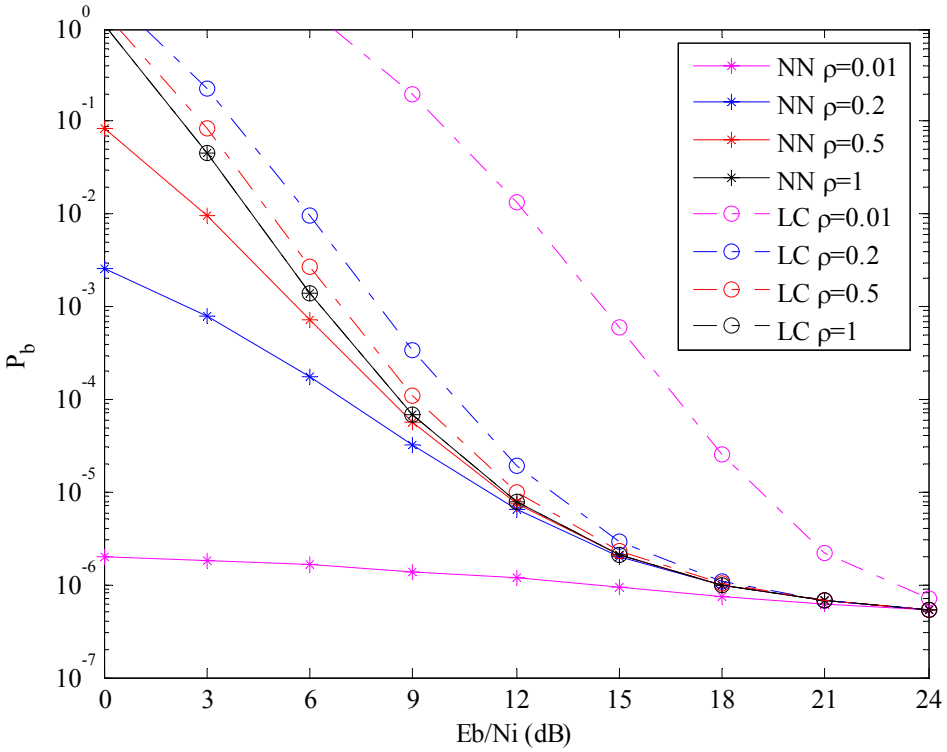

Figure 12. Comparison of the noise-normalized and linear-combining receivers with PNI for various values of the coefficient ρ.

D. PERFORMANCE ANALYSIS WITH HOSTILE PULSE-NOISE INTERFERENCE IN A FADING CHANNEL

Now we examine the performance of the noise-normalized combining receiver for a fading channel with PNI. As in the case of the linear-combining receiver, the noise at the receiver differs from bit to bit since each bit is affected by different amounts of noise power σ_{x_k}. Some bits are affected by both AWGN and the interference signal (i bits),

and the rest are affected only by AWGN ($d-i$ bits). Hence, the noise power at the output of the integrator is given by Equation (4.16).

If we combine Equations (4.6), (4.10), and (4.16), we have, since the decision variable Z is a GRV, the mean

$$\overline{Z} = \sum_{k=1}^{i} \frac{\sqrt{2}a_c}{\sqrt{\sigma_o^2 + \sigma_j^2}} + \sum_{k=1}^{d-i} \frac{\sqrt{2}a_c}{\sigma_o} \tag{4.21}$$

and the variance

$$\sigma_z^2 = \sum_{k=1}^{d} C^2 = d \tag{4.22}$$

The conditional probability P_d can be obtained in the same way as for the case of AWGN with the difference that the noise is no longer uniform, but i bits of the d bits are jammed, and the remaining $d-i$ bits of the d bits are not jammed. Hence,

$$\begin{aligned} P_d\left(\sum_{k=1}^{d} a_c\right) &= Q\left(\frac{\sqrt{2}\left(\sum_{k=1}^{i} \frac{a_c}{\sqrt{\sigma_o^2 + \sigma_j^2}} + \sum_{k=1}^{d-i} \frac{a_c}{\sigma_o}\right)}{d}\right) \\ &= Q\left(\sqrt{\frac{2}{d}}\left(\sum_{k=1}^{i} \gamma_{b_{k_j}} + \sum_{k=1}^{d-i} \gamma_{b_{k_o}}\right)\right) = Q\left(\sqrt{\frac{2}{d}}\left(\gamma_{b_j} + \gamma_{b_o}\right)\right) \end{aligned} \tag{4.23}$$

where

$$\gamma_{b_j} = \sum_{k=1}^{i} \gamma_{b_{k_j}} = \sum_{k=1}^{i} \frac{a_c}{\sqrt{\sigma_j^2 + \sigma_o^2}} \tag{4.24}$$

and

$$\gamma_{b_o} = \sum_{k=1}^{d-i} \gamma_{b_{k_0}} = \sum_{k=1}^{d-i} \frac{a_c}{\sigma_o} \tag{4.25}$$

Now it is time to evaluate the overall PDF $f_{\Gamma_b}(\gamma_b)$, which generally can be done only numerically, but first we must evaluate the PDFs of $\gamma_{b_{k_j}}$ and $\gamma_{b_{k_o}}$. The PDF $f_{\Gamma_{b_{k_j}}}$ of

the random variable representing the k^{th} bit $\gamma_{b_{k_j}}$ can be evaluated from Equation (2.6) by the change of the of variables

$$f_{\Gamma_{b_{k_j}}}(\gamma_{b_{k_j}}) = \left|\frac{da_c}{d\gamma_{b_{k_j}}}\right| f_{A_c}(a_c)\Big|_{a_c=\gamma_{b_{k_j}}\sigma_{x_j}} \tag{4.26}$$

where $f_{A_c}(a_c)$ is the Nakagami-*m* PDF as defined in Equation (2.6). From Equation (4.24) we have

$$\left|\frac{da_c}{d\gamma_{b_{k_j}}}\right| = \sigma_{x_j} \tag{4.27}$$

As we see, Equations (4.26) and (4.27) are the same as Equations (3.37) and (3.38), respectively, and as a result the PDF $f_{\Gamma_{b_{k_j}}}$ is

$$f_{\Gamma_{b_{k_j}}}(\gamma_{b_{k_j}}) = \frac{2}{\Gamma(m)}\left(m\overline{\gamma_{b_{k_j}}}\right)^m \left(\gamma_{b_{k_j}}\right)^{2m-1} e^{\left(-m\gamma_{b_{k_j}}^2\,\overline{\gamma_{b_{k_j}}}\right)} \tag{4.28}$$

where

$$\overline{\gamma_{b_{k_j}}} = \frac{\sigma_{x_j}^2}{\overline{a_c^2}} = \frac{\frac{1}{r}\left(\frac{N_o}{T_b}+\frac{1}{\rho}\frac{N_i}{T_b}\right)}{\overline{a_c^2}} = \frac{1}{r}\left[\left(\frac{E_b}{N_o}\right)^{-1}+\frac{1}{\rho}\left(\frac{E_b}{N_i}\right)^{-1}\right] \tag{4.29}$$

The PDF $f_{\Gamma_{b_{k_o}}}$ is the same as Equation (3.19) and for convenience is repeated:

$$f_{\Gamma_{b_{k_o}}}(\gamma_{b_{k_o}}) = \frac{2}{\Gamma(m)}\left(m\overline{\gamma_{b_{k_o}}}\right)^m \left(\gamma_{b_{k_o}}\right)^{2m-1} e^{\left(-m\gamma_{b_{k_o}}^2\,\overline{\gamma_{b_{k_o}}}\right)} \tag{4.30}$$

where

$$\overline{\gamma_{b_{k_o}}} = \frac{\sigma_o^2}{\overline{a_c^2}} = \frac{N_o}{T_s\overline{a_c^2}} = \frac{N_o}{rT_b\overline{a_c^2}} = \frac{1}{r}\frac{N_o}{E_b} = \frac{1}{r}\left(\frac{E_b}{N_o}\right)^{-1} \tag{4.31}$$

Having found the PDFs $f_{\Gamma_{bk_j}}$ and $f_{\Gamma_{bk_j}}$, we obtain their Laplace transforms $F_{\Gamma_{bk_j}}$ and $F_{\Gamma_{bk_j}}$ with Equation (3.24). The Laplace transform of the overall PDF of the jammed bits is

$$F_{\Gamma_{b_j}} = \left\{ F_{\Gamma_{bk_j}} \right\}^i \tag{4.32}$$

and the Laplace transform of the overall PDF of the bits that are not jammed is

$$F_{\Gamma_{b_o}} = \left\{ F_{\Gamma_{bk_o}} \right\}^{d-i} \tag{4.33}$$

Hence, the Laplace transform of the PDF of all d bits, jammed and otherwise, is

$$F_{\Gamma_b} = \left\{ F_{\Gamma_{bk_j}} \right\}^i \times \left\{ F_{\Gamma_{bk_o}} \right\}^{d-i} \tag{4.34}$$

As discussed in the previous chapter, we obtain the inverse Laplace transform using Equation (3.26). Finally, combining Equations (3.12), (3.16), (4.23) and the result of the numerical inversion of (4.34) using (3.26), we obtain the P_b of the noise-normalized combining receiver.

1. Performance Analysis for Different Fading Conditions

For BPSK/QPSK modulation with $r = 1/2$ and the weight structure B_d and the free distance d_{free} given in Table 2, we get Figure 13, where the probability P_b for different fading conditions is plotted for different values of the coefficient ρ. All the figures are for $E_b / N_o = 15\,\text{dB}$.

As *m* increase the receiver's performance decreases. In other words, as the fading conditions get less severe, the performance improves. Also, as E_b/N_i increases, the probability P_b for the same values of the parameter *m* converge since, as E_b/N_i increases, the interfering noise becomes AWGN. Finally, the difference in required

E_b/N_i for a specific P_b between m=0.5 and m=1 and between m=1 and m=2 generally increases as the coefficient ρ increases. This is something that also happens with the linear-combining receiver.

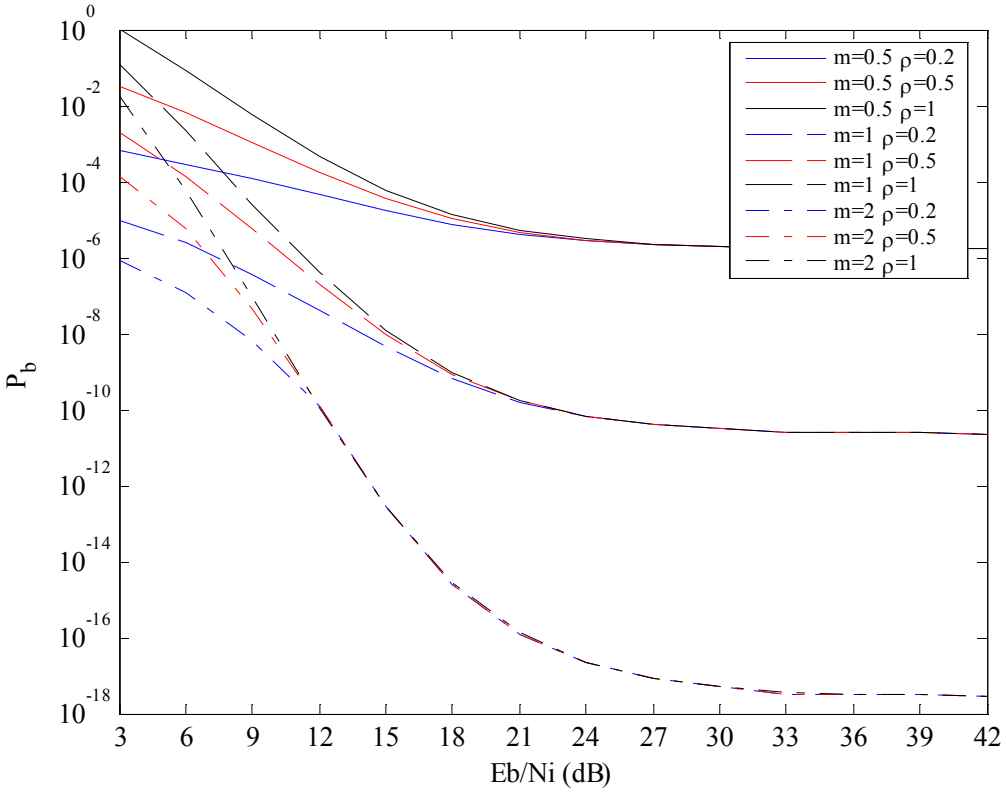

Figure 13. Noise-normalized receiver with PNI for various fading conditions and different values of the coefficient ρ.

2. Comparison of the Noise–Normalized Combining Receiver with the Linear-Combining Receiver

From Figures 14, 15, and 16, it is clear that the performance of the noise-normalized combining receiver is always better than the performance of the linear-combining receiver when $\rho < 1$. For the case of ρ=1, the two receivers have the same performance. Both of the receivers converge to the same probability P_b as E_b/N_i increases for the same fading conditions since the power of the interference becomes negligible. In order to maintain the same level of probability P_b, the linear-combining receiver requires much more power for a small ρ, while when ρ increases (the jammer's

instantaneous power decreases), the additional power required by the linear-combining receiver decreases. This is obvious in Figures 17 and 18 which are a portion of Figures 14 and 15, respectively, shown with an expanded scale.

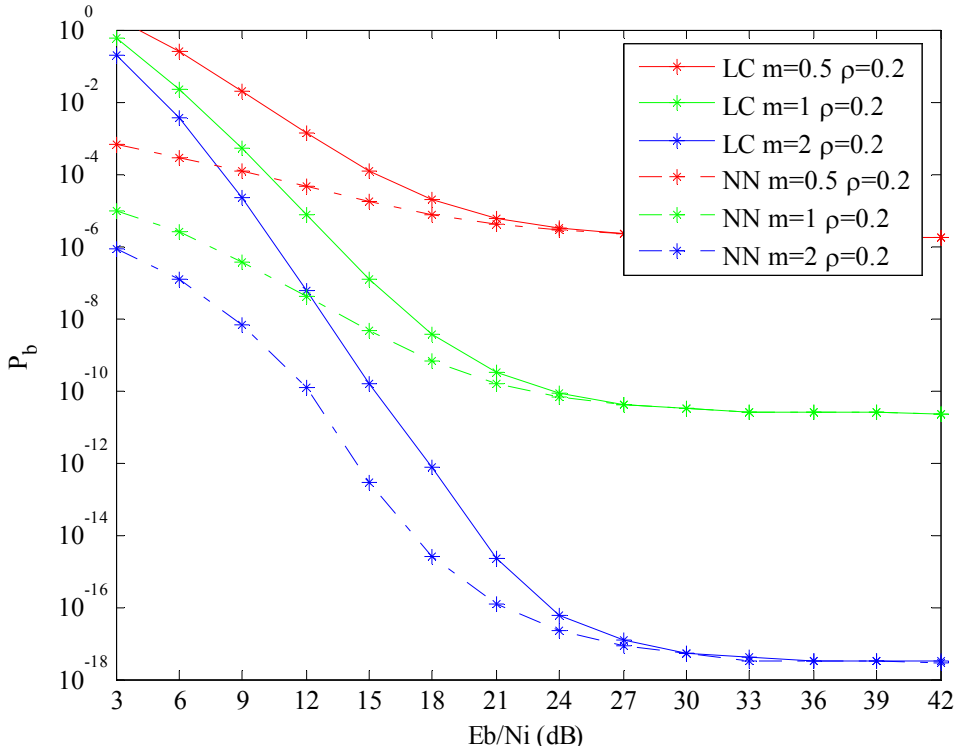

Figure 14. Comparison of the noise-normalized and the linear-combining receivers with PNI for various fading conditions and ρ=0.2.

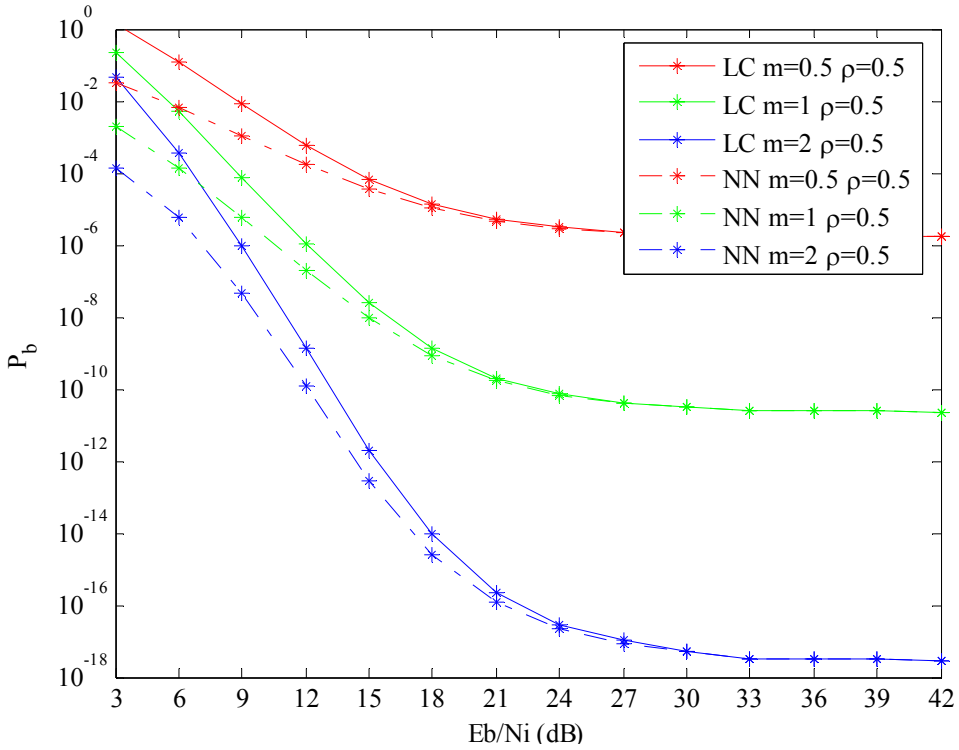

Figure 15. Comparison of the noise-normalized and the linear-combining receivers with PNI for various fading conditions and ρ=0.5.

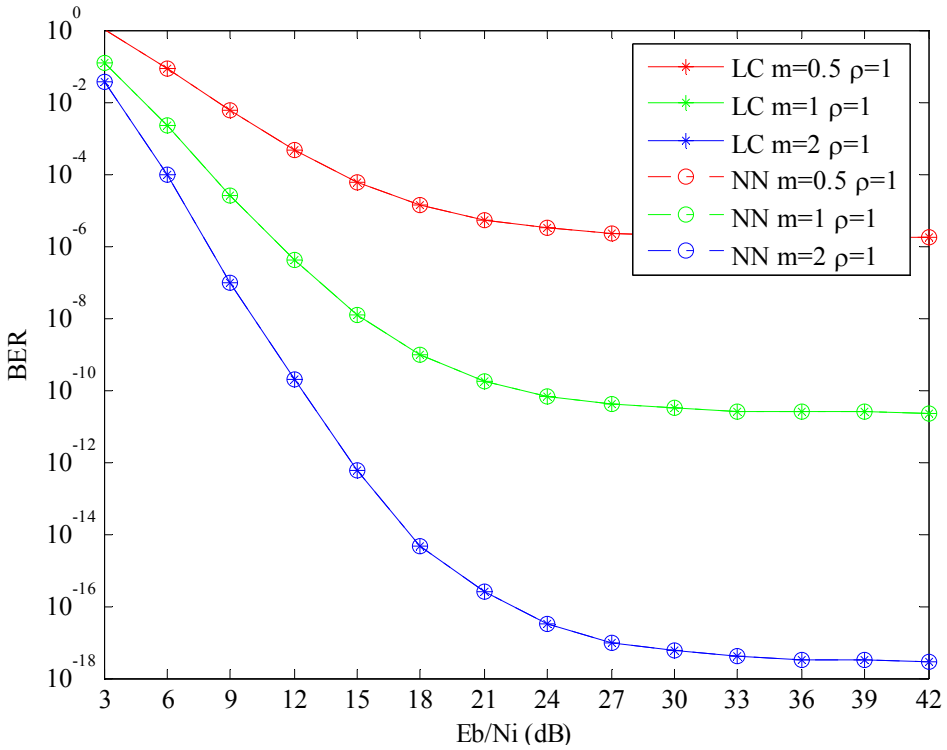

Figure 16. Comparison of the noise-normalized and the linear-combining receivers with PNI for various fading conditions and ρ=1.

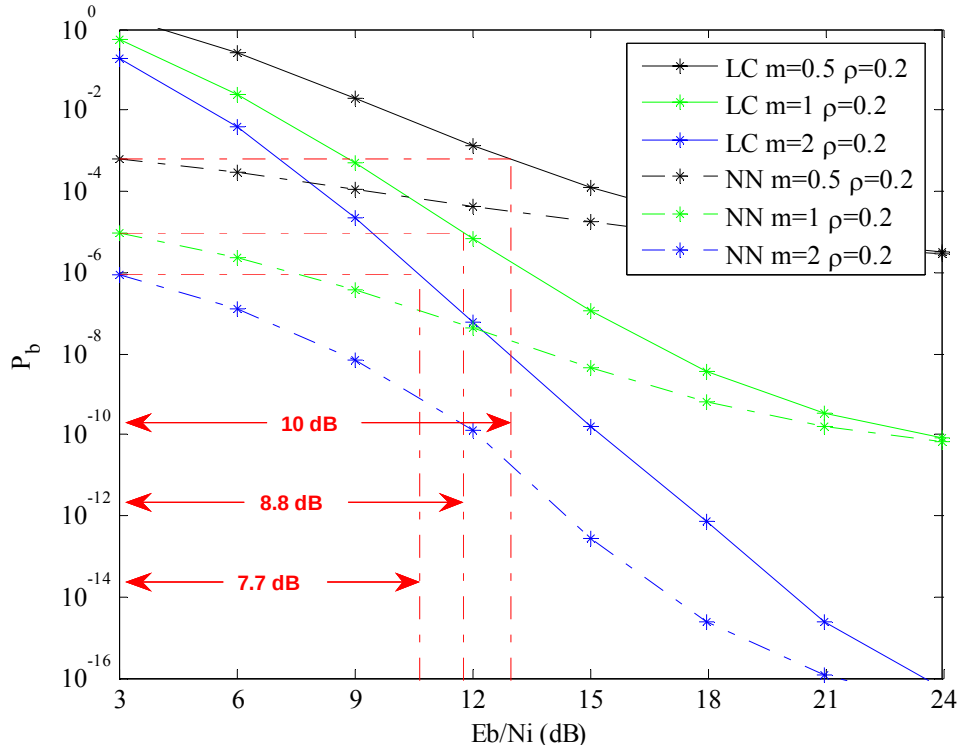

Figure 17. Comparison of the noise-normalized and the linear-combining receivers with PNI for various fading conditions and ρ=0.2 [$Eb/Ni \in [3,24]$].

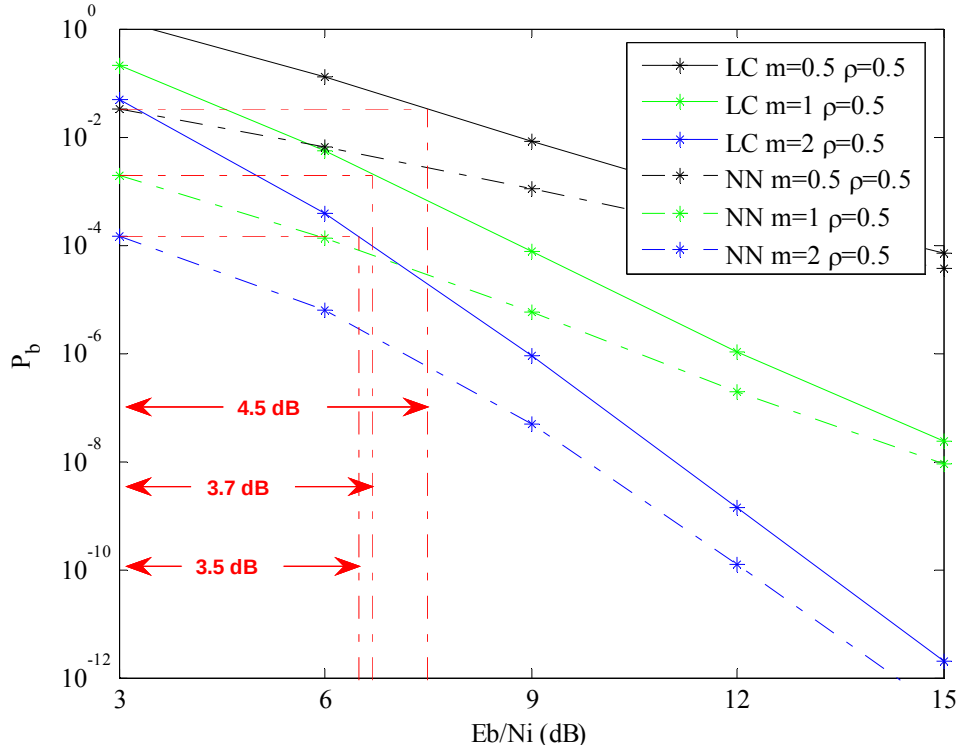

Figure 18. Comparison of the noise-normalized and the linear-combining receivers with PNI for various fading conditions and ρ=0.5 [$Eb/Ni \in [3,15]$].

E. SUMMARY

In this chapter we examined the performance of OFDM signals transmitted over frequency-selective, slowly fading Nakagami channels in an AWGN plus pulse-interference environment with a noise-normalized combining receiver and Viterbi soft decision decoding.

In the next chapter, we examine a modification of the noise-normalized combining receiver that is designed to operate with much coarser side information than the noise-normalized receiver; i.e. the exact noise power for every received bit is not known, but whether a bit is jammed or not is assumed known.

THIS PAGE INTENTIONALLY LEFT BLANK

V. PERFORMANCE ANALYSIS OF OFDM SIGNALS TRANSMITTED OVER FREQUENCY-SELECTIVE, SLOWLY FADING NAKAGAMI CHANNELS IN AN AWGN PLUS PULSE-INTERFERENCE ENVIRONMENT WITH MODIFIED NOISE-NORMALIZED COMBINING AND VITERBI SOFT DECISION DECODING (SDD)

In this chapter we examine the performance of OFDM signals transmitted over frequency-selective, slowly fading Nakagami channels in an AWGN plus pulse-interference environment using a modified noise-normalized combining receiver and Viterbi soft decision decoding.

A major problem that the designer of the noise-normalized combining receiver has to face is that it is very difficult to measure the power of the jammer in order to use it as side information for the receiver. In order to overcome this difficulty, an alternative solution is proposed in order to design a type of noise normalized receiver which does not require side information such as the exact noise power of the jammer.

A. THE MODIFIED NOISE-NORMALIZED COMBINING RECEIVER

The modified noise-normalized combining receiver (MNN) is designed to operate with much coarser side information; i.e., the exact noise power of every received bit is not known, but whether a bit is jammed or not is known.

The modified noise-normalized combining receiver for BPSK modulation with soft decision Viterbi decoding is equivalent to Figure 19 for the purpose of finding P_d.

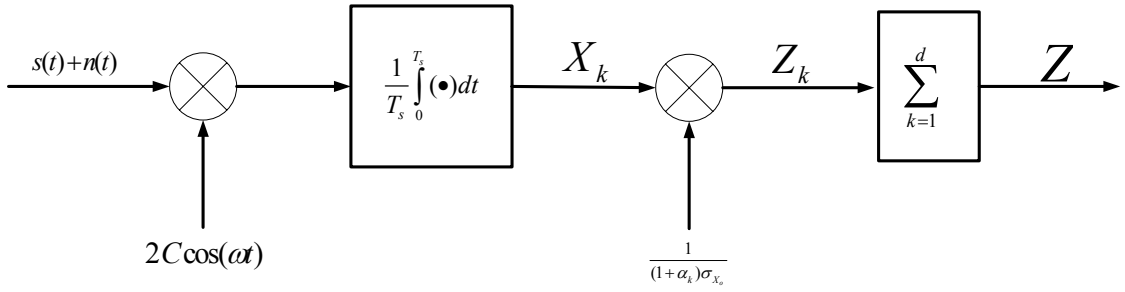

Figure 19. The modified noise-normalized combining receiver.

At the input of the receiver is the desired signal $s(t) = \sqrt{2}a_c d(t)\cos(\omega_c t)$ where a_c represents the amplitude of the received signal, $d(t)$ the information waveform, T_s the time duration of a symbol, and ω_c is the frequency of the sub-carrier signal. At the input of the receiver, the signal is corrupted by the noise $n(t)$. The integrator's output X_k is modelled as a GRV and has the mean and variance as given by Equations (3.3) and (3.4), respectively.

After the integrator, the signal X_k is divided by $(1+a_k)\sigma_o$ to yield

$$Z_k = \frac{X_k}{(1+\alpha_k)\sigma_o} \tag{5.1}$$

or

$$X_k = Z_k(1+\alpha_k)\sigma_o \tag{5.2}$$

where

$$\alpha_k = \begin{cases} 0 \text{ if } \sigma_k^2 = \sigma_o^2 \\ \alpha \text{ if } \sigma_k^2 > \sigma_o^2 \end{cases} \tag{5.3}$$

Since X_k is a GRV, Z_k is also a GRV. The PDFs of random variables X_k are given by Equations (3.1) and (3.2). Changing variables, we get the PDF of Z_k from

$$f_{Z_k}(z_k) = \left|\frac{dx_k}{dz_k}\right| f_{X_k}(x_k)\Big|_{X_k = Z_k(1+\alpha_k)\sigma_o} \tag{5.4}$$

From Equation (5.2), we have

$$\left|\frac{dx_k}{dz_k}\right| = \sigma_o(1+\alpha_k) \tag{5.5}$$

Therefore, from Equations (3.1), (5.2), (5.4), and (5.5), we get

$$f_{Z_k}(z_k) = \frac{\sigma_o(1+\alpha_k)}{\sqrt{2\pi}\sigma_{x_k}} \exp\left[-\frac{(Z_k\sigma_o(1+\alpha_k) - \overline{X_k})^2}{2\sigma_{x_k}^2} \right]$$

$$= \frac{1}{\sqrt{2\pi}\left(\frac{C\sigma_k}{\sigma_o(1+\alpha_k)} \right)} \exp\left[-\frac{\left(Z_k - \frac{\sqrt{2}Ca_c}{\sigma_o(1+a_k)} \right)^2}{2\left(\frac{C\sigma_k}{\sigma_o(1+\alpha_k)} \right)^2} \right] \tag{5.6}$$

From Equation (5.6), we see that mean and variance of Z_k are, respectively,

$$\overline{Z_k} = \frac{\sqrt{2}Ca_c}{\sigma_o(1+\alpha_k)} \tag{5.7}$$

and

$$\sigma_{z_k}^2 = \left(\frac{C\sigma_k}{\sigma_o(1+\alpha_k)} \right)^2 \tag{5.8}$$

The decision variable for the sequence of d bits is the summation of independent, random variables

$$Z = \sum_{k=1}^{d} Z_k \tag{5.9}$$

Hence, Z is also a GRV with mean

$$\overline{Z} = \sum_{k=1}^{d} \frac{\sqrt{2}Ca_c}{\sigma_o(1+\alpha_k)} \tag{5.10}$$

and variance

$$\sigma_z^2 = \sum_{k=1}^{d} \left(\frac{C\sigma_k}{\sigma_o(1+\alpha_k)} \right)^2 \tag{5.11}$$

B. PERFORMANCE ANALYSIS IN A FADING CHANNEL WITH AWGN

The performance analysis of the modified noise-normalized combining receiver in a fading channel with AWGN is now be examined. The modified noise-normalized combining receiver and the noise normalized receiver are identical as far as the output of

the integrator. Since the receiver is subject only to AWGN, we can assume that each bit is corrupted by the same amount of noise power, $\sigma_o^2 = N_o / T_s$, so

$$\sigma_k = \sigma_o \tag{5.12}$$

Thus, Equation (5.11) can be rewritten as

$$\sigma_z^2 = \sum_{k=1}^{d} \left(\frac{C\sigma_o}{\sigma_o} \right)^2 = dC^2 \tag{5.13}$$

We now assume that the constant *C* is equal to one.

The probability P_d is given in Equation (3.5). Substituting (5.10) and (5.13) into (3.5), we get

$$P_d\left(\sum_{k=1}^{d} a_c \right) = Q\left(\frac{\sum_{k=1}^{d} \frac{\sqrt{2}a_c}{\sigma_o}}{\sqrt{d}} \right) = Q\left(\sqrt{\frac{2}{d}} \sum_{k=1}^{d} \frac{a_c}{\sigma_o} \right) \tag{5.14}$$

If we substitute the $\sum_{k=1}^{d} \frac{a_c}{\sigma_0}$ with γ_b, we have the same conditional probability P_d as with the linear-combining receiver

$$P_d\left(\gamma_b\right) = Q\left(\sqrt{\frac{2}{d}} \gamma_b \right) \tag{5.15}$$

where

$$\gamma_b = \sum_{k=1}^{d} \gamma_{b_k} = \sum_{k=1}^{d} \frac{a_c}{\sigma_o} \tag{5.16}$$

As can be seen, Equation (5.15) is identical to Equation (3.14) and Equation (5.16) is identical to Equation (3.17); therefore, the probability of bit error of the modified noise-normalized combining receiver is the exactly same as that of the linear-combining receiver. This is expected since the receiver is subject to AWGN only and there is no interference. The upper bound on P_b of the modified noise-normalized

combining receiver is the same as that plotted in Figure 6 as a function of the SNR at the receiver for different values of the parameter *m*.

C. PERFORMANCE ANALYSIS WITH HOSTILE PULSE-NOISE INTERFERENCE IN A NON FADING CHANNEL

We now examine the modified noise-normalized combining receiver's performance in a non fading channel with PNI.

As for the linear-combining receiver and noise-normalized combining receiver, the noise that arrives at the receiver differs from bit to bit and each bit is affected by a different amount of noise power σ_{x_k}. A number of bits are affected by both AWGN and the interference signal (i bits), and the rest are affected by only AWGN ($d-i$ bits). Hence, the noise power at the output of the integrator for each received bit is given by Equation (4.16).

Since the signal $s(t)$ is transmitted over a non fading channel, the amplitude of the signal does not change due to the channel from bit to bit. Hence, Equations (5.7) and (5.10) can be rewritten

$$\overline{Z_k} = \frac{\sqrt{2}A_c}{\sigma_o(1+\alpha_k)} \tag{5.17}$$

and

$$\overline{Z} = \sum_{k=1}^{d-i} \frac{\sqrt{2}A_c}{\sigma_o} + \sum_{k=1}^{i} \frac{\sqrt{2}A_c}{\sigma_o(1+\alpha)} = (d-i)\frac{\sqrt{2}A_c}{\sigma_o} + i\frac{\sqrt{2}A_c}{\sigma_o(1+\alpha)} \tag{5.18}$$

If we combine Equations (5.11) and (4.16), we have for the variance of Z

$$\sigma_z^2 = \sum_{k=1}^{i} \frac{\sigma_o^2+\sigma_j^2}{\sigma_o^2(1+\alpha)^2} + \sum_{k=1}^{d-i} \frac{\sigma_o^2}{\sigma_o^2} = \frac{i}{(1+\alpha)^2}\left(1+\frac{\sigma_j^2}{\sigma_o^2}\right) + (d-i) \tag{5.19}$$

The conditional probability P_d is calculated by combining Equations (3.5), (5.18) and (5.19):

$$P_d\left(\sum_{k=1}^{d} A_c\right) = Q\left(\sqrt{\frac{\left((d-i)\frac{\sqrt{2}A_c}{\sigma_o} + i\frac{\sqrt{2}A_c}{\sigma_o(1+\alpha)}\right)^2}{(d-i) + \frac{i}{(1+\alpha)^2}\left(1+\frac{\sigma_j^2}{\sigma_o^2}\right)}}\right)$$
$$= Q\left(\sqrt{2r\frac{E_b}{N_o}\frac{\left((d-i)+i\frac{1}{(1+\alpha)}\right)^2}{(d-i)+\frac{i}{(1+\alpha)^2}\left(1+\frac{1}{\rho}\left(\frac{E_b}{N_i}\right)^{-1}\Big/\left(\frac{E_b}{N_o}\right)^{-1}\right)}}\right) \tag{5.20}$$

The upper bound on P_b for the modified noise-normalized combining receiver can be evaluated by combining Equations (3.12), (3.33), and (5.20).

1. Performance Analysis for the Same Values of the Coefficient ρ

For BPSK/QPSK modulation, where the data rates are 6 and 12 Mbps, respectively, the code rate is $r = 1/2$ and the weight structure B_d and the free distance d_{free} are given in Table 2, P_b for the same values of the coefficient ρ is plotted in Figures 20 through 25. All the figures are for $E_b / N_o = 5\,\text{dB}$.

We see that for small values of E_b/N_i, the larger the coefficient α is, the better performance we have. There is a crossover value of E_b/N_i which depends on the coefficient ρ, above which smaller values of α lead to better performance than for larger ones.

We also see that for small values of the coefficient ρ and for all values of the coefficient α, the modified noise-normalized combining receiver has better performance than the linear-combining receiver. For small values of the coefficient ρ and for large values of α, the modified noise-normalized receiver has better performance than the noise-normalized receiver as well. As $\rho \to 1$, the three receivers have almost the same performance no matter what the value of α, and for $\rho = 1$, they have exactly the same performance as expected. The best choice for α depends on ρ and E_b/N_i. For very small

values of ρ, like ρ=0.01, larger α gives better performance without regard to E_b/N_i, but for larger values of ρ (i.e., $\rho \geq 0.1$), for small values of E_b/N_i, the larger the coefficient α is, the better the performance.

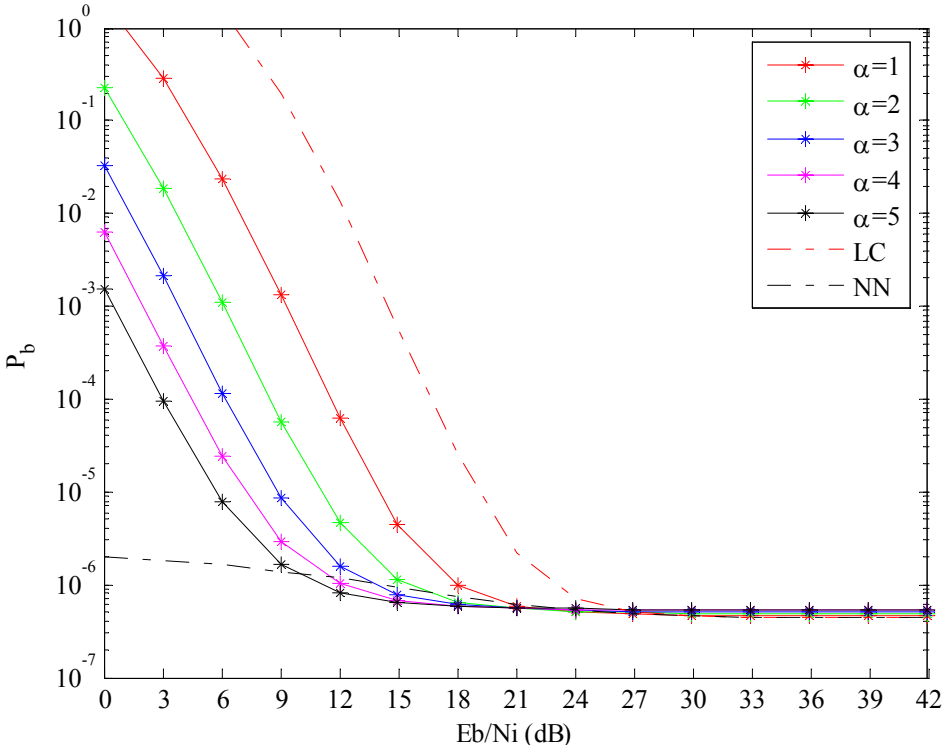

Figure 20. Modified noise-normalized receiver with PNI for non fading different values of the coefficient α and ρ=0.01.

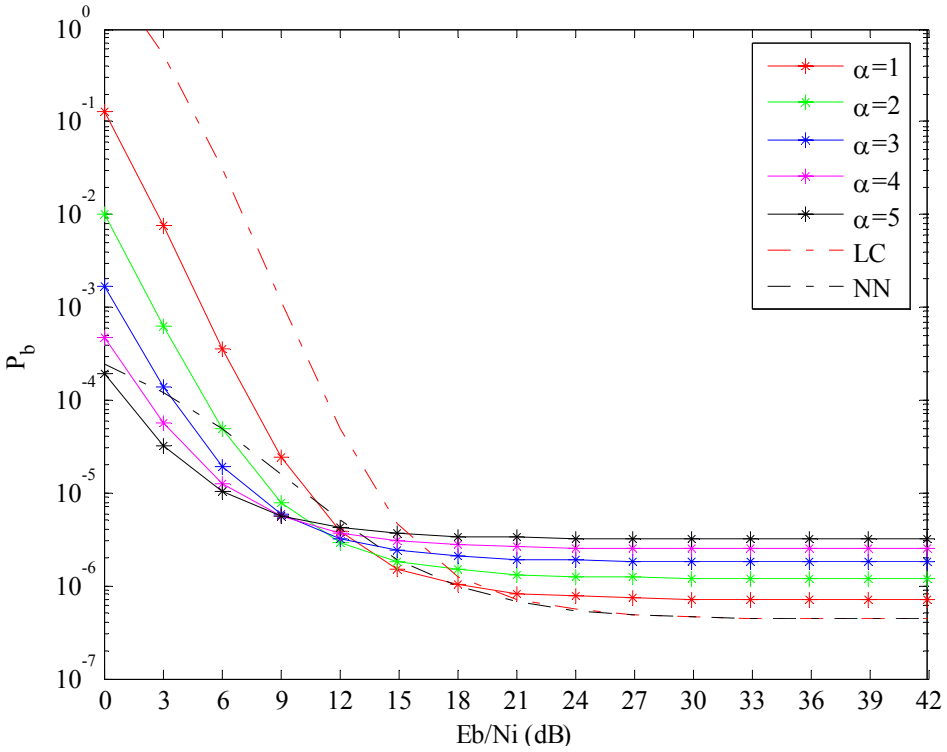

Figure 21. Modified noise-normalized receiver with PNI for non fading different values of the coefficient α and ρ=0.1.

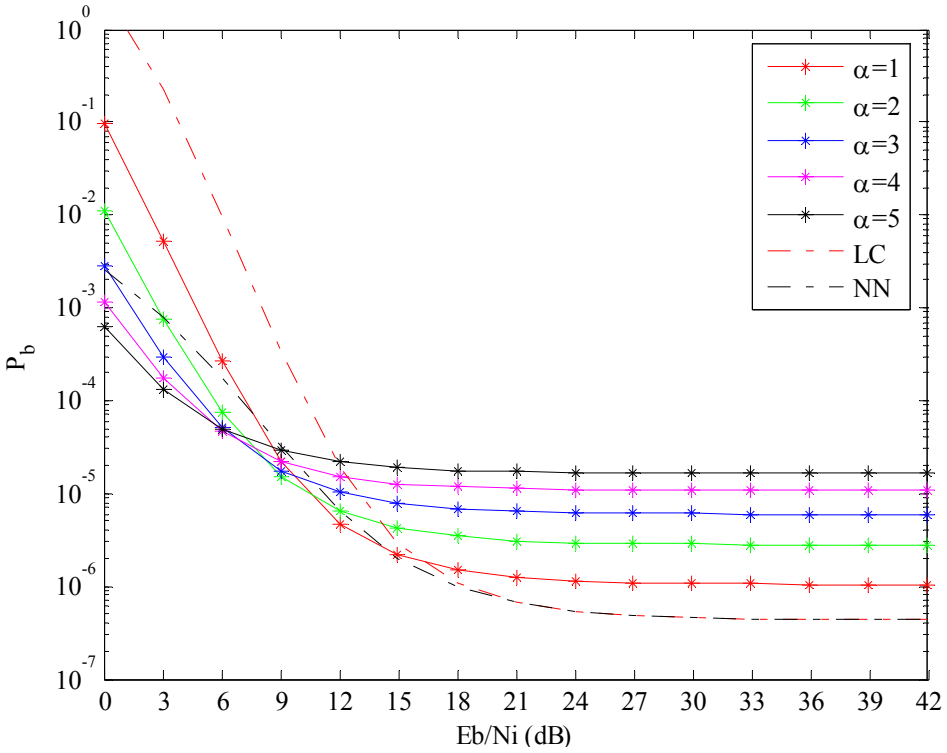

Figure 22. Modified noise-normalized receiver with PNI for non fading different values of the coefficient α and ρ=0.2.

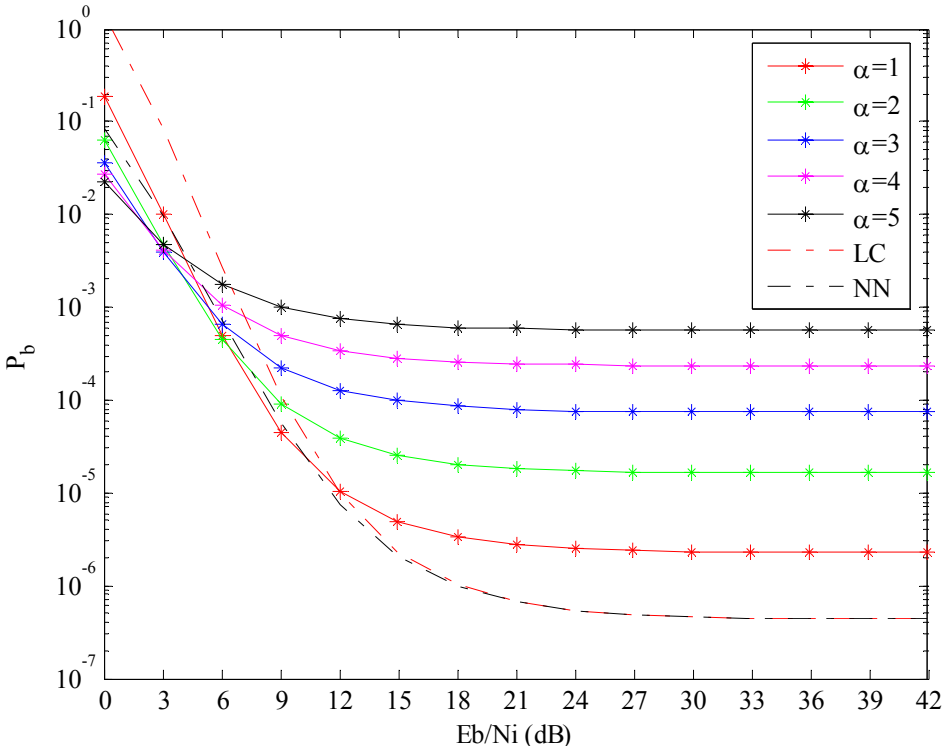

Figure 23. Modified noise-normalized receiver with PNI for non fading different values of the coefficient α and ρ=0.5.

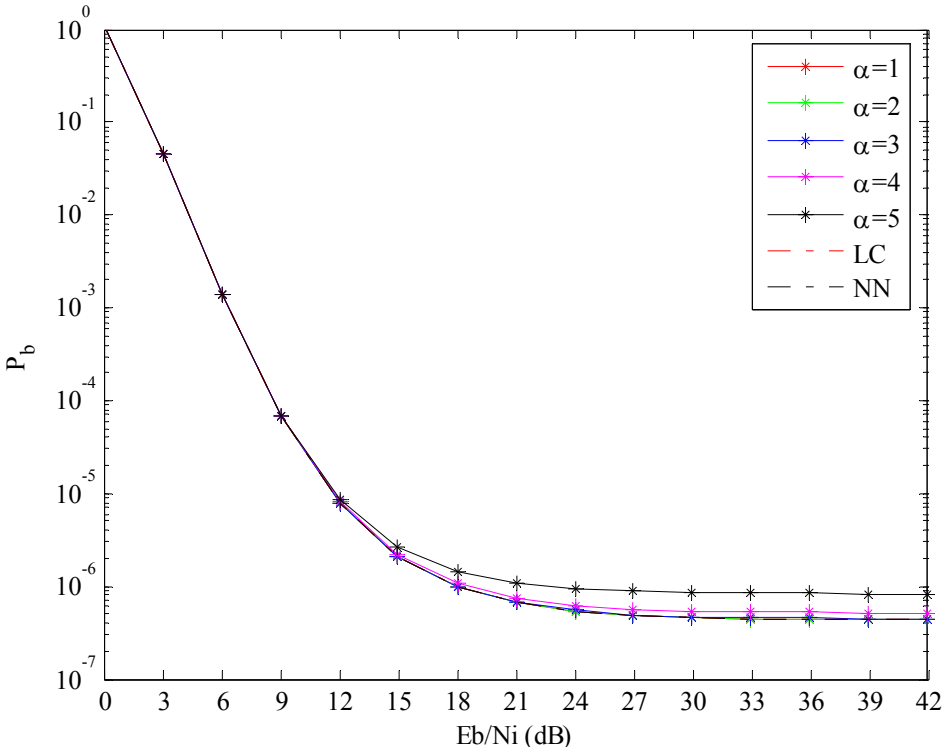

Figure 24. Modified noise-normalized receiver with PNI for non fading different values of the coefficient α and ρ=0.9999.

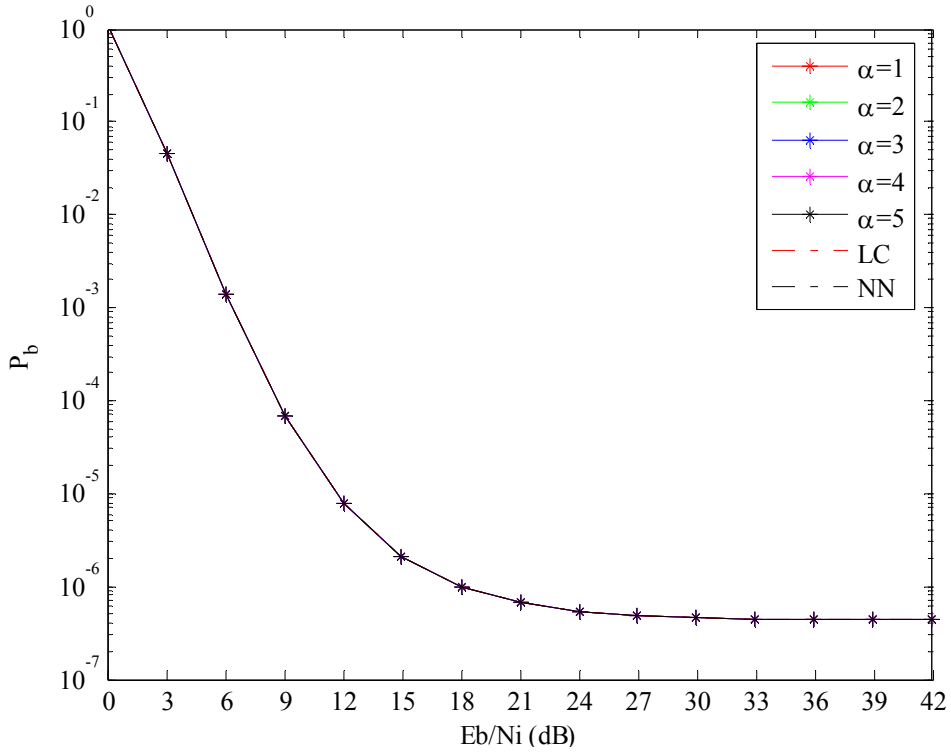

Figure 25. Modified noise-normalized receiver with PNI for non fading different values of the coefficient α and ρ=1

2. Performance Analysis for the Same Values of the Coefficient α

For BPSK/QPSK modulation, where the data rates are 6 and 12 Mbps, respectively, the code rate is $r = 1/2$ and the weight structure B_d and the free distance d_{free} are given in Table 2, P_b for the same values of the coefficient α is plotted in Figures 26, 27, 28, 29, 30, and 31. All the figures are for $E_b / N_o = 5\,dB$.

We notice that as the coefficient α becomes larger, the difference in P_b for $E_b/N_i = 0\ dB$ and $E_b/N_i = 42\ dB$ decreases, i.e., the difference for ρ=0.1 and α=1 is $\Delta(P_b) \approx 1.1 \cdot 10^{-1}$, but for α=7, $\Delta(P_b) \approx 5.9 \cdot 10^{-5}$ We also see that for large values of the coefficient α, the smaller the parameter ρ is the better the performance. This is obvious for $\alpha \geq 7$.

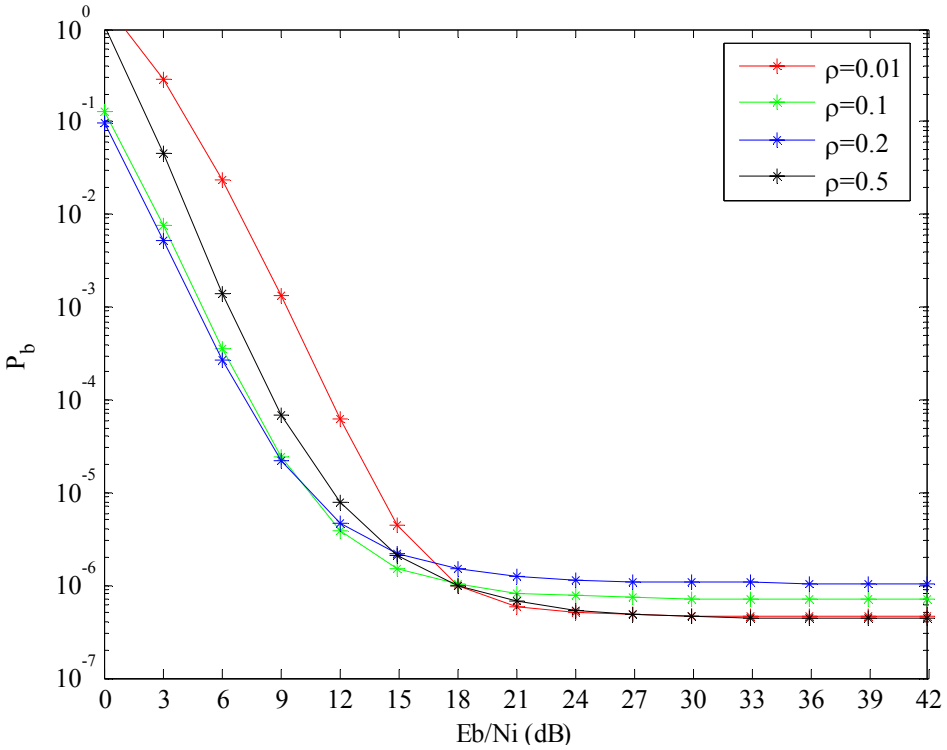

Figure 26. Modified noise-normalized receiver with PNI for non fading different values of the coefficient ρ and α=1.

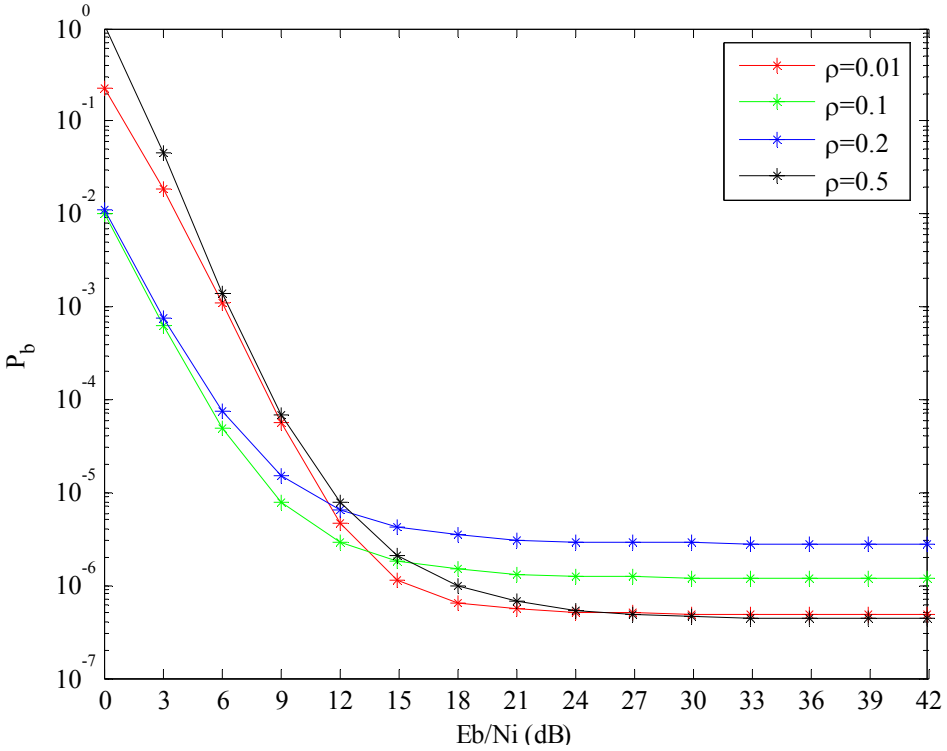

Figure 27. Modified noise-normalized receiver with PNI for non fading different values of the coefficient ρ and α=2.

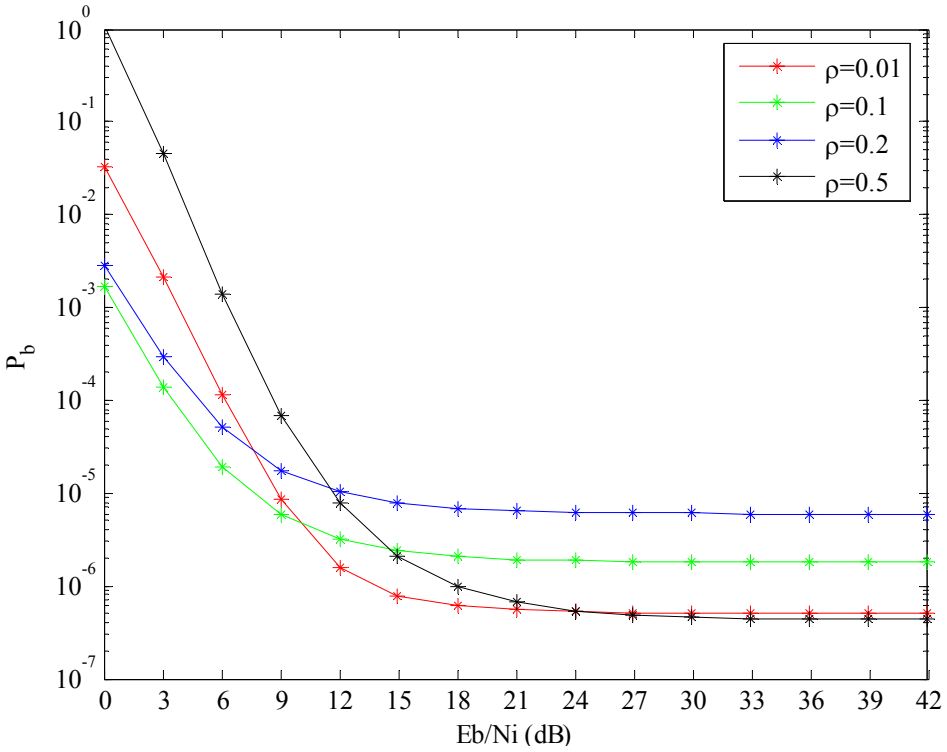

Figure 28. Modified noise-normalized receiver with PNI for non fading different values of the coefficient ρ and α=3.

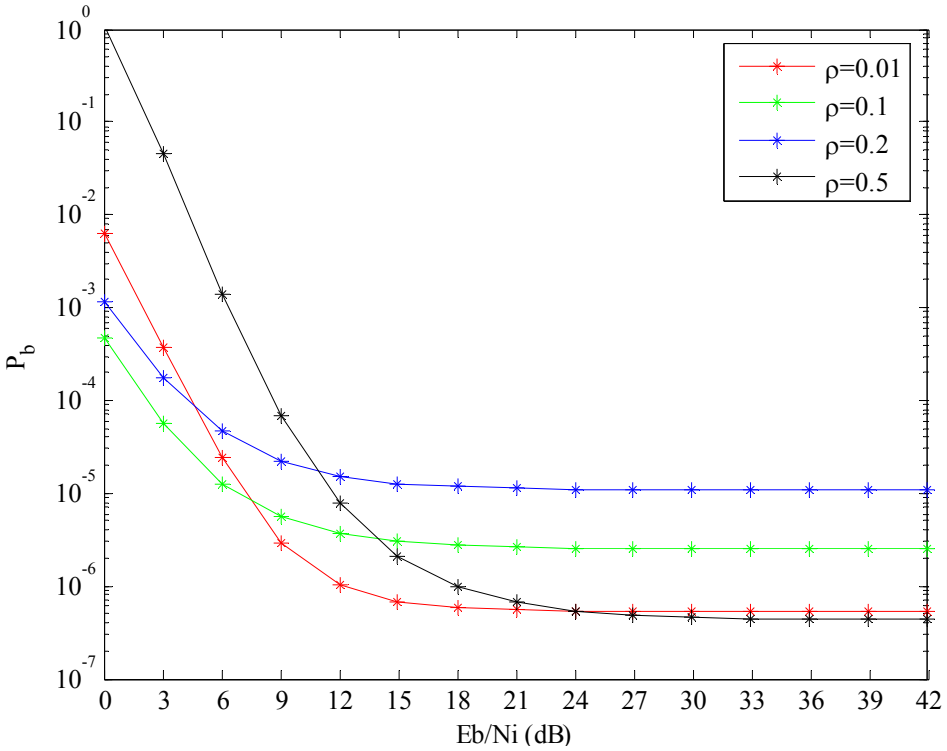

Figure 29. Modified noise-normalized receiver with PNI for non fading different values of the coefficient ρ and α=4.

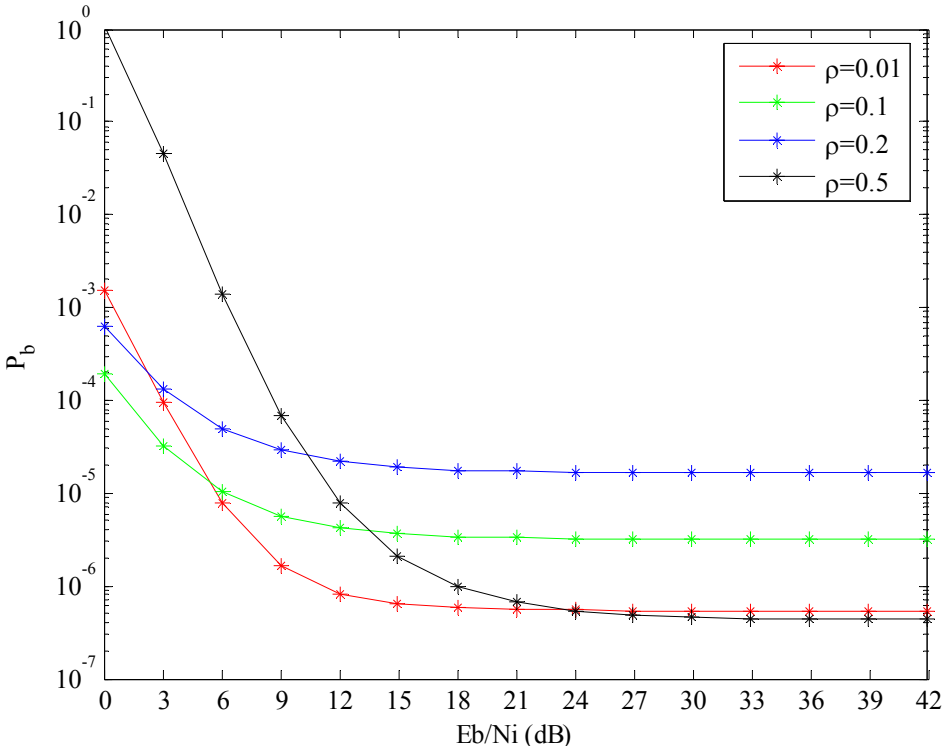

Figure 30. Modified noise-normalized receiver with PNI for non fading different values of the coefficient ρ and α=5.

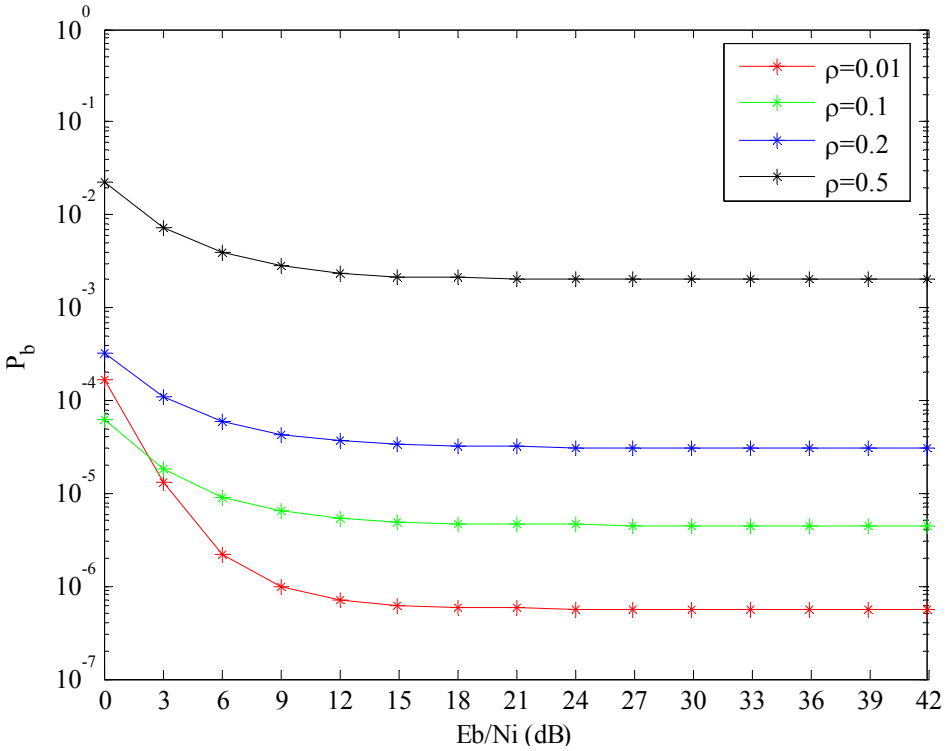

Figure 31. Modified noise-normalized receiver with PNI for non fading different values of the coefficient ρ and α=7.

D. PERFORMANCE ANALYSIS WITH HOSTILE PULSE-NOISE INTERFERENCE IN A FADING CHANNEL

Having examined the performance of the modified noise-normalized receiver for a non fading channel, we now examine its performance for a fading channel with PNI.

The noise power at the output of the integrator for each received bit is given in Equation (4.16). Since the signal $s(t)$ is transmitted over a Nakagami fading channel, the amplitude of the signal changes from bit to bit, and Equations (5.18) must be rewritten as

$$\overline{Z} = \sum_{k=1}^{d-i} \frac{\sqrt{2}a_c}{\sigma_o} + \sum_{k=1}^{i} \frac{\sqrt{2}a_c}{\sigma_o(1+\alpha)} \tag{5.21}$$

The variance is the same as for no fading and is given by Equation (5.19). The conditional probability P_d is calculated by combining Equations (3.5), (5.19), and (5.21):

$$\begin{aligned} P_d\left(\sum_{k=1}^{d} A_c\right) &= Q\left(\frac{\sum_{k=1}^{d-i} \frac{\sqrt{2}a_c}{\sigma_o} + \sum_{k=1}^{i} \frac{\sqrt{2}a_c}{\sigma_o(1+\alpha)}}{\sqrt{(d-i) + \frac{i}{(1+\alpha)^2}\left(1+\frac{\sigma_j^2}{\sigma_o^2}\right)}}\right) \\ &= Q\left(\frac{\sqrt{2}\left(\gamma_{b_o} + \gamma_{b_j}\right)}{\sqrt{(d-i) + \frac{i}{(1+\alpha)^2}\left(1+\frac{\sigma_j^2}{\sigma_o^2}\right)}}\right) \end{aligned} \tag{5.22}$$

where

$$\gamma_{b_j} = \sum_{k=1}^{i} \gamma_{b_{k_j}} = \sum_{k=1}^{i} \frac{a_c}{\sigma_o(1+\alpha)} \tag{5.23}$$

and

$$\gamma_{b_o} = \sum_{k=1}^{d-i} \gamma_{b_{k_0}} = \sum_{k=1}^{d-i} \frac{a_c}{\sigma_o} \tag{5.24}$$

The PDF $f_{\Gamma_{b_{k_j}}}$ of the random variable representing the k^{th} bit $\gamma_{b_{k_j}}$ is obtained from

$$f_{\Gamma_{b_{k_j}}}(\gamma_{b_{k_j}}) = \left|\frac{da_c}{d\gamma_{b_{k_j}}}\right| f_{A_c}(a_c)\Big|_{a_c=\gamma_{b_{k_j}}\sigma_o(1+\alpha)} \tag{5.25}$$

where $f_{A_c}(a_c)$ is the Nakagami-*m* PDF as defined in Equation (2.6). From Equation (5.23) we get

$$\left|\frac{da_c}{d\gamma_{b_{k_j}}}\right| = \sigma_o(1+\alpha) \tag{5.26}$$

so

$$\begin{aligned} f_{\Gamma_{b_{k_j}}}(\gamma_{b_{k_j}}) &= \sigma_o(1+\alpha)\frac{2}{\Gamma(m)}\left(\frac{m}{\overline{a_c^2}}\right)^m \left(\gamma_{b_{k_j}}\sigma_o(1+\alpha)\right)^{2m-1} e^{\left(-\frac{m\left(\gamma_{b_{k_j}}\sigma_o(1+\alpha)\right)^2}{\overline{a_c^2}}\right)} \\ &= \frac{2}{\Gamma(m)}\left(\frac{m\sigma_o^2(1+\alpha)^2}{\overline{a_c^2}}\right)^m \left(\gamma_{b_{k_j}}\right)^{2m-1} e^{\left(-\frac{m\gamma_{b_{k_j}}^2\sigma_o^2(1+\alpha)^2}{\overline{a_c^2}}\right)} \end{aligned} \tag{5.27}$$

If we substitute $\overline{\gamma_{b_j}} = \frac{\sigma_o^2(1+\alpha)^2}{\overline{a_c^2}}$, Equation (5.27) simplifies to

$$f_{\Gamma_{b_k}}(\gamma_{b_{k_j}}) = \frac{2}{\Gamma(m)}\left(m\overline{\gamma_{b_j}}\right)^m \left(\gamma_{b_{k_j}}\right)^{2m-1} e^{\left(-m\gamma_{b_{k_j}}^2\,\overline{\gamma_{b_j}}\right)} \tag{5.28}$$

where

$$\overline{\gamma_{b_j}} = \frac{\sigma_o^2(1+\alpha)^2}{\overline{a_c^2}} = \frac{N_o(1+\alpha)^2}{T_s\overline{a_c^2}} = \frac{(1+\alpha)^2}{r}\left(\frac{E_b}{N_o}\right)^{-1} \tag{5.29}$$

The PDF $f_{\Gamma_{b_{k_o}}}$ is the same as Equation (5.19) and for convenience is repeated:

$$f_{\Gamma_{b_{k_o}}}(\gamma_{b_{k_o}}) = \frac{2}{\Gamma(m)}\left(m\overline{\gamma_{b_{k_o}}}\right)^m \left(\gamma_{b_{k_o}}\right)^{2m-1} e^{\left(-m\gamma_{b_{k_o}}^2\,\overline{\gamma_{b_{k_o}}}\right)} \tag{5.30}$$

where

$$\overline{\gamma_{b_{k_o}}} = \frac{\sigma_o^2}{\overline{a_c^2}} = \frac{N_o}{T_s \overline{a_c^2}} = \frac{N_o}{rT_b \overline{a_c^2}} = \frac{1}{r}\frac{N_o}{E_b} = \frac{1}{r}\left(\frac{E_b}{N_o}\right)^{-1} \tag{5.31}$$

The overall PDF $f_{\Gamma_b}(\gamma_b)$ must be evaluated numerically from Equation (3.26), combined with Equations (4.34), (5.28), and (5.30).

Having found the overall PDF, we are now ready to calculate to the upper bound on the probability P_b using Equations (3.12), (3.16), (5.22) and the numerical calculation of the PDF found above.

1. Performance Analysis for Fading Channels

The performance of the modified noise-normalized combining receiver for different fading conditions is now examined. For $r = 1/2$ and for the weight structure B_d and the free distance d_{free} of Table 2, we get Figures 32, 33, and 34 where the probability of bit error is plotted for the same fading conditions and for different values of the coefficients ρ and α. All the figures are for $E_b / N_o = 15\,\text{dB}$.

We see that P_b for different values of α does not converge for large E_b/N_i. For small values of E_b/N_i, the modified noise-normalized receiver has better performance than the linear-combining receiver but worse than the noise-normalized. The value of E_b/N_i where the modified noise-normalized receiver is better than linear-combining becomes smaller as the parameter *m* becomes larger. Finally, for small values of E_b/N_i, the larger the coefficient α is, the better the performance. The best value of α depends on the parameter *m* and the coefficient ρ.

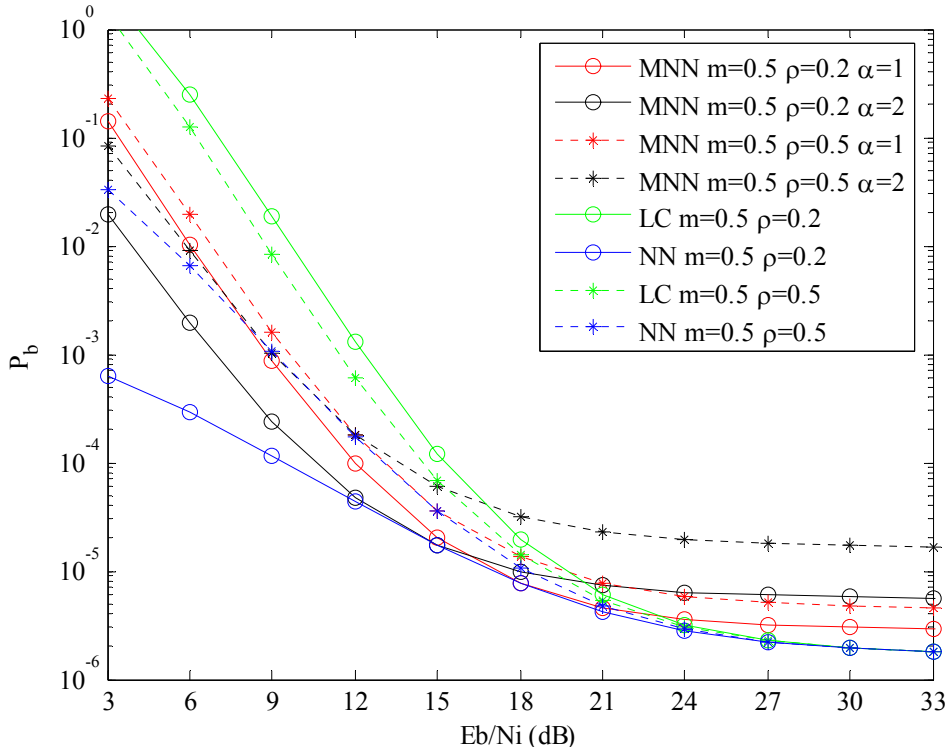

Figure 32. Modified noise-normalized receiver with PNI for different values of the coefficients ρ and α with m=0.5.

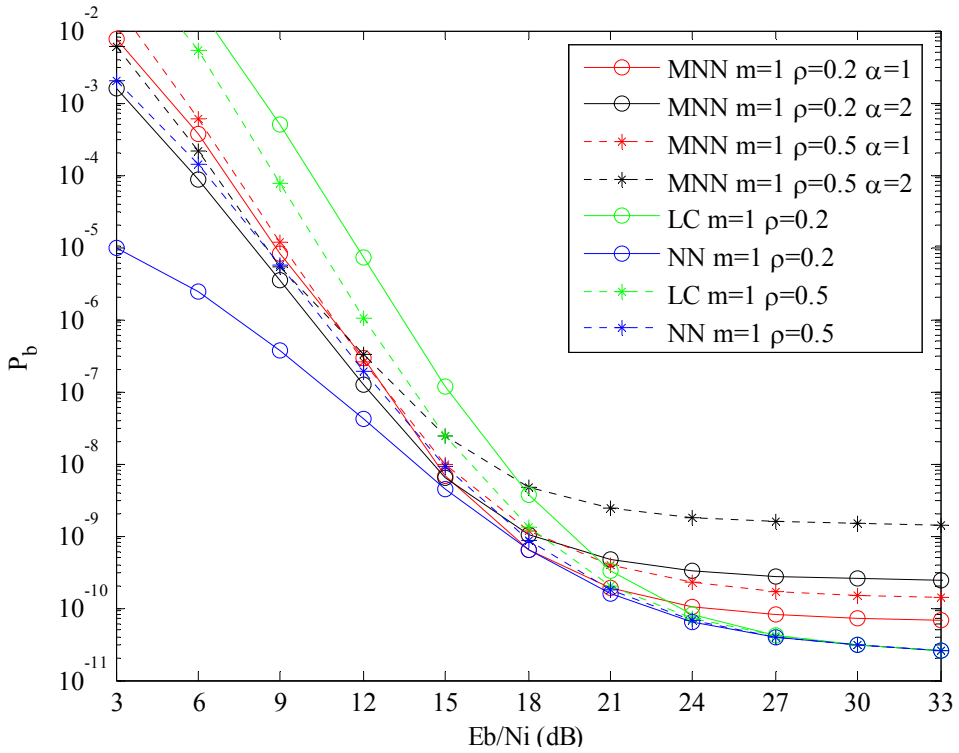

Figure 33. Modified noise-normalized receiver with PNI for different values of the coefficients ρ and α with m=1.

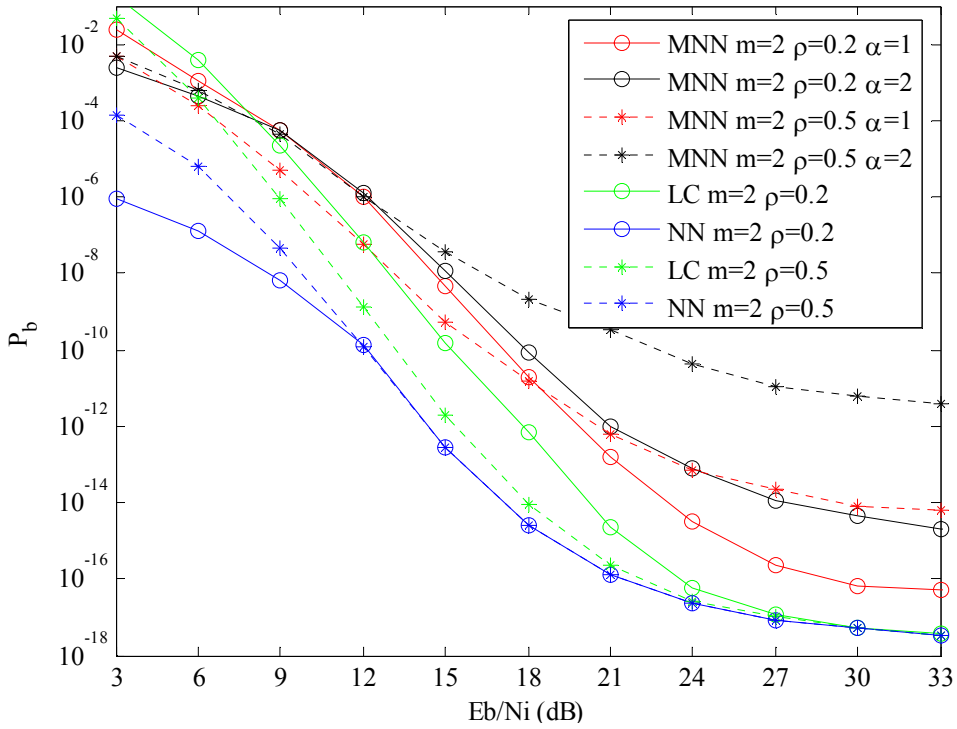

Figure 34. Modified noise-normalized receiver with PNI for different values of the coefficients ρ and α with m=2.

2. Performance Analysis as Function of the Coefficient α

If we compare the performance of the modified noise-normalized combining receiver for the same values of the coefficient α, we see that for small values of the parameter m (more severe fading conditions), the larger the coefficient ρ is, the better the performance of the receiver. This does not happen for less severe fading conditions. For example, for m=2, where the performance of the receiver for small values of the E_b/N_i is better for ρ=0.2 than for ρ=0.5. We see that for m=1, the performance is better than for m=0.5, but for m=2, for small values of the E_b/N_i, the performance is worse. In other words, the receiver behaves better for more severe fading conditions than for less severe.

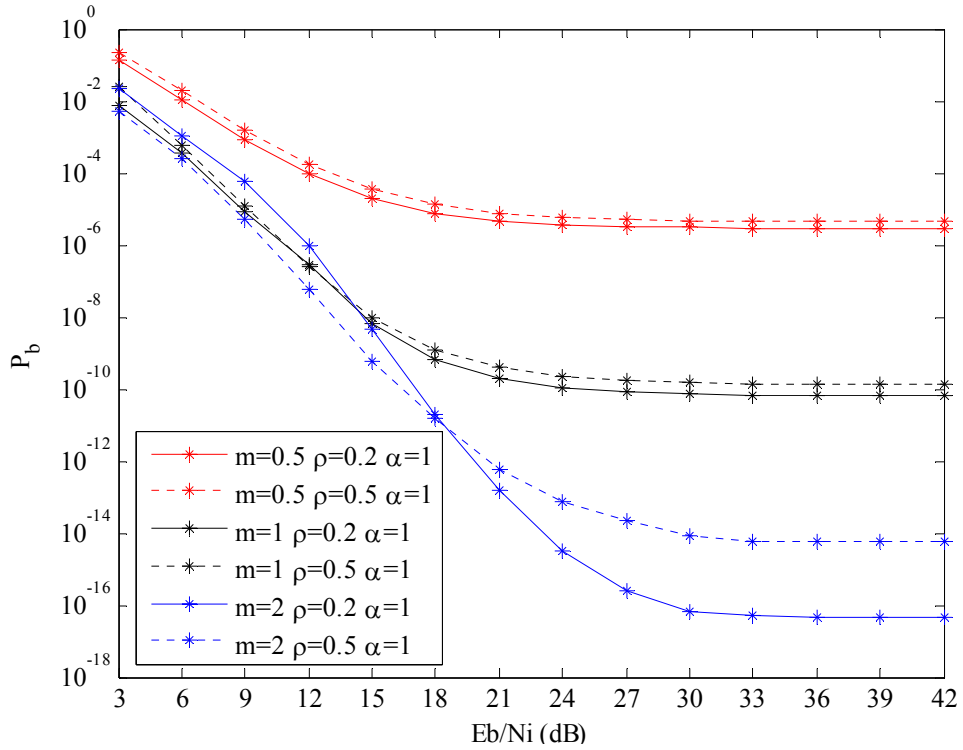

Figure 35. Modified noise-normalized combining receiver for different fading conditions and for different values of the coefficient ρ with α=1.

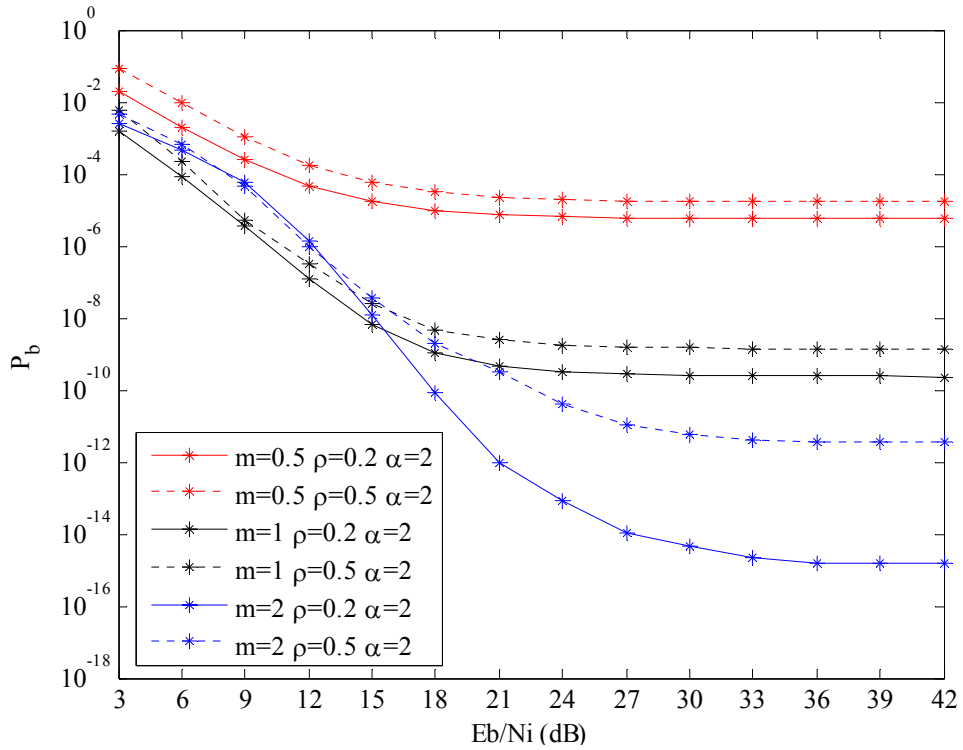

Figure 36. Modified noise-normalized combining receiver for different fading conditions and for different values of the coefficient ρ with α=2.

3. Performance Analysis for the Same Value of the Coefficient ρ.

In Figures 37 and 38 we have plotted P_b for the same values of the coefficient ρ. We see that for the same values of the parameter m and small values of E_b/N_i, the receiver has better performance for small values of α than for large. The value of the E_b/N_i where this property reverses depends on the value of ρ. The larger ρ is, this property reverses for larger values of the E_b/N_i. We notice as before that for m=1, the performance is better than for m=0.5 for all E_b/N_i, but for m=2 and small values of the E_b/N_i, the performance of the receiver is worse than for m=1.

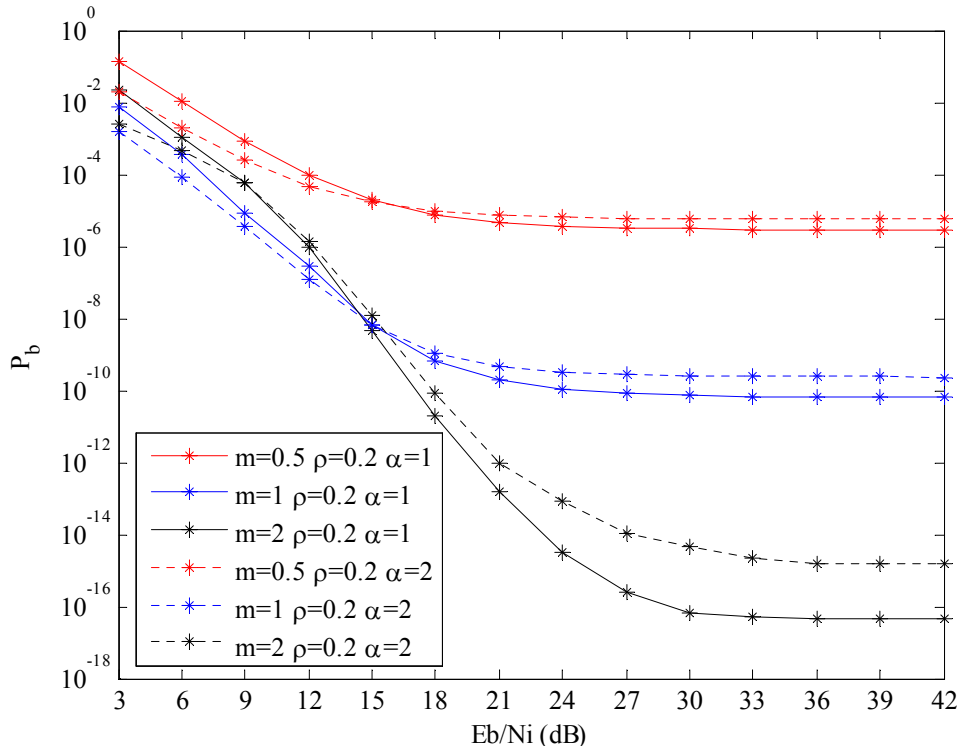

Figure 37. Modified noise-normalized combining receiver for different fading conditions and for different values of the coefficient α with ρ=0.2.

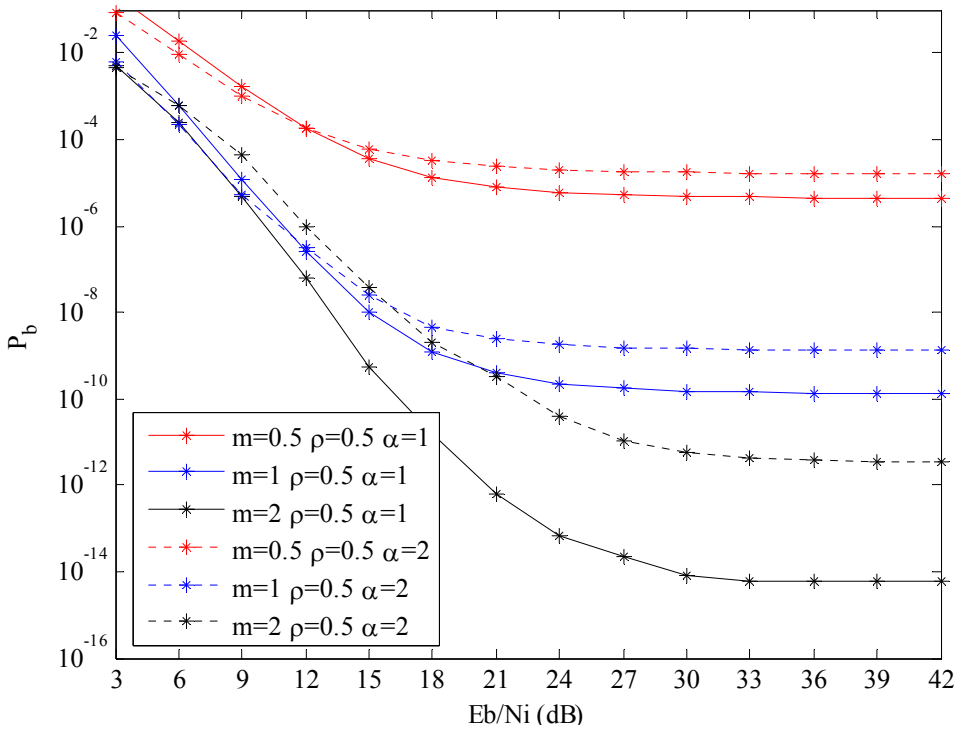

Figure 38. Modified noise-normalized combining receiver for different fading conditions and for different values of the coefficient α with ρ=0.5.

E. SUMMARY

In this chapter we examined the performance of OFDM signals transmitted over frequency-selective, slowly fading Nakagami channels in an AWGN plus pulse-interference environment using a modified noise-normalized combining receiver. This receiver is an alternative to the noise-normalized receiver, where the goal is to design a type of receiver which does not require detailed side information such as the exact noise power of the interference.

In the next chapter we investigate the noise-normalized combining receiver with normalization error, which is another alternative to the noise-normalized combining receiver, where the noise power of the receiver is imperfectly estimated and used to improve performance when PNI is present.

THIS PAGE INTENTIONALLY LEFT BLANK

VI. PERFORMANCE ANALYSIS OF OFDM SIGNALS TRANSMITTED OVER FREQUENCY-SELECTIVE, SLOWLY FADING NAKAGAMI CHANNELS IN AN AWGN PLUS PULSE-INTERFERENCE ENVIRONMENT WITH NOISE-NORMALIZED COMBINING WITH NORMALIZATION ERROR AND VITERBI SOFT DECISION DECODING (SDD)

In this chapter the performance of OFDM signals transmitted over frequency-selective, slowly fading Nakagami channels in an AWGN plus pulse-interference environment with noise-normalized combining with normalization error and Viterbi soft decision decoding is examined.

The noise-normalized combining receiver with normalization error is another approximation of the noise-normalized combining receiver. For this receiver, the noise power of the receiver is estimated and this estimation is used to improve performance when PNI is present.

A. THE NOISE-NORMALIZED COMBINING RECEIVER WITH NORMALIZATION ERROR

The model of the noise-normalized combining receiver with normalization error (NNne), when BPSK modulation is used, is presented in Figure 39.

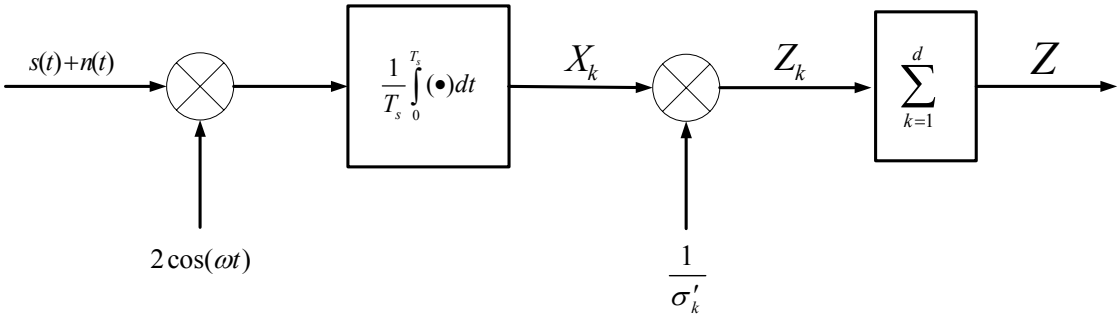

Figure 39. The noise-normalized combining receiver with normalization error.

As we see in Figure 39, X_k is divided after the integrator by an estimation of the noise power which is given by

$$\sigma_k'^2 = \begin{cases} \sigma_o^2 + \alpha\sigma_j^2, & \text{when PNI is operational} \\ \sigma_o^2, & \text{otherwise} \end{cases} \tag{6.1}$$

where σ_o^2 is the AWGN noise power, σ_j^2 is the interference noise power and α is a constant that indicates the normalization error. When α=1, there are no errors.

As in all cases already examined, the integrator's output X_k is modelled as a GRV with the mean and the variance given by Equations (3.3) and (3.4), respectively.

After the integrator, the random variable X_k is divided by the noise power given in Equation (6.1), so the signal becomes

$$Z_k = \frac{X_k}{\sigma_k'} \tag{6.2}$$

or

$$X_k = Z_k \sigma_k' \tag{6.3}$$

Since X_k is a GRV, Z_k is also a GRV. The PDFs of random variables X_k are given by Equations (3.1) and (3.2). Changing variables, we get the PDF of Z_k from

$$f_{Z_k}(z_k) = \left|\frac{dX_k}{dZ_k}\right| f_{X_k}(x_k)\Big|_{Z_k = Z_k\sigma_k'} \tag{6.4}$$

From Equation (6.3), we have

$$\left|\frac{dX_k}{dZ_k}\right| = \sigma_k' \tag{6.5}$$

Therefore,

$$f_{Z_k}(z_k) = \frac{\sigma_k'}{\sqrt{2\pi}\sigma_{x_k}} e^{\left[-\frac{(z_k\sigma_k' - \overline{X_k})^2}{2\sigma_{x_k}^2}\right]} = \frac{1}{\sqrt{2\pi}\left(\sigma_k/\sigma_k'\right)} e^{\left[-\frac{(z_k - (\overline{X_k}/\sigma_k'))^2}{2\left(\sigma_k^2/\sigma_k'^2\right)}\right]} \tag{6.6}$$

From Equation (6.6), we see that the mean of Z_k is

$$\overline{Z_k} = \frac{\overline{X}}{\sigma'_k} = \frac{\sqrt{2}a_c}{\sigma'_k} \tag{6.7}$$

and the variance is

$$\sigma^2_{z_k} = \frac{\sigma^2_k}{\sigma'^2_k} \tag{6.8}$$

The decision variable for the sequence of d bits is given by

$$Z = \sum_{k=1}^{d} Z_k \tag{6.9}$$

Hence, from Equations (6.7) and (6.8),

$$\overline{Z} = \sum_{k=1}^{d} \frac{\sqrt{2}a_c}{\sigma'_k} = \sum_{k=1}^{d-i} \frac{\sqrt{2}a_c}{\sigma_o} + \sum_{k=1}^{i} \frac{\sqrt{2}a_c}{\sqrt{\sigma_o^2 + \alpha\sigma_j^2}} \tag{6.10}$$

and

$$\sigma_z^2 = \sum_{k=1}^{d} \frac{\sigma_k^2}{\sigma'^2_k} = \sum_{k=1}^{d-i} \frac{\sigma_o^2}{\sigma_o^2} + \sum_{k=1}^{i} \frac{\sigma_o^2 + \sigma_j^2}{\sigma_o^2 + \alpha\sigma_j^2} = (d-i) + i\frac{1+\left(\sigma_j^2/\sigma_o^2\right)}{1+\alpha\left(\sigma_j^2/\sigma_o^2\right)} \tag{6.11}$$

since Z is the sum of d independent, Gaussian random variables.

B. PERFORMANCE ANALYSIS IN A FADING CHANNEL WITH AWGN

The performance analysis of this receiver with AWGN with soft decision Viterbi decoding is now examined. The noise-normalized combing receiver with normalization error is identical to the other receivers examined in previous chapters at the output of the integrator. The receiver is subject only to AWGN; therefore, each bit is corrupted by the same amount of noise power $\sigma_o^2 = N_o / T_s$. Hence,

$$\sigma_k = \sigma_o \tag{6.12}$$

and Equations (6.10) and (6.11) can be rewritten as

$$\overline{Z} = \sum_{k=1}^{d} \frac{\sqrt{2}a_c}{\sigma'_k} = \sum_{k=1}^{d} \frac{\sqrt{2}a_c}{\sigma_o} \tag{6.13}$$

and

$$\sigma_z^2 = \sum_{k=1}^{d} \frac{\sigma_k^2}{\sigma_k'^2} = \sum_{k=1}^{d} \frac{\sigma_o^2}{\sigma_o^2} = d \tag{6.14}$$

The probability P_d is given in Equation (3.5). Substituting (6.13) and (6.14) into (3.5), we get

$$P_d\left(\sum_{k=1}^{d} a_c\right) = Q\left(\frac{\sum_{k=1}^{d} \frac{\sqrt{2}a_c}{\sigma_o}}{\sqrt{d}}\right) = Q\left(\sqrt{\frac{2}{d}}\sum_{k=1}^{d} \frac{a_c}{\sigma_o}\right) \tag{6.15}$$

If we substitute $\sum_{k=1}^{d} \frac{a_c}{\sigma_0}$ with γ_b, we obtain the same conditional probability P_d as for the linear-combining receiver

$$P_d\left(\gamma_b\right) = Q\left(\sqrt{\frac{2}{d}}\gamma_b\right) \tag{6.16}$$

where

$$\gamma_b = \sum_{k=1}^{d} \gamma_{b_k} = \sum_{k=1}^{d} \frac{a_c}{\sigma_o} \tag{6.17}$$

Equation (6.16) is identical to Equation (3.14), and Equation (6.17) is identical to Equation (3.17); therefore, the probability of bit error of the noise-normalized combining receiver with normalization error is the same exactly as for linear-combining. This is expected since the receiver is subject only to AWGN, and the normalization has no effect.

C. PERFORMANCE ANALYSIS WITH HOSTILE PULSE-NOISE INTERFERENCE IN A NON FADING CHANNEL

Having examined the performance of the noise-normalized combining receiver with normalization error in a fading channel with AWGN, the performance of the receiver for a non fading channel with PNI is now examined.

As was the case in the proceeding chapters, the noise that arrives at the receiver differs from bit to bit since each bit is affected by different amounts of noise power σ_{x_k}. A number of bits are affected by both AWGN and the interference signal (i bits), and the remaining are affected by AWGN only ($d-i$ bits). As a result, the noise power at the output of the integrator for each received bit is given in Equation (4.16).

Since the channel is non fading, Equation (6.10) can be written

$$\overline{Z} = (d-i)\frac{\sqrt{2}A_c}{\sigma_o} + i\frac{\sqrt{2}A_c}{\sqrt{\sigma_o^2 + \alpha\sigma_j^2}} \tag{6.18}$$

The combination of Equations (3.5), (6.11), and (6.18) gives us

$$P_d\left(\sum_{k=1}^{d} A_c\right) = Q\left(\sqrt{\frac{\left((d-i)\frac{\sqrt{2}A_c}{\sigma_o} + i\frac{\sqrt{2}A_c}{\sqrt{\sigma_o^2+\alpha\sigma_j^2}}\right)^2}{(d-i) + i\frac{1+\left(\sigma_j^2/\sigma_o^2\right)}{1+\alpha\left(\sigma_j^2/\sigma_o^2\right)}}}\right)$$

$$= Q\left(\sqrt{2r\frac{E_b}{N_o}\frac{\left((d-i) + \frac{i}{\sqrt{1+\frac{\alpha}{\rho}\left[\left(\frac{E_b}{N_i}\right)^{-1}\Big/\left(\frac{E_b}{N_o}\right)^{-1}\right]}}\right)^2}{\frac{1+\frac{1}{\rho}\left[\left(\frac{E_b}{N_i}\right)^{-1}\Big/\left(\frac{E_b}{N_o}\right)^{-1}\right]}{(d-i) + i\frac{1+\frac{\alpha}{\rho}\left[\left(\frac{E_b}{N_i}\right)^{-1}\Big/\left(\frac{E_b}{N_o}\right)^{-1}\right]}{1+\frac{\alpha}{\rho}\left[\left(\frac{E_b}{N_i}\right)^{-1}\Big/\left(\frac{E_b}{N_o}\right)^{-1}\right]}}}}\right) \tag{6.19}$$

The combination of Equations (3.12), (3.33), and (6.19) gives us the probability P_b for the noise-normalized combining receiver with normalization error.

1. Performance Analysis for the Same Value of the Coefficient α.

For BPSK/QPSK modulation, $r = 1/2$, and the weight structure B_d and the free distance d_{free} given in Table 2, we get Figures 40, 41, and 42 for the same value of the coefficient α. All the figures are for $E_b / N_o = 5\,\text{dB}$.

As we can see, for α=0.1 (when our estimation of the power of the jammer is poor), the performance of the receiver is worse than for larger values of the coefficient α unless E_b/N_i □ 1. For small E_b/N_i, the smaller ρ is, the better the performance of the noise-normalized receiver with normalization error. This does not happen for large values of E_b/N_i. For α=1 and α=2, as the coefficient ρ gets smaller, the performance of the receiver improves when $\rho < 1$. In other words, as the instantaneous jammer's power increases, the performance of the receiver improves.

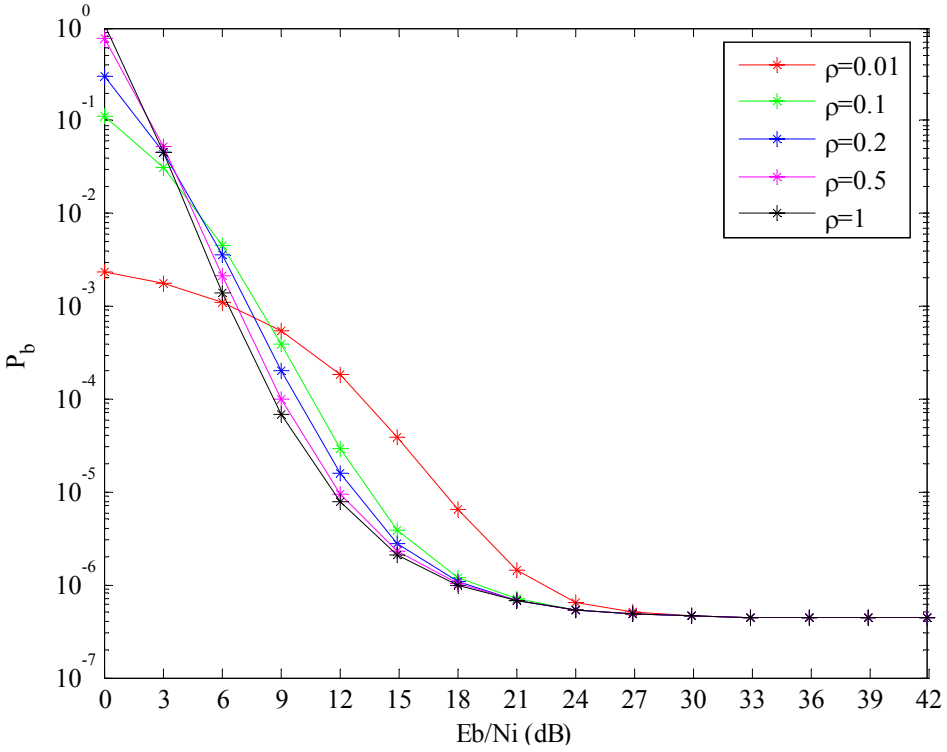

Figure 40. Noise-normalized combining receiver with normalization error with PNI for non fading for α =0.1.

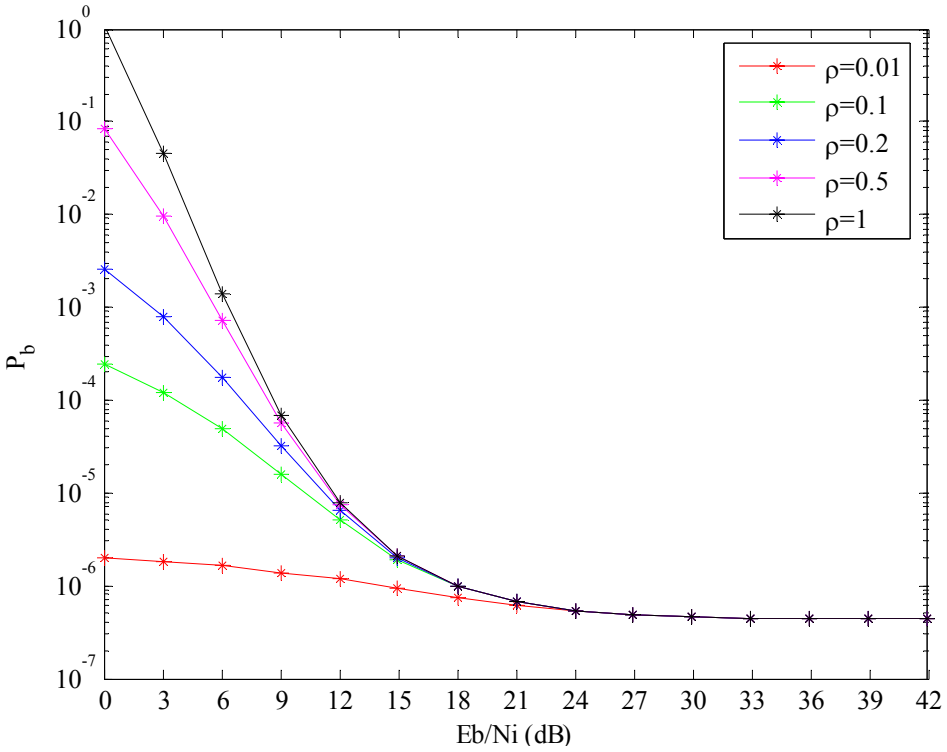

Figure 41. Noise-normalized combining receiver with normalization error with PNI for non fading for α =1.

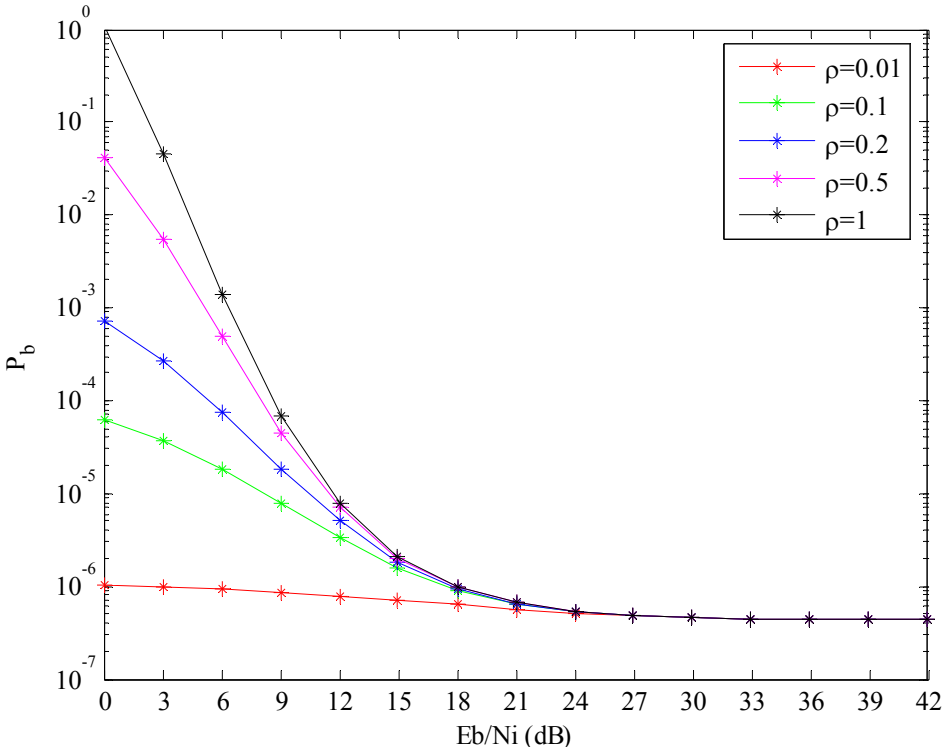

Figure 42. Noise-normalized combining receiver with normalization error with PNI for non fading for α =2.

2. Performance Analysis for the Same Value of the Coefficient ρ.

For BPSK/QPSK modulation, $r = 1/2$, and the weight structure B_d and the free distance d_{free} given in Table 2, we get Figures 43, 44, 45, 46, and 47 for the probability of bit error for the same value of the coefficient ρ. All the figures are for $E_b / N_o = 5\,\text{dB}$.

We first note that for α=1, the performance of the noise-normalized combining receiver with normalization error is exactly the same as the noise-normalized combining receiver, which is expected since the noise-normalized combining receiver with normalization error is identical to the noise-normalized combining receiver for α=1. The second thing we notice is that for any value of the coefficient α, the modified noise-normalized combining receiver with normalization error has better performance than the linear-combining receiver. We also see that when we overestimate the jammer's power, the receiver has better performance than when we underestimate the jammer's power. Finally, when we overestimate the jammer's power, the receiver has better performance than the ideal noise-normalized combining receiver. For example, for ρ=0.2, α=2, and $P_b = 1.1\times10^{-3}$, the noise-normalized combining receiver requires about 3.1 dB more power in order to achieve the same performance and the linear-combining receiver requires 8.4 dB more power than the noise-normalized combining receiver with normalization error.

Finally, we see that for small values of E_b / N_i, there are values of E_b / N_i where the modified noise-normalized receiver has better performance than the noise-normalized receiver with normalization error. The values of E_b / N_i, where this happens depends on the coefficient ρ.

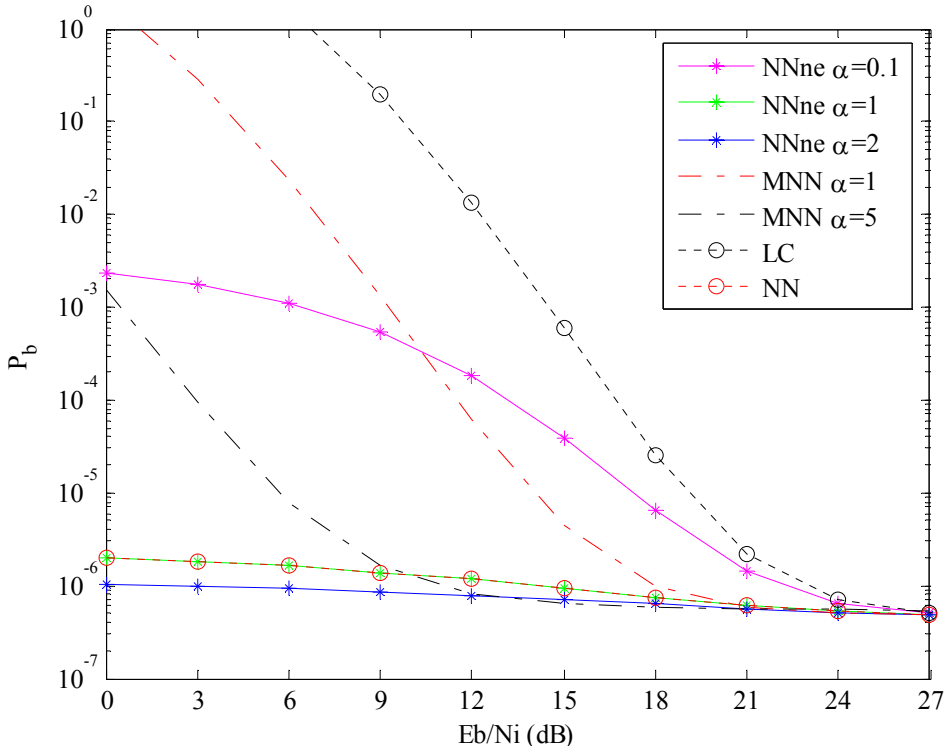

Figure 43. Noise-normalized combining receiver with normalization error with PNI for non fading for ρ=0.01.

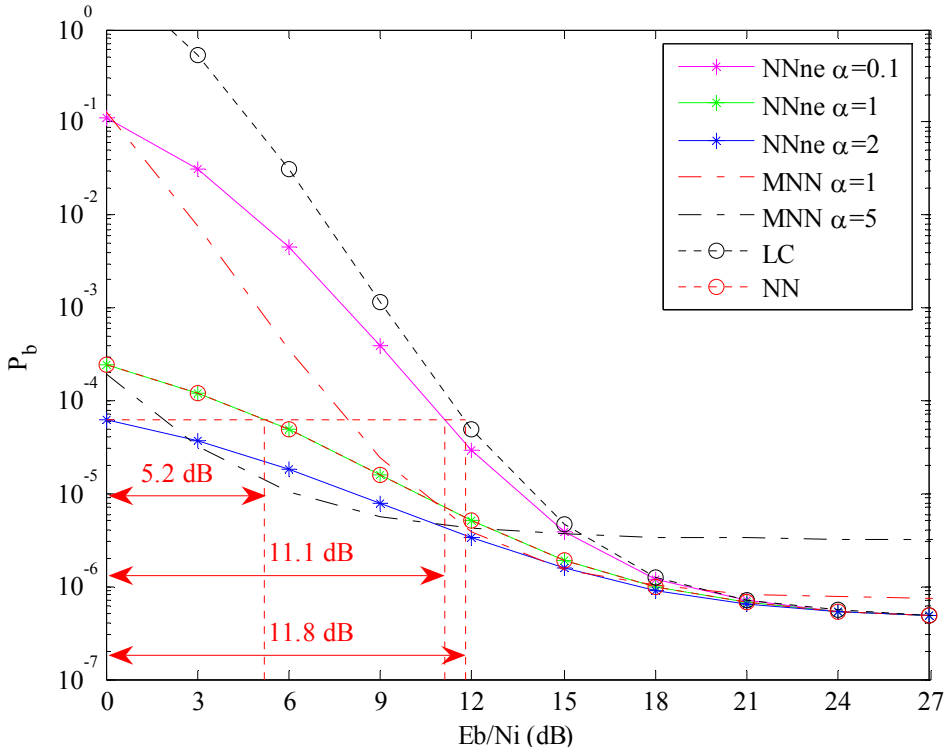

Figure 44. Noise-normalized combining receiver with normalization error with PNI for non fading for ρ=0.1.

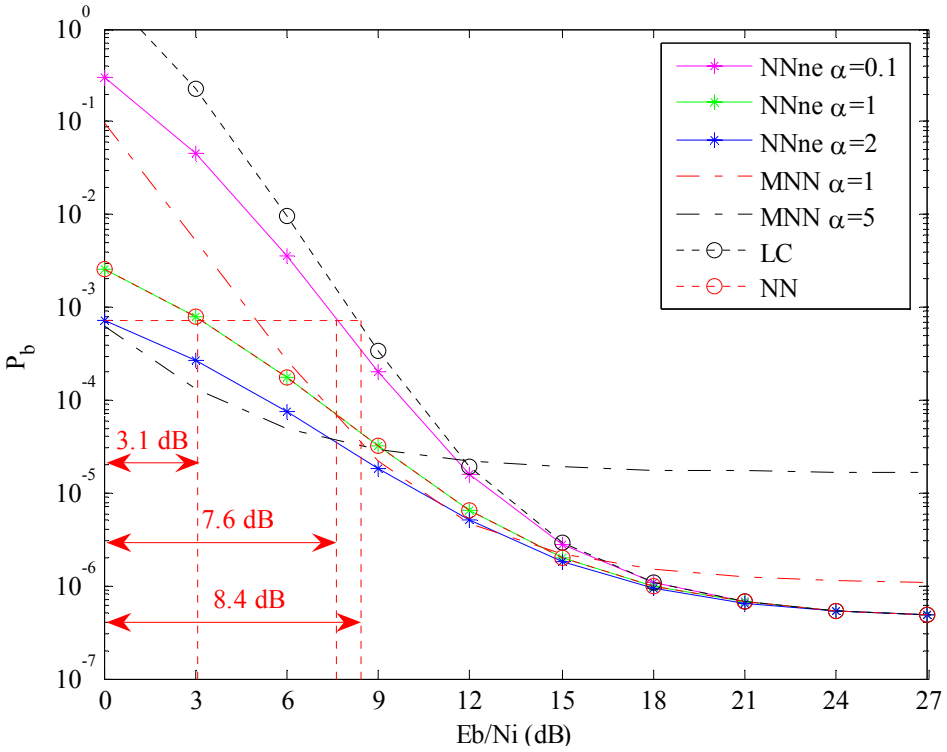

Figure 45. Noise-normalized combining receiver with normalization error with PNI for non fading for ρ=0.2.

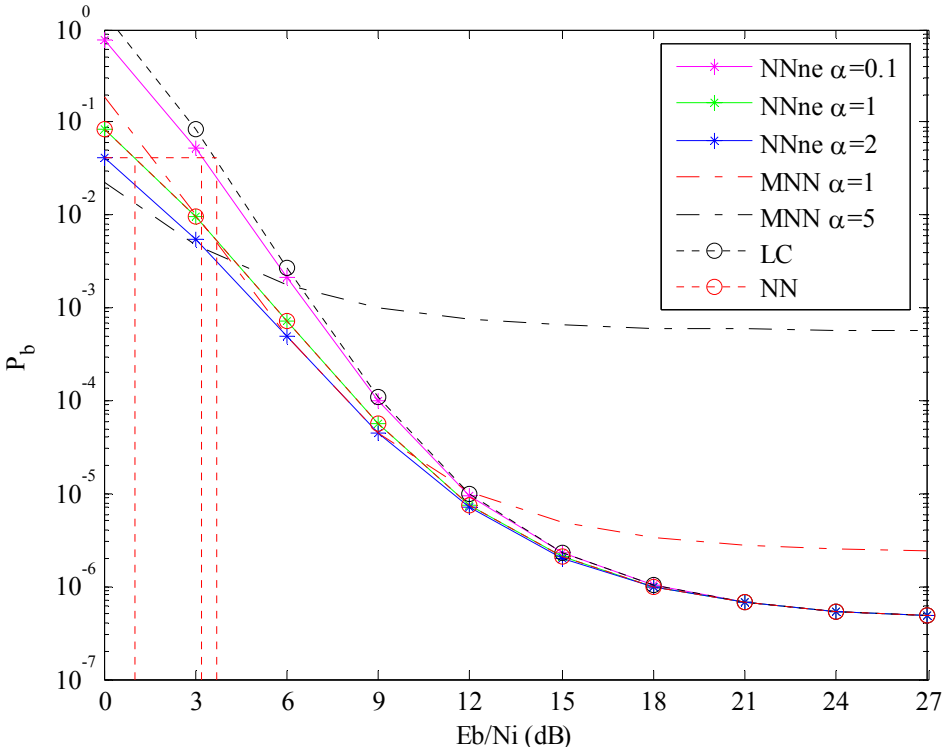

Figure 46. Noise-normalized combining receiver with normalization error with PNI for non fading for ρ=0.5.

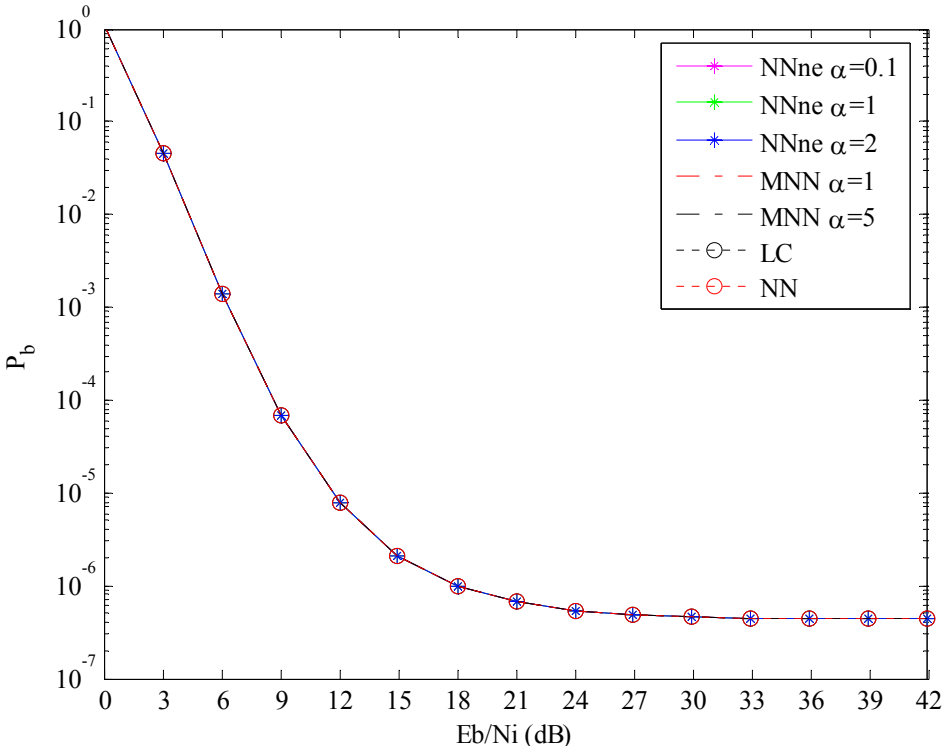

Figure 47. Noise-normalized combining receiver with normalization error with PNI for non fading for ρ=1.

D. PERFORMANCE ANALYSIS WITH HOSTILE PULSE-NOISE INTERFERENCE IN A FADING CHANNEL

For the case of interference, the noise power at the output of the integrator for each received bit is given by Equation (4.16). Due to the fading channel, the amplitude of the signal changes from bit to bit, and the mean of the random variable used to model the integrator output is given by Equation (6.10) and the variance by Equation (6.11). The conditional probability P_d is calculated by combining Equations (3.5), (6.10), and (6.11):

$$P_d\left(\sum_{k=1}^{d} A_c\right) = Q\left(\frac{\sum_{k=1}^{d-i}\frac{\sqrt{2}a_c}{\sigma_o} + \sum_{k=1}^{i}\frac{\sqrt{2}a_c}{\sqrt{\sigma_o^2+\alpha\sigma_j^2}}}{\sqrt{(d-i)+i\left(\left(1+\frac{\sigma_j^2}{\sigma_o^2}\right)\Big/\left(1+\alpha\frac{\sigma_j^2}{\sigma_o^2}\right)\right)}}\right)$$
$$= Q\left(\frac{\sqrt{2}\left(\gamma_{b_o}+\gamma_{b_j}\right)}{\sqrt{(d-i)+i\left(\left(1+\frac{\sigma_j^2}{\sigma_o^2}\right)\Big/\left(1+\alpha\frac{\sigma_j^2}{\sigma_o^2}\right)\right)}}\right) \tag{6.20}$$

where

$$\gamma_{b_j} = \sum_{k=1}^{i}\gamma_{b_{k_j}} = \sum_{k=1}^{i}\frac{a_c}{\sqrt{\sigma_o^2+\alpha\sigma_j^2}} \tag{6.21}$$

and

$$\gamma_{b_o} = \sum_{k=1}^{d-i}\gamma_{b_{k_0}} = \sum_{k=1}^{d-i}\frac{a_c}{\sigma_o} \tag{6.22}$$

The PDF $f_{\Gamma_{b_{k_j}}}$ of the random variable representing the k^{th} bit $\gamma_{b_{k_j}}$ is obtained from

$$f_{\Gamma_{b_{k_j}}}(\gamma_{b_{k_j}}) = \left|\frac{da_c}{d\gamma_{b_{k_j}}}\right| f_{A_c}(a_c)\Big|_{a_c=\gamma_{b_{k_j}}\sqrt{\sigma_o^2+\alpha\sigma_j^2}} \tag{6.23}$$

where $f_{A_c}(a_c)$ is the Nakagami-*m* PDF as defined in Equation (2.6). From Equation (6.21), we have

$$\left|\frac{da_c}{d\gamma_{b_{k_j}}}\right| = \sqrt{\sigma_o^2+\alpha\sigma_j^2} \tag{6.24}$$

so

$$f_{\Gamma_{b_{k_j}}}(\gamma_{b_{k_j}}) = \sqrt{\sigma_o^2+\alpha\sigma_j^2}\,\frac{2}{\Gamma(m)}\left(\frac{m}{\overline{a_c^2}}\right)^m\left(\gamma_{b_{k_j}}\sqrt{\sigma_o^2+\alpha\sigma_j^2}\right)^{2m-1}\exp\left(-\frac{m\left(\gamma_{b_{k_j}}\sqrt{\sigma_o^2+\alpha\sigma_j^2}\right)^2}{\overline{a_c^2}}\right) \quad (6.25)$$

$$= \frac{2}{\Gamma(m)}\left(\frac{m\left(\sigma_o^2+\alpha\sigma_j^2\right)}{\overline{a_c^2}}\right)^m\left(\gamma_{b_{k_j}}\right)^{2m-1}\exp\left(-\frac{m\gamma_{b_{k_j}}^2\left(\sigma_o^2+\alpha\sigma_j^2\right)}{\overline{a_c^2}}\right)$$

If we substitute $\overline{\gamma_b} = \frac{\left(\sigma_o^2+\alpha\sigma_j^2\right)}{\overline{a_c^2}}$ into Equation (6.25), we get

$$f_{\Gamma_{b_k}}(\gamma_{b_{k_j}}) = \frac{2}{\Gamma(m)}\left(m\overline{\gamma_{b_j}}\right)^m\left(\gamma_{b_{k_j}}\right)^{2m-1}e^{\left(-m\gamma_{b_{k_j}}^2\,\overline{\gamma_{b_j}}\right)} \quad (6.26)$$

where

$$\overline{\gamma_{b_j}} = \frac{\left(\sigma_o^2+\alpha\sigma_j^2\right)}{\overline{a_c^2}} = \frac{\left(N_o+\alpha\frac{N_i}{\rho}\right)}{T_s\overline{a_c^2}} = \frac{1}{r}\left(\left(\frac{E_b}{N_o}\right)^{-1}+\frac{\alpha}{\rho}\left(\frac{E_b}{N_i}\right)^{-1}\right) \quad (6.27)$$

The PDF $f_{\Gamma_{b_{k_o}}}$ is the same with as Equation (3.17) and for convenience is repeated:

$$f_{\Gamma_{b_{k_o}}}(\gamma_{b_{k_o}}) = \frac{2}{\Gamma(m)}\left(m\overline{\gamma_{b_{k_o}}}\right)^m\left(\gamma_{b_{k_o}}\right)^{2m-1}e^{\left(-m\gamma_{b_{k_o}}^2\,\overline{\gamma_{b_{k_o}}}\right)} \quad (6.28)$$

where

$$\overline{\gamma_{b_{k_o}}} = \frac{\sigma_o^2}{\overline{a_c^2}} = \frac{N_o}{T_s\overline{a_c^2}} = \frac{N_o}{rT_b\overline{a_c^2}} = \frac{1}{r}\frac{N_o}{E_b} = \frac{1}{r}\left(\frac{E_b}{N_o}\right)^{-1} \quad (6.29)$$

As in previous chapters, the overall PDF is evaluated numerically from Equation (3.26), using Equations (4.34), (3.22), (6.26), and (6.28).

Now with the use of Equations (3.12), (3.16), (5.22), and the numerical calculation of the PDF found above, we can calculate P_b.

1. Performance Analysis for the Same Fading Conditions

The performance of the noise-normalized combining receiver with normalization error for the same fading conditions is now examined. For $r = 1/2$ and for the weight structure B_d and the free distance d_{free} from Table 2, we get Figures 48 to 56 where P_b is plotted for the same fading conditions but for different values of the coefficients ρ and α. All the figures are for $E_b / N_o = 15\,\text{dB}$.

The first thing we notice is that for α=1 the noise-normalized combining receiver has the same performance as the noise-normalized combining receiver with normalization error. This is expected since the two receivers are identical for α=1. The second thing we notice is that for values of α greater than one (overestimation of the jammer's power), the performance is better than the performance of noise-normalized combining receiver, but the improvement is not large. Also, even for small values of the coefficient α (underestimation of the jammer's power), the performance of the noise-normalized combining receiver with normalization error is better than the performance of the linear-combining receiver. Finally, we see that for ρ=1, all the receivers have the same performance.

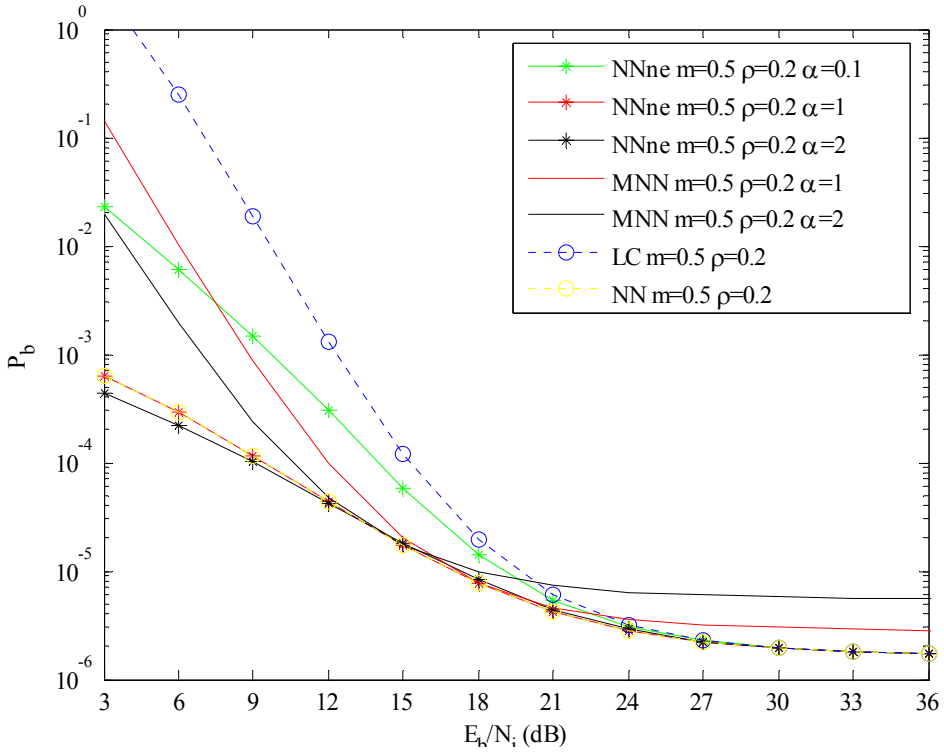

Figure 48. Noise-normalized combining receiver with normalization error with PNI for different values of the coefficient α with m=0.5 and ρ=0.2.

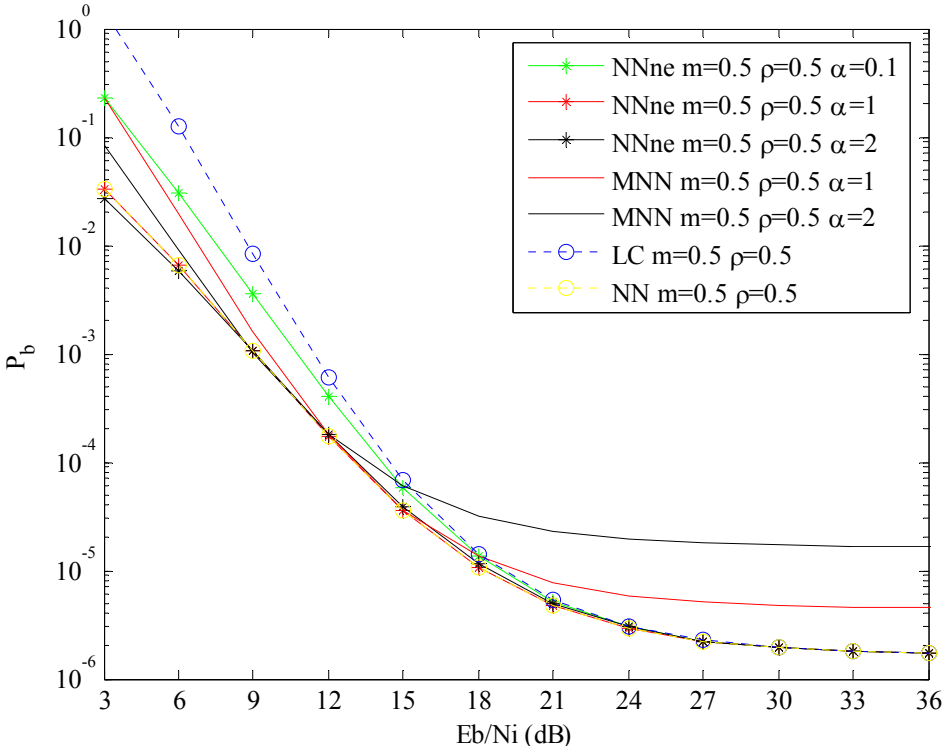

Figure 49. Noise-normalized combining receiver with normalization error with PNI for different values of the coefficient α with m=0.5 and ρ=0.5.

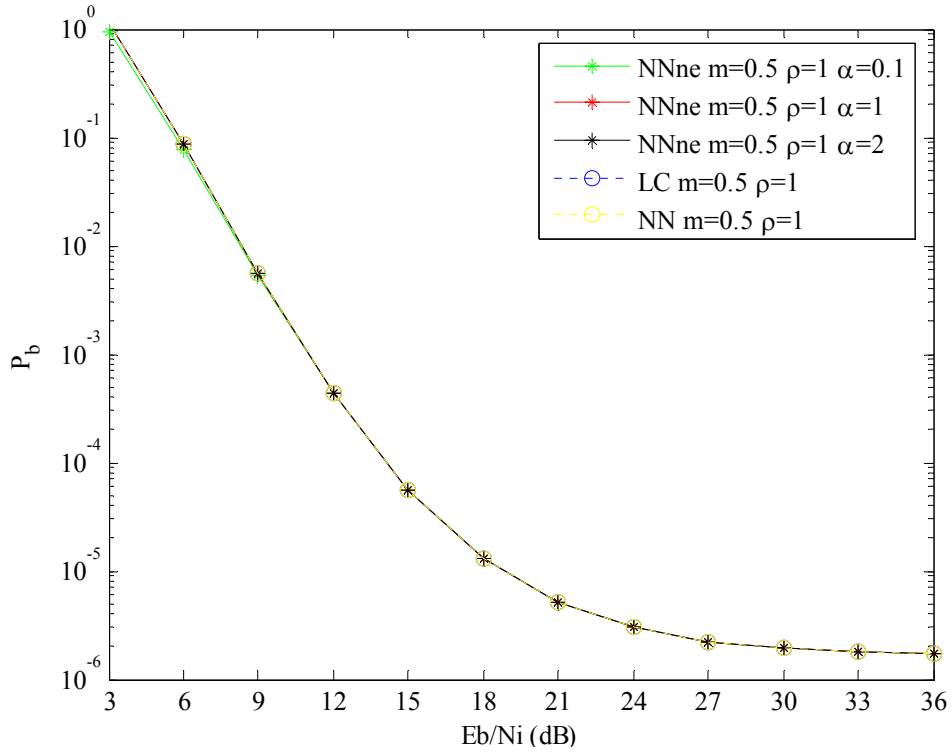

Figure 50. Noise-normalized combining receiver with normalization error with PNI for different values of the coefficient α with m=0.5 and ρ=1.

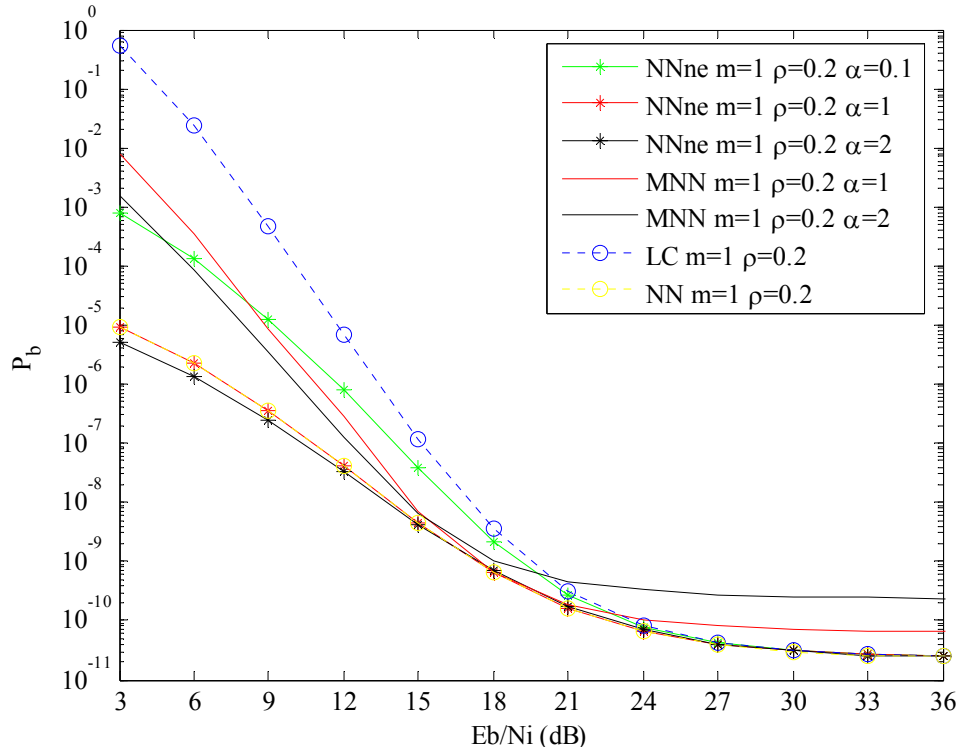

Figure 51. Noise-normalized combining receiver with normalization error with PNI for different values of the coefficient α with m=1 and ρ=0.2.

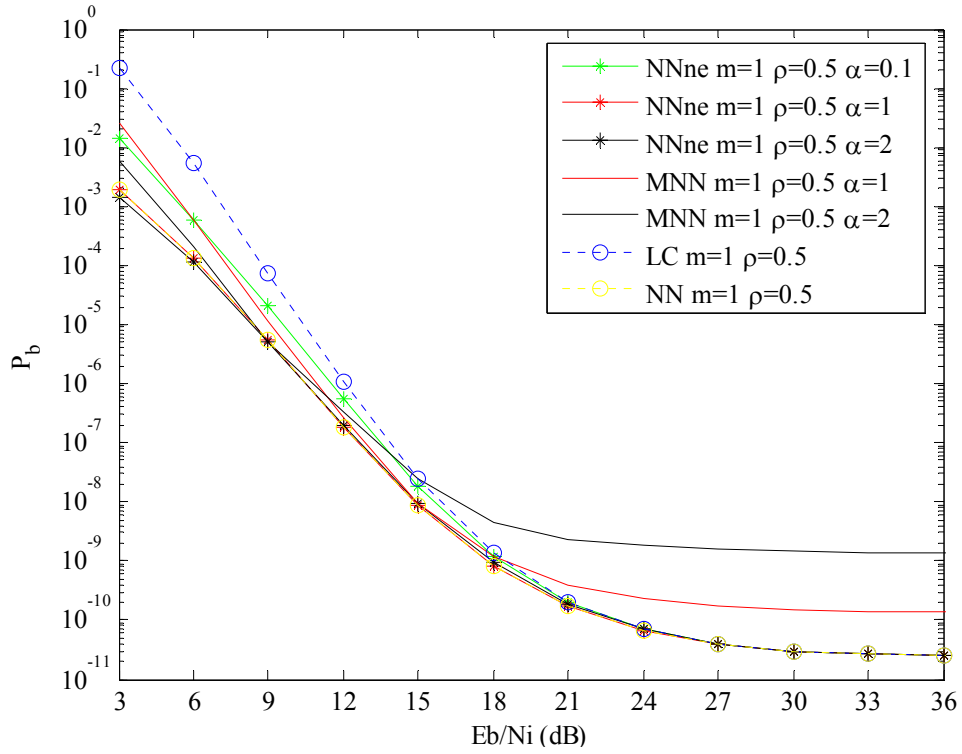

Figure 52. Noise-normalized combining receiver with normalization error with PNI for different values of the coefficient α with m=1 and ρ=0.5.

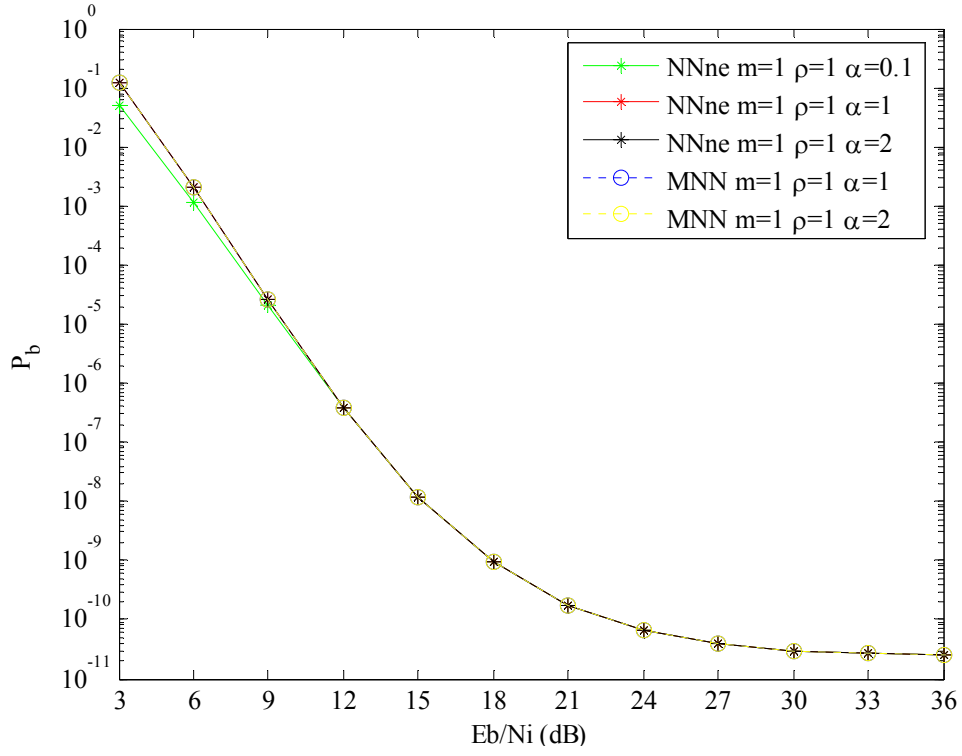

Figure 53. Noise-normalized combining receiver with normalization error with PNI for different values of the coefficient α with m=1 and ρ=1.

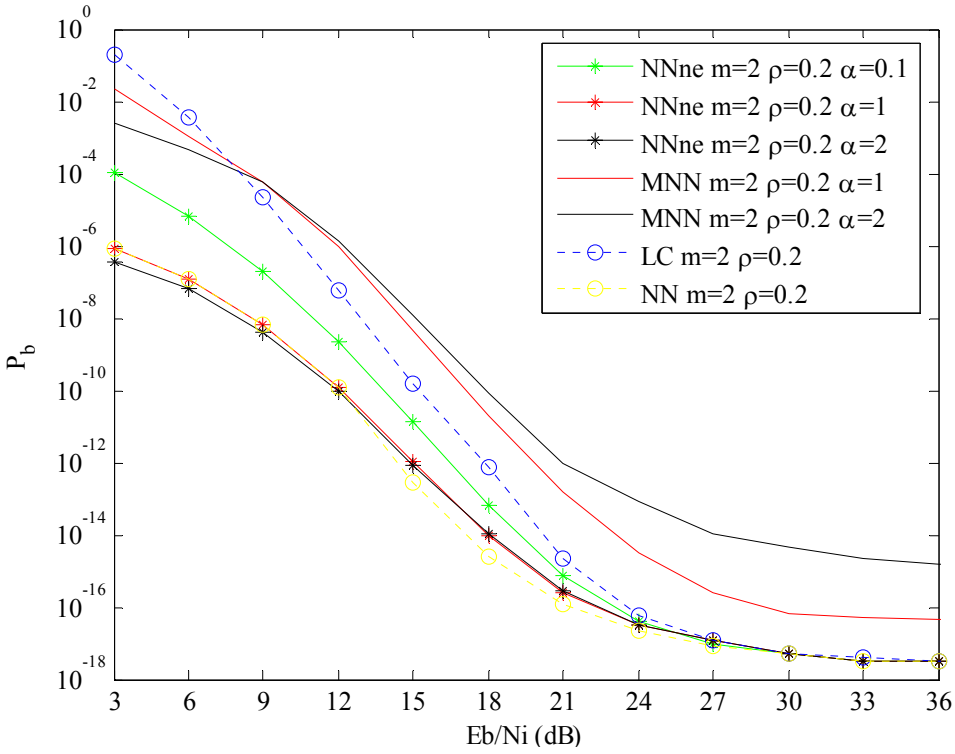

Figure 54. Noise-normalized combining receiver with normalization error with PNI for different values of the coefficient α with m=2 and ρ=0.2.

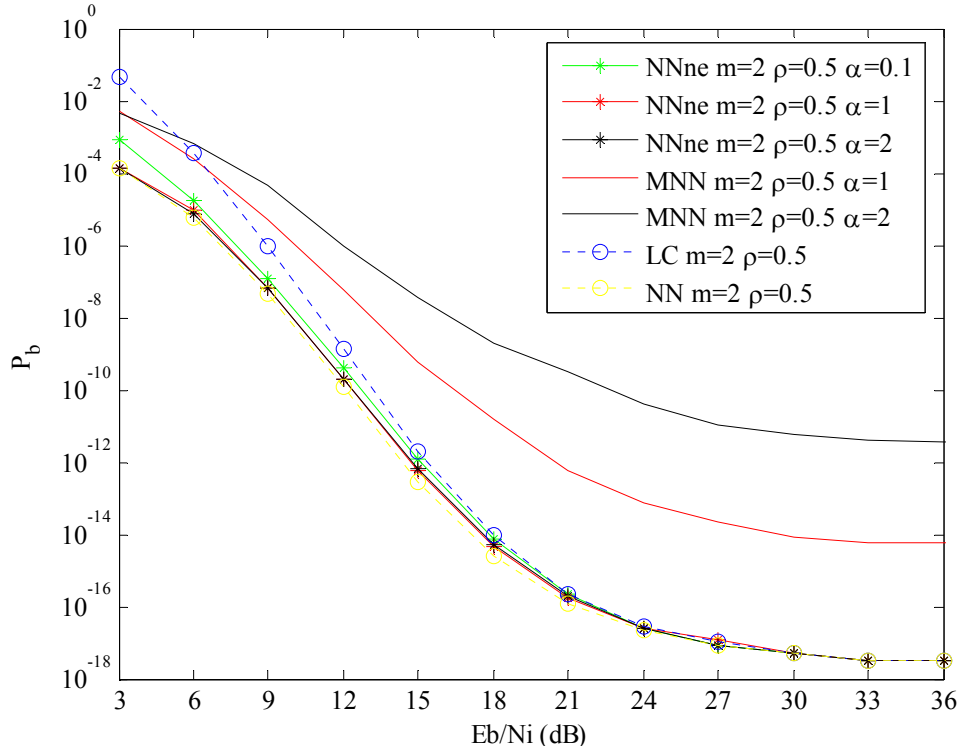

Figure 55. Noise-normalized combining receiver with normalization error with PNI for different values of the coefficient α with m=2 and ρ=0.5.

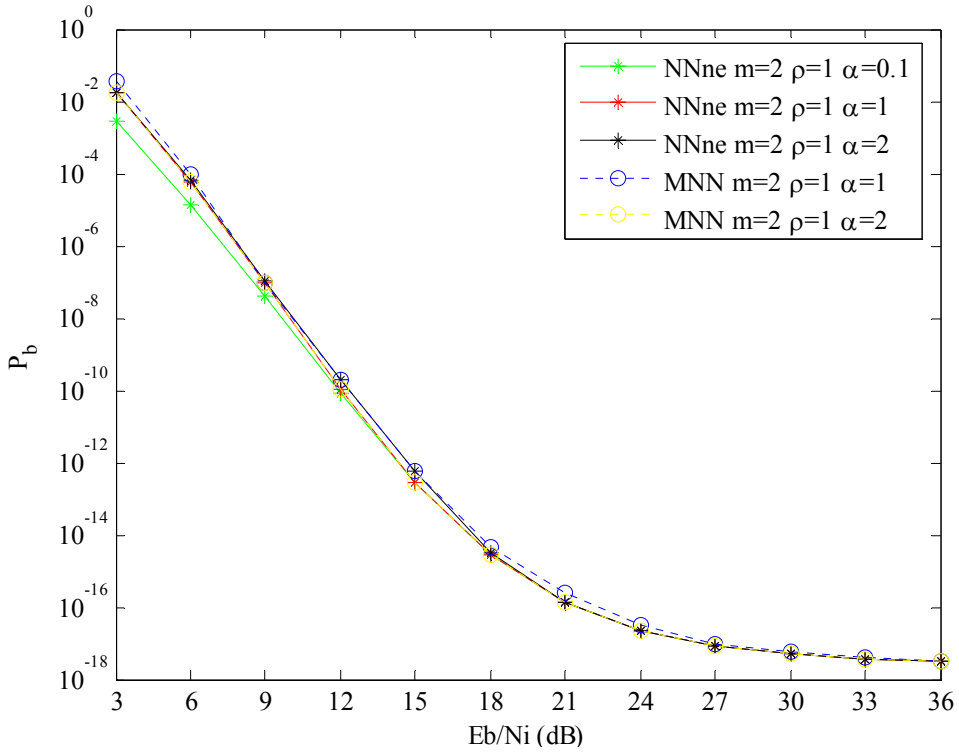

Figure 56. Noise-normalized combining receiver with normalization error with PNI for different values of the coefficient α with m=2 and ρ=1.

2. Performance Analysis for the Same Value of the Coefficient α

If we compare the performance of the noise-normalized combining receiver with normalization error for the same values of the coefficient α, we notice that for small values of the parameter m (m=0.5), the smaller the coefficient ρ is the better the performance is, but for less severe fading conditions and small values of E_b/N_i, the larger the coefficient ρ is the better the performance is. This changes for larger values of E_b/N_i, where the larger the coefficient ρ is the better the performance. The performance crossover point depends on the coefficient ρ and the parameter m. Finally, for the same value of the coefficients α and ρ, the larger the parameter m is, the better the performance of the receiver. In other words, the less severe fading conditions lead to better performance regardless of ρ or α.

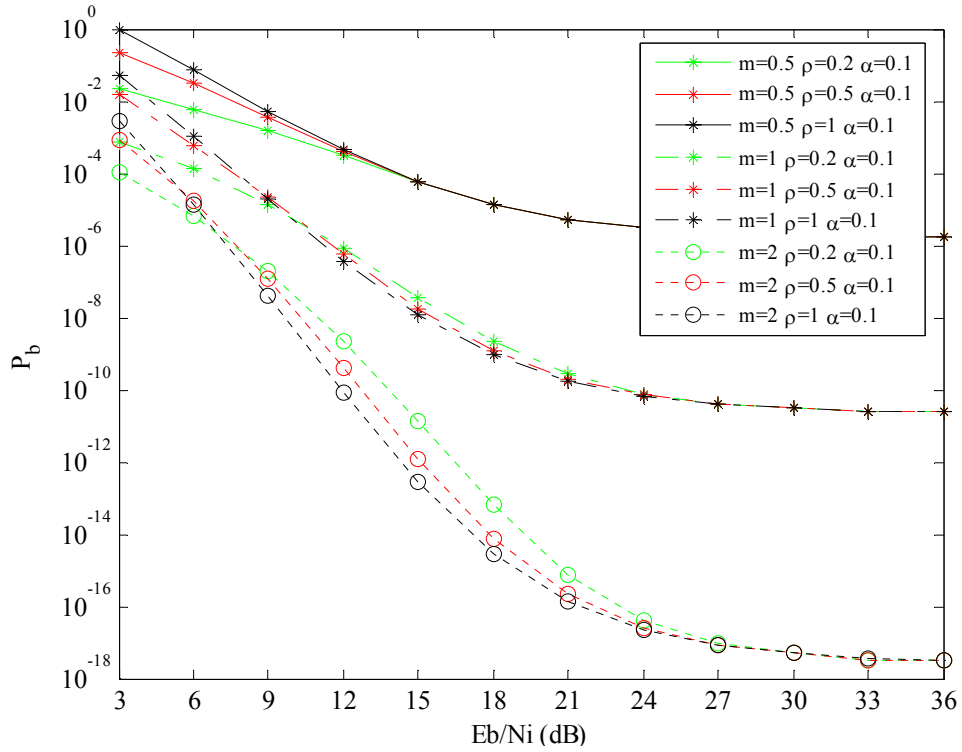

Figure 57. Noise-normalized combining receiver with normalization error for different fading conditions, different values of the coefficient ρ, and α=0.1.

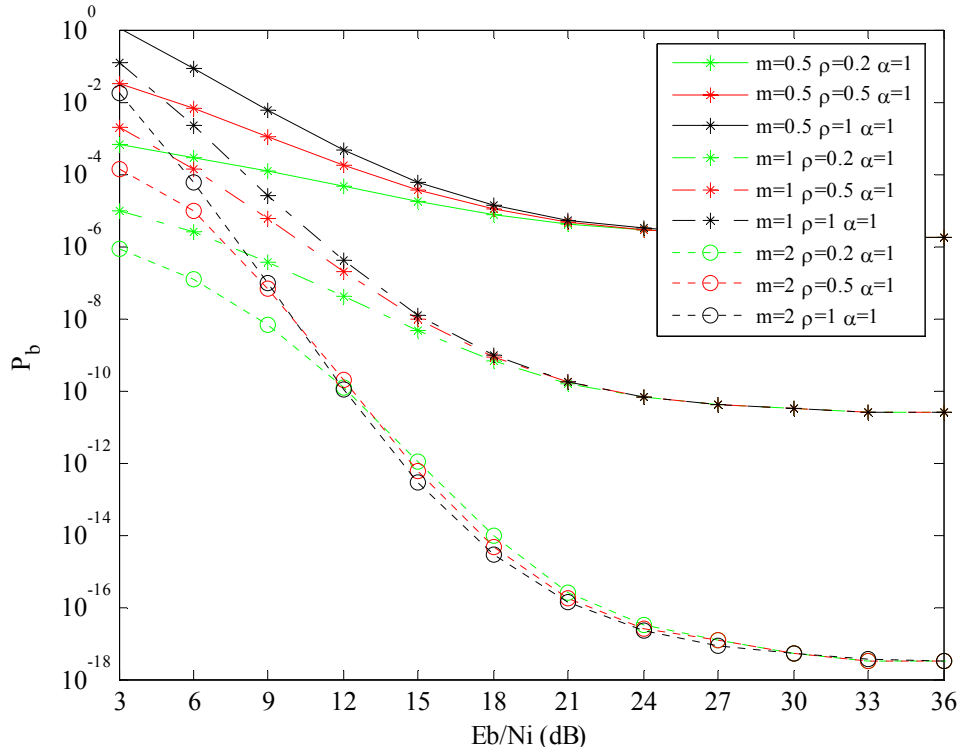

Figure 58. Noise-normalized combining receiver with normalization error for different fading conditions, different values of the coefficient ρ, and α=1.

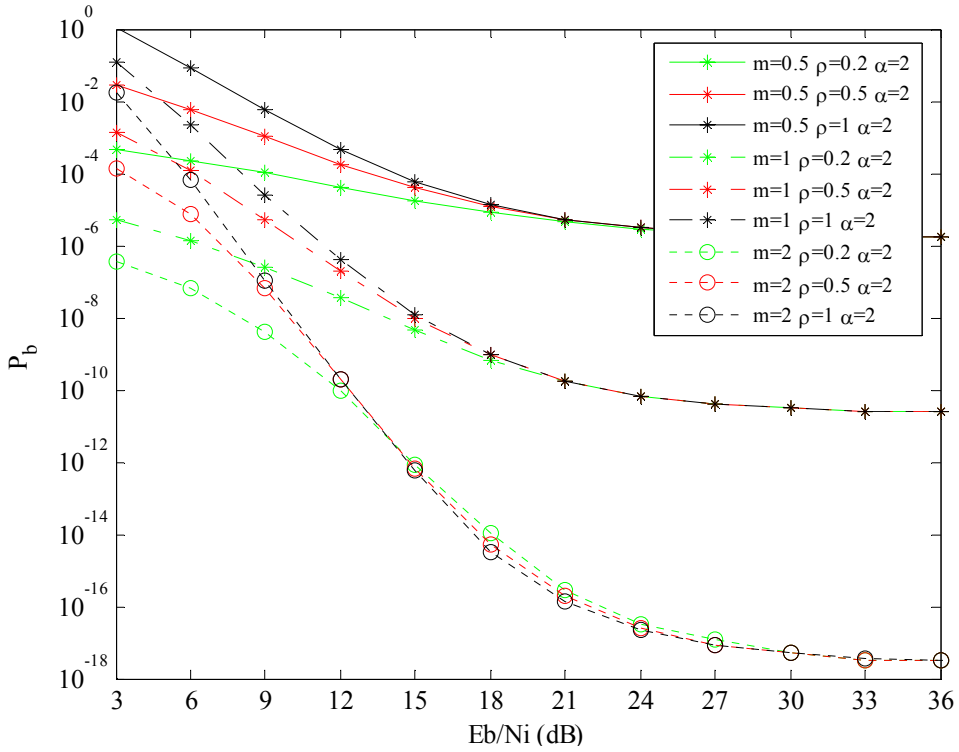

Figure 59. Noise-normalized combining receiver with normalization error for different fading conditions, different values of the coefficient ρ, and α=2.

3. Performance Analysis for the Same Value of the Coefficient ρ

The last analysis that we consider is for constant ρ. As the coefficient α increases, performance improves. In other words, as our estimation improves or when we overestimate the jammer's noise power, the performance of the receiver improves. Finally, as the parameter m increases, performance improves. As fading conditions get less severe, performance improves.

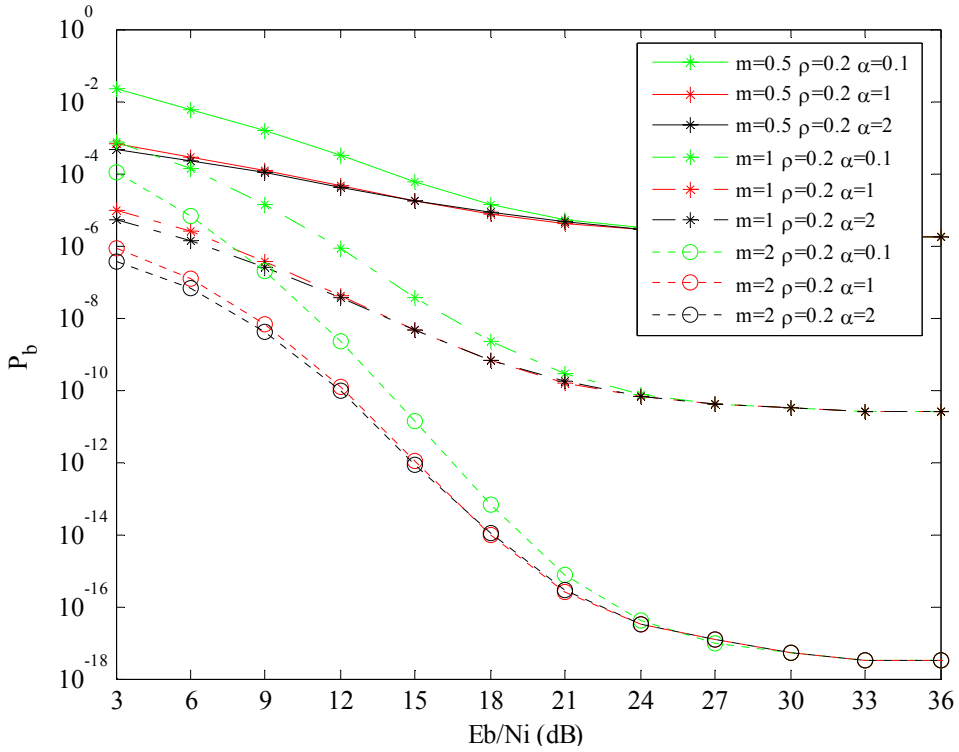

Figure 60. Noise-normalized combining receiver with normalization error for different fading conditions, different values of the coefficient α, and ρ=0.2.

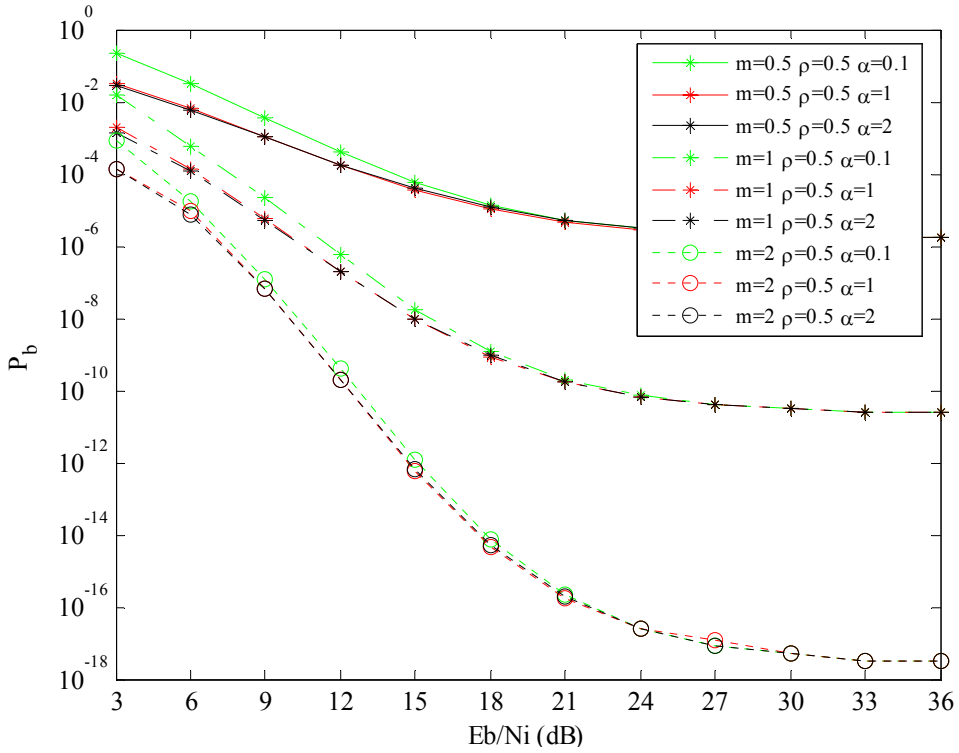

Figure 61. Noise-normalized combining receiver for different fading conditions, for different values of the coefficient α, and ρ=0.5.

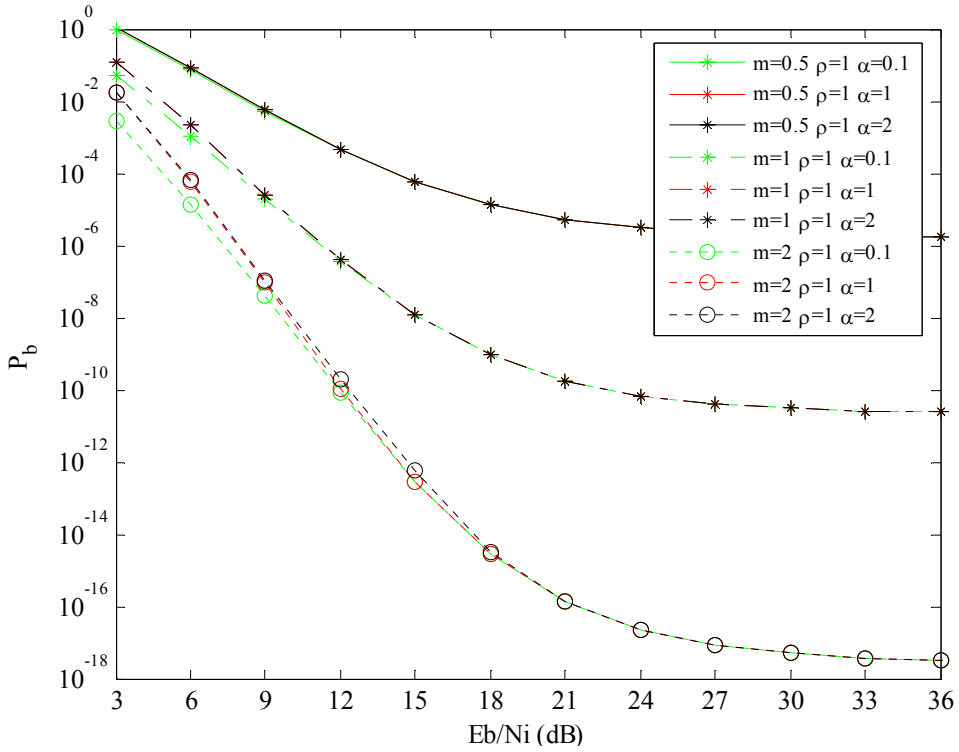

Figure 62. Noise-normalized combining receiver with normalization error for different fading conditions, different values of the coefficient α, and ρ=1.

Having examined the performance of the noise-normalized receiver with normalization error, we conclude in the next chapter with comments on the performance of the receivers examined in Chapters III, IV, V, and VI.

THIS PAGE INTENTIONALLY LEFT BLANK

VII. CONCLUSIONS

The performance of the *IEEE* 802.11*g* WLAN standard receiver for the 6 and 12 Mbps data rates for signal transmitted over flat fading Nakagami channels in a PNI environment was investigated in this thesis for BPSK and QPSK modulation and the code rate specified by the WLAN standard. Receiver performance with Viterbi SDD was analyzed for AWGN alone and for AWGN plus PNI. Moreover, the performance of the *IEEE* 802.11*g* WLAN standard receiver was examined for different scenarios, one where no side information was considered to be available (linear-combining receiver), one when side information was available (in other words, the amplitude of the received signal and the noise power that corrupts every received bit were assumed known), and one when partial side information was considered to be available. In this case, the exact noise power for every received bit was not known, but whether a bit was jammed or not was known (modified noise-normalized receiver and noise-normalized receiver with normalization error). In each case we studied the effect of PNI in non fading channels as well as the effect of AWGN only and AWGN plus PNI in fading channels. In this closing chapter, the main conclusions of the analyses are summarized.

A. SUMMARY OF THESIS FINDINGS

At this point we summarize the findings for the four different receivers examined in Chapters III through VI for both AWGN and AWGN plus PNI.

1. Conclusions on the Effect of AWGN in a Fading Channel

The first comment about the effect of AWGN in a fading channel is that the performance of all receivers examined in this thesis is identical. It was proven analytically that the implementation of the noise-normalized receiver as well as the implementation of the modified noise-normalized receiver and the noise-normalized receiver with normalization error has no effect on receiver performance.

2. Conclusions on the Effect of Hostile Pulse Noise Interference in a non Fading Channel

One general comment is that the noise-normalized receiver with normalization error can achieve even better performance than the noise-normalized receiver with exact estimation of the interference noise. When the estimation was correct, the noise-normalized receiver with normalization error and the noise-normalized receiver had identical performance, but overestimation of the interference power leads to better performance for the noise-normalized receiver with normalization error.

For small values of E_b/N_i, the modified noise-normalized receiver (for large values of α) and the noise-normalized receiver with normalization error have the best performance. Which of the two have the best performance depends on the coefficient ρ. For larger E_b/N_i, the noise-normalized receiver with normalization error always has the best performance. On the other hand, the modified noise-normalized receiver (for larger values of α) and the linear combining receiver have the poorest performance. For small values of E_b/N_i, the linear-combining receiver has the worse performance, and for large values of the E_b/N_i, the modified noise-normalized receiver has the worst performance. All the receivers had identical performance for ρ=1, or in other words, for barrage noise.

Another finding regarding the effect of hostile PNI in a non fading channel is that for the linear-combining receiver, as $\rho \to 1$, performance improves, while the opposite is true for the receivers with noise-normalization. As $\rho \to 0$, the performance of the various noise-normalized receivers improves, especially the modified noise-normalized receiver when $\alpha \geq 7$.

3. Conclusions on the Effect of Hostile Pulse Noise Interference in a Fading Channel

The first comment about the effect of hostile PNI in a fading channel is that the noise-normalized receiver with normalization error always has the best performance for all fading and interference conditions when the normalization error is overestimated. For small values of E_b/N_i, all the noise-normalized receivers have better performance than

the linear-combining receiver. For large values of E_b/N_i, the modified noise-normalized receiver has poorer performance than the other receivers examined.

Commenting on all the receivers' performance, we note that each receiver's performance improves as we move from severe to moderate fading conditions. Moreover, it is important to note that, when ρ=1, all four receivers have identical performance.

B. FUTURE WORK

Due to limitations of the mathematical program used for the numerical evaluation of P_b, some cases of interest were not examined. In addition, there are several areas in which follow-on research is recommended. Since P_b for non-binary modulation types was not examined, the performance of higher data rates and code rates should be examined. The performance of the noise-normalized receiver with normalization error for large overestimation (i.e. α=10) should also be examined, and the performance of all receivers for even more moderate fading conditions (i.e., m=10) should be considered. Furthermore, since the computation of P_b is done numerically, a derivation of analytical closed form expressions would help reduce the computational complexity required to obtain results.

THIS PAGE INTENTIONALLY LEFT BLANK

LIST OF REFERENCES

[1] Institute of Electrical and Electronics Engineers Standard, 802.11a, Wireless LAN Medium Access Control (MAC) and Physical Layer (PHY) Specifications: High-Speed Physical Layer Extension in the 5 GHz Band, *IEEE*, New York, 16 September 1999.

[2] WHITE PAPER "*IEEE* 802.11g new draft standard clarifies future of wireless LAN" William Carney TEXAS INSTRUMENTS.

[3] J. S. Lee, L. E. Miller, and Y. K. Kim, "Probability of error analysis of a BFSK frequency-hopping system with diversity under partial-band jamming interference-Part II: Performance of square-law nonlinear combining soft decision receivers," *IEEE Trans. Commun*., vol. COM-32, pp. 1243–1250, December 1984.

[4] J. S. Lee, L. E. Miller, and R. H. French, "The analyses of uncoded performances for certain ECCM receiver design strategies for multihops/ symbol FH/MFSK waveforms," *IEEE J. Selected Areas Commun*., vol. SAC-3, pp. 611–620, September 1985.

[5] J. S. Lee, R. H. French, and L. E. Miller, "Errorcorrecting codes and nonlinear diversity combining against worst case partial-band noise jamming of FH/MFSK systems," *IEEE Trans. Commun*., vol. COM-36, pp. 471–478, April 1988.

[6] R. C. Robertson and T. T. Ha, "Error probabilities of fast frequency-hopped MFSK with noisenormalization combining in a fading channel with partial-band interference," *IEEE Trans. Commun*., vol. 40, pp. 404–412, February 1992.

[7] L. E. Miller, J. S. Lee, and A. P. Kadrichu, "Probability of error analysis of a BFSK frequency-hopping system with diversity under partial-band jamming interference-Part III: Performance of a square-law self-normalizing soft decision receiver," *IEEE Trans. Commun*., vol. COM-34, pp. 669-675, July 1986.

[8] R. C. Robertson and T. T. Ha, "Error probabilities of fast frequency-hopped FSK with selfnormalization combining in a fading channel with partial-band interference," *IEEE J. Sel. Areas Commun*., vol. 10, pp. 714–723, May 1992.

[9] R. C. Robertson and K. Y. Lee, "Performance of fast frequency-hopped MFSK receivers with linear and self-normalization combining in a Rician fading channel with partial-band interference," *IEEE J. Sel. Areas Commun*., vol. 10, pp. 731–741, May 1992.

[10] Richard Van Nee, Ramjee Prasand, OFDM for Wireless Multimedia Communications, Artech House Publisher, Boston, London, 2000.

[11] Proakis, J.G., Digital Communications, 4th ed., McGraw Hill, New York, NY, 2001.

[12] Kalogrias, Christos, "Performance analysis of the *IEEE* 802.11*a* WLAN standard optimum and sub-optimum receiver in frequency selective, slowly fading Nakagami channels with AWGN and pulsed-noise interference," Master's thesis, Naval Postgraduate School, Monterey, CA, 2004.

[13] Tsoumanis, Andreas, "Performance analysis of the effect of pulsed-noise interference on WLAN signals transmitted over a Nakagami fading channel," Master's thesis, Naval Postgraduate School, Monterey, CA, 2004.

THIS PAGE INTENTIONALLY LEFT BLANK

INITIAL DISTRIBUTION LIST

1. Defense Technical Information Center
   Ft. Belvoir, Virginia

2. Dudley Knox Library
   Naval Postgraduate School
   Monterey, California

3. Chairman, Code EC/Po
   Department of Electrical and Computing Engineering
   Naval Postgraduate School
   Monterey, California

4. Chairman, Code IS/Bo
   Department of Information Sciences
   Naval Postgraduate School
   Monterey, California

5. Professor R. Clark Robertson EC/Rc
   Department of Electrical and Computer Engineering
   Naval Postgraduate School
   Monterey, California

6. Professor David C. Jenn, EC/Jn
   Department of Electrical & Computer Engineering
   Naval Postgraduate School
   Monterey, California

7. Embassy of Greece,
   Office of Naval Attaché
   Washington, DC

8. Konstantinos Taxeidis
   Pl. Kaliga 3
   Athens, Greece